Geographia Technica

Technical Geography
an International Journal for the Progress of Scientific Geography

Volume 13, Geographia Technica No. 1/2018

www.technicalgeography.org

Cluj University Press

Geographia Technica

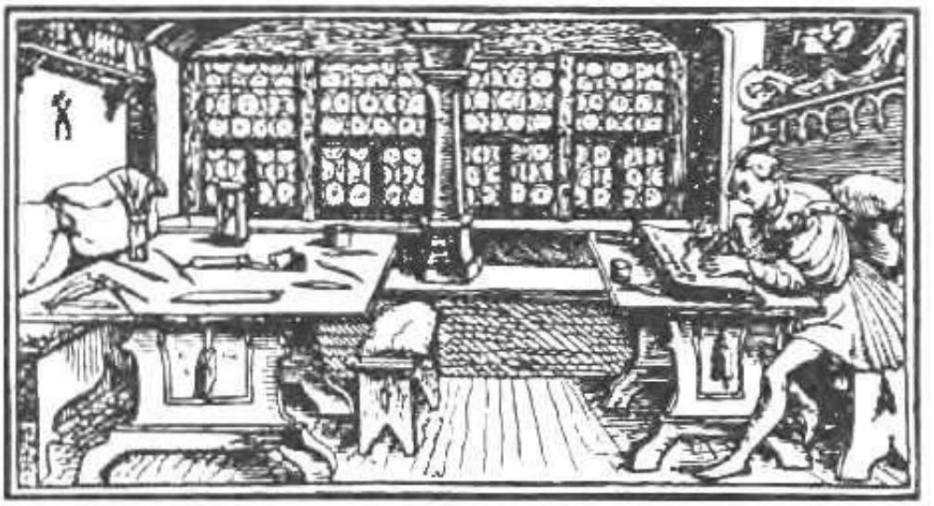

Technical Geography

an International Journal for the Progress of Scientific Geography

2018 – No. 1

Cluj University Press

ISSN: 1842 - 5135 (Printed version)
ISSN: 2065 - 4421 (Online version)

Babeș-Bolyai University
Cluj University Press
Director: Codruța Săcelean
Str. Hașdeu nr. 51
400371 Cluj-Napoca, România
Tel./fax: (+40)-264-597.401
E-mail: editura@editura.ubbcluj.ro
http://www.editura.ubbcluj.ro/

Asociatia Geographia Technica
2, Prunilor Street
400334 Cluj-Napoca, România
Tel. +40 744 238093
editorial-secretary@technicalgeography.org
http://technicalgeography.org/

Contents

Geographia Technica

Volume 13, Issue 1, spring 2018

An International Journal of Technical Geography

ISSN 2065-4421 (Online); ISSN 1842-5135 (printed)

REMOTE SENSING BASED ASSESSMENT OF VARIATION OF SPATIAL DISPARITIES

József BENEDEK[1], Kinga IVAN[2]

DOI: 10.21163/GT_2018.131.01

ABSTRACT:
The aim of this paper is to identify the relationship between the spatial and temporal variation of spatial disparities (measured with Gross Domestic Product, GDP) and night-time lights at regional (county) level in Romania. The analysis presumed using night-time lights data captured by the DMSP-OLS satellites, in addition to official statistical data expressing economic income (GDP). The DMSP-OLS night-time lights data collected by the National Oceanic and Atmospheric Administration (NOAA) has a spatial resolution of 30 arc second and is available for the period of 1992-2013. The delimitation of unlit and lit areas was performed using ArcGIS software. The lower value of light intensity reflects less developed areas and those with higher value reflects more developed areas. The assessment relationship between GDP and night lights value was made using statistical correlation. The results show a strong linear correlation between the GDP and night lights value. It means that night-time lights are an excellent proxy for measuring spatial (regional) disparities. Moreover, based on the linear dependence and the spatial relation between these two datasets, we will be able in the future to go one step further and measure the level of spatial disparities at local level (cities and communes), where official statistical data is not recorded.

Key-words: *Night-time light, Spatial disparities, DMSP-OLS satellite images, Romania.*

1. INTRODUCTION

Remote sensing offers a wide range of satellite imagery which is widely used in various fields such as geography, environmental studies, spatial planning, topography or economics. Depending on the time when these images were taken we distinguish satellite images captured during the day and satellite images captured at night. Lately more and more attention has been paid to the use of satellite images captured at night in order to determine socio-economic data corresponding to micro scale spatial units, where official statistical data is not available. Night-time lights (NTL) resulting from the illumination of public and private spaces, roads or from the use of vehicles during night, reflects the intensity of human economic activity of an area (Chen & Nordhaus, 2011; Henderson et al., 2012; Mellander et al., 2015; Pinkovskiy & Sala-I-Martin, 2016). Information on the degree of night-time illumination of a spatial unit can be obtained on a global scale for a period of more than 20 years with the assistance of remote sensing. In this context, using remote sensing and Geographic Information System (GIS) may provide new perspectives for assessing economic performance at national and sub-national level. Satellite images also offer a great potential for the spatial and temporal analysis of the degree of night-time illumination of a spatial unit. Night-time lights (NTL) data captured by the satellites in order to estimate economic growth is a topical one, being used lately in numerous studies.

[1]*University of Miskolc, Institute of World and Regional Economics, 3515 Miskolc, Hungary, jozsef.benedek@ubbcluj.ro;*
[2]*Babeş-Bolyai University, 400006 Cluj-Napoca, Romania, kinga.ivan@ubbcluj.ro.*

Elvidge et al. (1997) have conducted research on the relationship between illuminated areas and GDP for 21 countries, obtaining a very strong correlation between the two analyzed variables. Henderson et al. (2012) has used night-time lights data to measure the real income growth, and Henderson et al. (2011) analyzed the relation between night-time lights and GDP, having also obtained a very strong correlation.

Night-time lights data have been used by Villa (2016) in assessing the effects of social transfers on the economic growth at local level. The study revealed that social transfers have generated positive effects on economic growth in Columbia. Ghosh et al. (2013) have used satellite images captured at night to measure human welfare. In another approach Jean et al. (2016) have used high resolution satellite images captured during the day to make predictions about the spatial distribution of economic well-being in five countries in Africa. In other studies the decoupling between the energy consumption and economic growth was examined (Szlávik and Sebestyén Szép, 2017).

In the present paper we proposed to analyze the relation between the night-time lights variation and economic spatial disparities at national and sub-national level in Romania for the period 2000-2013. Thus we have followed the temporal variation analysis of night-time lights (NTL) at national and sub-national level in Romania, respectively the relationship between the mean of night-time light (NTL) value and Gross Domestic Product (GDP). Similar concerns had Iuga (2015) who having analyzed the link between the evolution of climate change and socio-economic development in Romania, using as key indicator the real Gross domestic product (GDP) per capita. The scientific and practical relevance of our study is related to the major bottlenecks in measuring spatial disparities and economic development in Romania: 1. GDP is directly measured only at national level, the regional GDP being calculated indirectly with two years average delay from the national GDP calculations; 2. there is no statistical record of GDP on the local level (cities and communes). The practical relevance of this issue is given by the fact that GDP is used as main indicator for the designation of areas eligible for European or national development support schemes.

2. STUDY AREA AND DATA

Romania is situated in the south-eastern part of Europe, its territory comprises 238 391 km² and its population reached 19 760 314 inhabitants in 2016 (Eurostat Database, 2017).

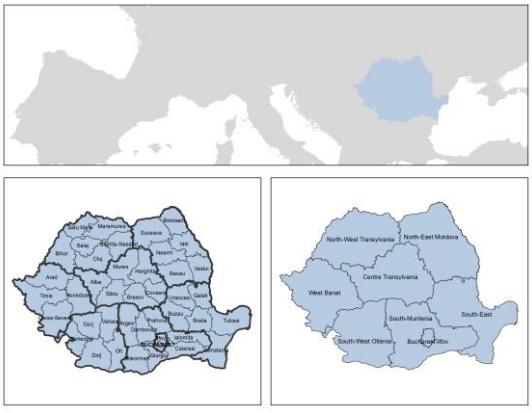

Fig. 1. Romanian counties (left) and development regions (right) *(Source: authors).*

The country is organized in 41 administrative counties (*judete* in Romanian) and Bucharest municipality (**Fig. 1**). The counties (NUTS-3 units) are grouped in 8 development regions (NUTS-2 level): North-West Transylvania, North-East Moldova, Center Transylvania, West Banat, South-West Oltenia, South-Muntenia, Bucharest-Ilfov, South-East (Black Sea) (**Fig. 1**). Both sub-national levels (NUTS-2 and 3) are the basic territorial units for the distribution of EU and national founded development policies.

Remote sensing provides data of global scale on artificial illumination during the night. A dataset that proved to be very useful and has been used in many studies, is DMSP-OLS night-time lights data (**Fig. 2**) collected and offered by the National Oceanic and Atmospheric Administration (NOAA). These data have a spatial resolution of 30 arc second (1 km^2) and can be obtained free of charge from the NOAA database for the period 1992-2013 (NOAA, 2017).

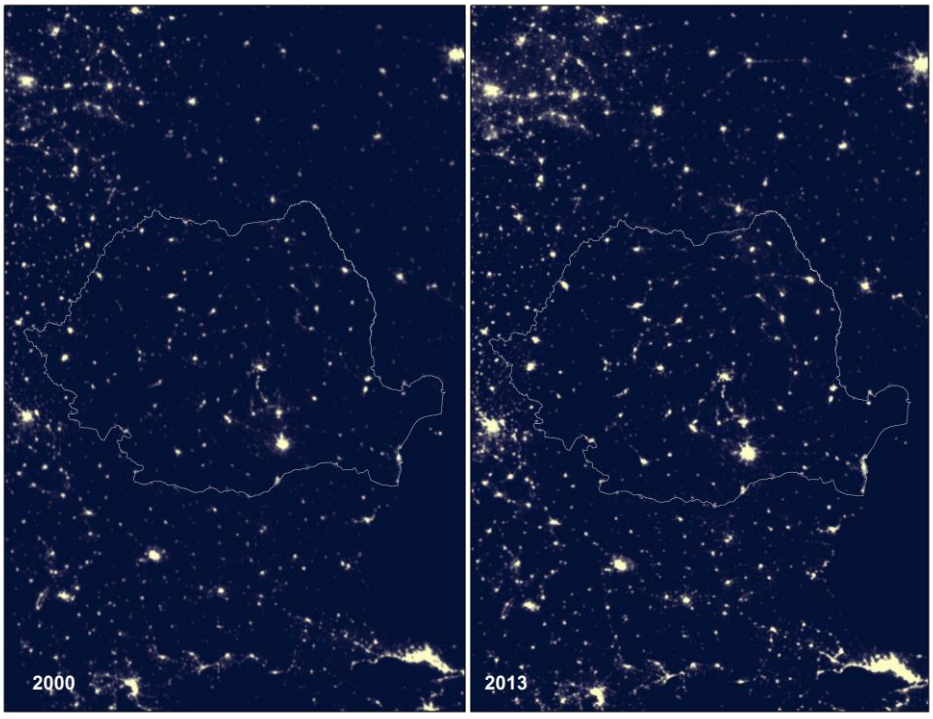

Fig. 2. DMSP-OLS night-time lights in Romania between 2000 and 2013 *(Source of data: NOAA, 2017).*

DMSP - OLS satellites orbit Earth and record light intensity with the help of the OLS sensors in every location on Earth from 20:30 until 22:00 local time, between 65° north latitude and 65°south latitude (Villa, 2016). The intensity of night-time lights reflects light both inside and outside their premises (Henderson et al., 2012). The main indicator of both spatial economic disparities and economic output is the Gross Domestic Product (GDP), more exactly the Gross Domestic Product relative to the total population of the considered area (GDP per capita). The values of GDP at national and sub-national level have been extracted for the period 2000-2013 from the Eurostat Database (Eurostat Database, 2017).

3. METHODOLOGY

3.1. Evaluation of temporal variation of night-time illumination

The GIS (Geographic Information System) tool has been used to extract the night-time illumination data at national and sub-national level in Romania. DMSP (Defense Meteorological Satellite Program) satellite imagery purchased from the National Oceanic and Atmospheric Administration database (NOAA, 2017), a total number of 14 images (from 2000 to 2013), have been processed in ArcGIS 10.4, which allowed us to delimit the unlit and lit areas.

The value of light intensity measured by the DMSP-OLS satellites is ranging from 0-63 Digital Number. 0 values correspond to unlit areas, and those with 63 to high lit areas. From the illuminated areas those with a lower value of the light intensity reflect less developed areas, and those with a higher value reflect the more developed ones. In order to group areas depending on the light intensity value first we removed the unlit areas, those with 0 value. Thus in the first phase unlit areas have been eliminated for each reference year and illuminated areas have been delimited. This process has been carried out with the assistance of Set Null function of ArcGIS 10.4, in which zero values were assigned to all DN $\leq$ 0 values. Subsequently with the assistance of Zonal Statistics function, the mean night-time value was calculated, then the surface of illuminated areas at national, regional and county level for each reference year (**Fig. 3)**.

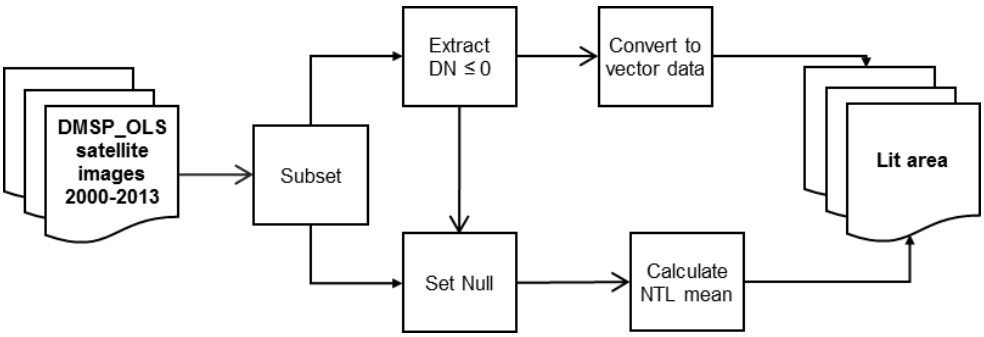

Fig. 3. Flowchart of extracting lit areas.

Values thus obtained were matched with the statistical data corresponding to the analyzed spatial units. Then using the data on the total illuminated area corresponding to each reference year, the growth rate of night-time light (NTL) has been calculated as follow:

$$NTL_{rate} = \frac{(NTL_1 - NTL_o)}{NTL_o} \text{ x } 100 \quad (1)$$

Where,

NTL_1 - represents night-time light area from the following year;
NTL_0 - represents night-time light area from the previous year;

3.2. Analysis of the relationship between mean of night-time light value and GDP

According to Henderson et al. (2012) lights in an area reflect the total intensity of income. In order to evaluate the link between economic output in Romania and night-time

illumination we used a statistical correlation. The GDP (and GDP per capita) is the classic indicator that dominates the methodology of measuring the level of the development at national and regional level (Pinkovskiy & Sala-I-Martin, 2016) and it is an important variable in analyzing economic growth (Henderson et al., 2012) and spatial disparities. In the research of the relation between luminosity and GDP, in some studies the sum of light intensity values were computed (Villa, 2016; Ghosh et al., 2013) while in other studies the mean of night light value (Mellander et al., 2015) or the lit area were used (Elvidge et al., 1997; Ebener et al., 2015). According to Mellander et al. (2015) in the present research we used the mean of night-time light (NTL) value.

The intensity of linear relationship between the mean of night-time light value and GDP was determined using by Pearson correlation coefficient (r). The Pearson correlation coefficient (r) of two variables, x_i and y_i, was calculated on the basis of the following equation (Lee & Wong, 2001):

$$r = \frac{\frac{\sum_{i=1}^{n} xiyi}{n} - \overline{X} \bullet \overline{Y}}{SxSy} \tag{2}$$

where, $\overline{X}$ and $\overline{Y}$ represent the mean of x and y, and S_x and S_y represent standard deviation of x and y, calculated with the formulas:

$$Sx = \sqrt{\frac{\sum_{n=1}^{n} x^2}{n} - \overline{X}^2} \quad Sy = \sqrt{\frac{\sum_{n=1}^{n} y^2}{n} - \overline{Y}^2} \tag{3}$$

4. RESULTS AND DISCUSSIONS

The graphical representation showing the variation of illuminated areas and GDP (Gross Domestic Product at current market prices) in Romania for the period 2000-2013 illustrates that the these two variables have similar trends, excepting the year of 2013, when the illuminated areas decrease. The decline of the illuminated area is explained by the population decline in the year of 2013 (**Fig. 4**).

It can be noted that with the increase or decrease of the GDP, the illuminated areas in Romania follow the same trend. This trend is supported by the statistical results obtained by analyzing the relationship between mean of night-time light value and GDP on national level, where the calculated Pearson correlation coefficient was 0.70, which fact indicates a strong link between these two variables.

This means that night-time light can be used as proxy for economic output and spatial economic disparities in Romania. In addition, its growth trend reflects well the trend of economic growth and development.

Fig. 4. Development rate (in %) of illuminated areas and of the GDP in Romania in the period 2000 - 2013.

On regional level the degree of correlation between the mean of night-time light and GDP in the period 2000-2013 was very high in Bucharest-Ilfov Region. The statistical analysis has identified three clusters within the distribution: the first one corresponding with the period between 2000-2002 (r=0.83), the second one between 2003-2009 (r=0.94) and the third one between 2010-2013 (r=-0.78) (**Fig. 5a**). The fifth-order polynomial dynamics from **Fig. 5b** (R^2 = 0.86) adjusts much better to the cloud of points than the simple linear regression from **Fig. 5a**. This overall curve highlights more precisely the influence of GDP on night-time light, namely the dynamics of well-being in Romania.

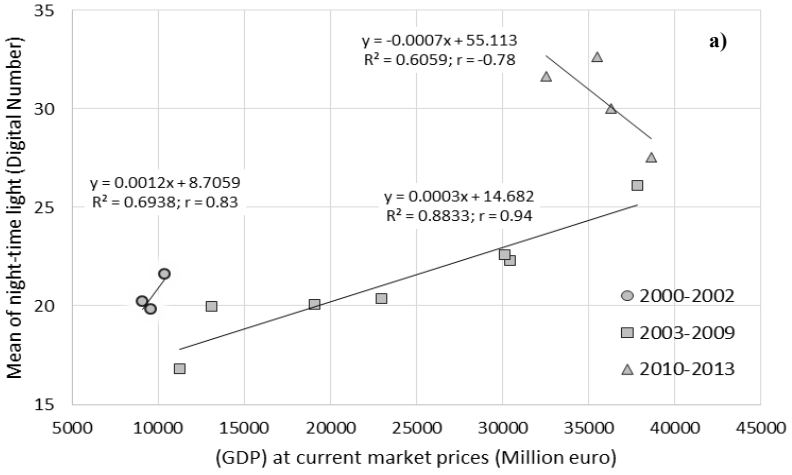

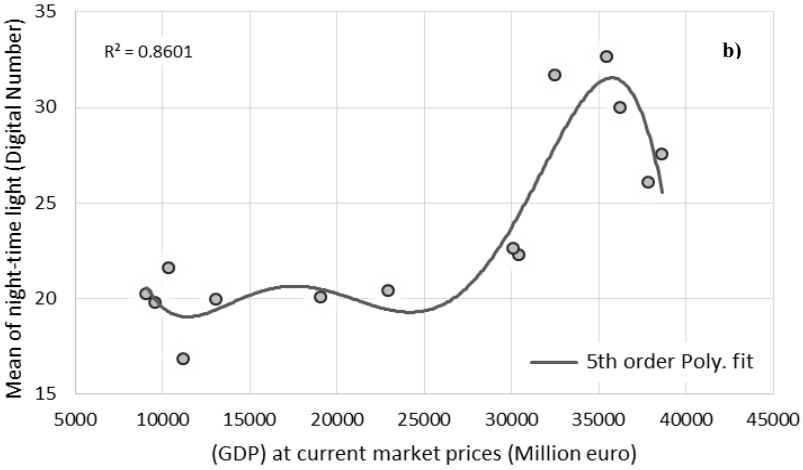

Fig. 5. Graph correlating illumination and GDP, in Bucharest- Ilfov Region (2000–2013).

For other development regions, the results showed a similar high statistical link for three of them: West Banat Region (r=0.75), South-East Region (r=0.71), North-West Transylvania Region (r=0.70), and slightly lower relation in the case of the rest of four regions: North-East Moldova Region (r=0.55), South-Muntenia Region (r=0.64), Centre Transylvania Region (r=0.68) and South-West Oltenia Region (r=0.69).

Based on these results we can state that, on national and regional level, the variation of illumination largely reflects the intensity of economic activity in Romania. Therefore, the night-time illumination can be used as an alternative proxy to the GDP for the measurement of economic and social development.

On county level, following the analysis of the degree of dependence between the mean of night-time light and GDP (**Table 1**), we have distinguished four categories of counties: a) economic activity was very highly reflected by illumination, $r \geq 0.80$; b) economic activity was highly reflected by illumination $r < 0.80$ and $r \geq 0.65$; c) economic activity was medium-level reflected by illumination $r < 0.65$ and $r \geq 0.50$; d) economic activity was lowly reflected by illumination $r < 0.50$ (**Fig. 6**).

As a general observation, we can see from **Fig. 6** and **Table 1** that for the large number of cases the correlation between night-time illumination and GDP was strong.

We have few exemptions, with low correlation, where further research is needed. Our main hypothesis for these cases is that their official GDP is underestimated. The counties in this category ($r < 0.5$) have low levels of GDP and are characterized by a strong outmigration (Benedek & Török, 2014; Benedek, 2015).

The correlation increases in the case of counties with higher values of GDP and less outmigration. Future research is needed to fully understand and to clarify these spatial differences on county levels. That means in the same time, that the use of night-lights as proxy for GDP at county level faces some limitations.

Table 1.

The degree of dependence between GDP and mean of night-time light value.

GDP vs. night-time light (2000-2013)			
Sub-regions	**Pearson (r)**	**Sub-regions**	**Pearson (r)**
Bihor	0.84	Galati	0.60
Bistrita-Nasaud	0.51	Tulcea	0.63
Cluj	0.69	Vrancea	0.62
Maramures	0.51	Arges	0.58
Satu Mare	0.58	Calarasi	0.84
Salaj	0.59	Dambovita	0.65
Alba	0.69	Giurgiu	0.81
Brasov	0.75	Ialomita	0.68
Covasna	0.40	Prahova	0.56
Harghita	0.48	Teleorman	0.64
Mures	0.61	Bucuresti	0.74
Sibiu	0.80	Ilfov	0.79
Bacau	0.42	Dolj	0.78
Botosani	0.54	Gorj	0.74
Iasi	0.59	Mehedinti	0.22
Neamt	0.58	Olt	0.57
Suceava	0.61	Valcea	0.40
Vaslui	0.14	Arad	0.86
Braila	0.44	Caras-Severin	0.38
Buzau	0.63	Hunedoara	0.65
Constanta	0.81	Timis	0.80

Fig. 6. Illustration of the degree of dependence between mean of night-time light and GDP at county level.

5. CONCLUSIONS

Night-time lights data obtained by remote sensing proved to be useful in analyzing the lit area variation as well as in assessing the economic output differences on national and sub-national level in Romania. The study of the relationship between GDP and mean of night-time light value revealed a direct relationship between the two variables, both on national, regional and county level. These results demonstrate that night-time illumination reflects well the intensity of economic activity in Romania. Therefore, it can be used with confidence in estimating economic output differences and economic growth in Romania at national and regional level. However, its use at county level needs further investigations.

R E F E R E N C E S

Benedek, J. & Török, I. (2014) County-level demographic disparities in Romania. *Transylvanian Review*, 23 (2), 138-147.

Benedek, J. (2015) Spatial differentiation and core-periphery structures in Romania. *Eastern Journal of European Studies*, 6 (1), 49-61.

Chen, X. & Nordhaus, W. D. (2011) Using luminosity data as a proxy for economic statistics. *Proceedings of the National Academy of Sciences*, 108 (21), 8589-8594.

Ebener, S., Murray, C., Tandon, A. & Elvidge, C. C. (2005) From wealth to health: Modelling the distribution of income per capita at the sub-national level using night-time light imagery. *Int J Health Geogr*, 4 (5), 1-17.

Elvidge, C. D., Baugh, K. E., Kihn, E. A., Kroehl, H. W. & Davis, E. R. (1997) Mapping city lights with night-time data from the DMSP operational linescan system. *Photogrammetric Engineering & Remote Sensing*, 63 (6), 727-734.

EUROSTAT DATABASE (2017). – Available from: http://ec.europa.eu/eurostat/.[Accessed March 2017].

Ghosh, T., Anderson, S. J., Elvidge, C. D. & Sutton, P. C. (2013) Using nighttime satellite imagery as a proxy measure of human well-being. *Sustainability*, 5, 4988-5019.

Henderson, V., Storeygard, A. & Weil, D. N. (2011) A Bright Idea for Measuring Economic Growth. *American Economic Review: Papers & Proceedings*, 101 (3), 194-99.

Henderson, V., Storeygard, A. & Weil, D. N. (2012) Measuring economic growth from outer space. *American Economic Review*, 102 (2), 994-1028.

Iuga, C. (2015) Socioeconomic Development and Climate Change – Basic Components of Sustainable Development in European Union Countries. *Journal of Environmental Protection and Ecology*, 16 (3), 1168-1178.

Jean, N., Burke, M., Xie, M., Davis, W. M., Lobell, D. B. & Ermon, S. (2016) Combining satellite imagery and machine learning to predict poverty. *Science*, 353 (6301), 790-794.

Lee, J. & Wong, D.W.S.(2001) *Statistical Analysis with ArcView GIS*, John Wiley and Sons, New York.

Mellander, C., Lobo, J., Stolarick, K. & Matheson, Z. (2015) Night-Time Light Data: A Good Proxy Measure for Economic Activity? *PLoS ONE*, 10 (10), 1-18.

NOAA (2017). - National Oceanic and Atmospheric Administration. Available from: https://ngdc.noaa.gov/eog/ [Accessed January 2017].

Pinkovskiy, M. & Sala-I-Martin, X. (2016) Lights, camera,... income! Illuminating the national accounts-household surveys debate. *Quarterly Journal of Economics*, 131 (2), 579-631.

Szlávik, J. & Sebestyén Szép, T. (2017) Delinking of energy consumption and economic growth in the visegrad group. *Geographia Technica*, 12 (2), 139-149.

Villa, J. M. (2016) Social Transfers and Growth: Evidence from Luminosity Data. *Economic Development and Cultural Change*, 65 (1), 39-61.

HEAT WAVES FREQUENCY. A STUDY CASE OF IASI CITY, ROMANIA (1961-2016)

Roxana Simona BOCANCEA [1,2]

DOI: 10.21163/GT_2018.131.02

ABSTRACT:
Among the weather events generated by extreme temperatures, heat waves are some of the most harmful which in the recent years has obviously increased the nature of climate risk. The main reason why we decided to conduct such a research is due to the profound socio-economic impact of heat waves in urban areas. The aims of this study were to analyze heat waves at Iasi meteorological station based on the daily maximum temperature during 56-year period (1961-2016). The frequency and duration were analyzed by applying the 95th percentile method and choosing the length of an event of minimum three consecutive days. The results were showing that the most frequent heat waves are those lasting 3 and 4 days, but regarding the duration, the longest heat waves were considered during the summer of 2007, lasting 10 days at Iasi meteorological station. The main result is that the frequency trend is significantly increasing.

Key-words: *Heat waves, Climate change, Iasi Muncipality, Percentile 95th*

1. INTRODUCTION

In the last two decades many climate change studies have focused on extreme temperatures as they have significant impact on environment and society. One of the most harmful weather events generated by extreme temperatures are heat waves (HWs). Heat waves have discernible impacts including rise in mortality and morbidity (Knowlton et al., 2009; Bassil et al., 2007), an increased strain on infrastructure (power generation, water supply, transportation) (et al., 2003) and consequent impacts on society.

The socio-economic impact of heat waves has maintained the interest of scientists in this subject who has undertaken it in various ways. In Romania many studies of heat waves were conducted developed at regional or local scale. Some of the studies focus on the impacts and response to heat waves and some of the studies focus on the cause of the heat waves. In a recent research one, carried out by Sfica et al., 2017 were analyzed the synoptic conditions which generate heat waves and warm spells in Romania. The authors found two major conditions responsible of the heat waves, one being radiative type, respectively advective type. Another study focus on some of the important indices of the heat waves in Romania, such as amplitude, magnitude, number of events, duration and frequency which shows that most of the indices have statistically significant increasing trends (Croitoru et al., 2016).

For instance, in Romania the results of certain studies indicated changes in the extremes air temperature, pointing out their correlation with changes of large-scale circulation patterns. The connection between heat waves and large-scale circulation in southeastern Europe was investigated by Spinoni et al., 2010; Georgescu et al., 2013.

[1]*Alexandru Ioan Cuza University, 700505 Iasi, Romania*
[2]*Université de Lorraine, Laboratoire LOTERR-EA7304, 57045 Metz Cedex 01, France, roxana.bocancea@univ-lorraine.fr*

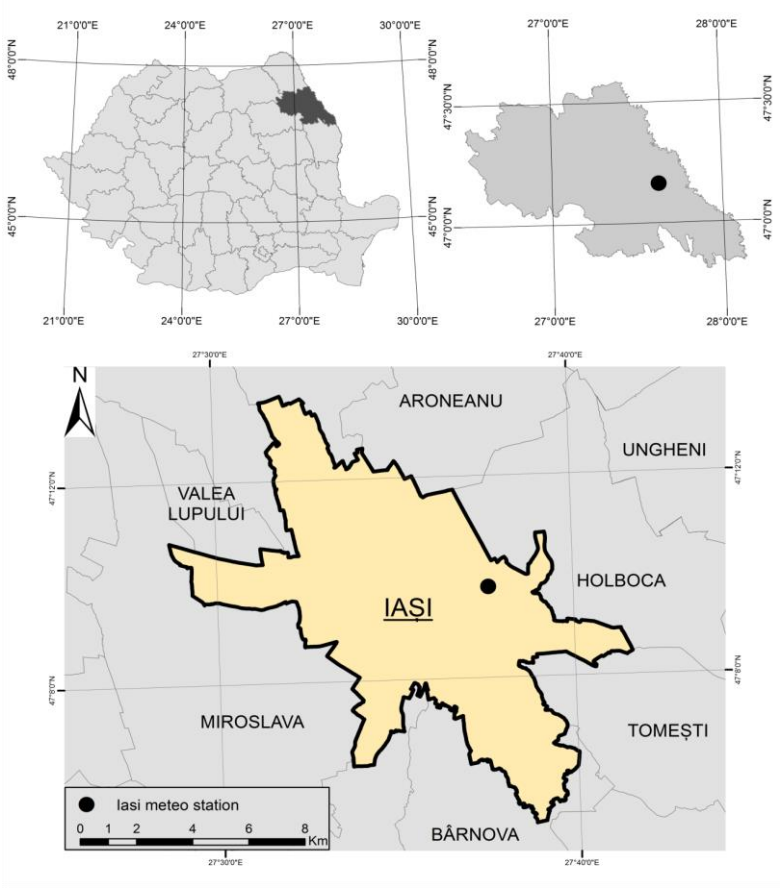

Fig 1. Location of the study area

The consequences of the heat waves are not always related to the hazard itself but also to the characteristics of the population in the affected areas. Therefore, are expected that heat waves will have more severe impact on vulnerable population groups as those with pre-existing health problems, socially isolated elderly people, homeless people, young children, people suffering from obesity and chronic diseases, also those with a low socio-economic status (Mattchies et al., 2008). The impacts of heat waves in Europe have increased the mortality in most of the main cities, due to the sensitivity of the population to high temperatures, as well as their ability to cope with heat exposure (Wilhelmi and Hayden, 2010). Most of the impact of a heat wave depends also on the frequency of high temperature over a longer time period, on the time of the year that they occur and also as an indirect consequence on the population are the influences of other phenomena such as slope instabilities and floods (IPCC, 2012). The most significant heat wave events that have affected European countries in the last decades being recorded within the EM-DAT database are listed in the **Table 1**.

Table 1.

The most significant heat waves events in Europe since 2003 (EM-DAT)

Most affected countries	Date	Number of victims
Russia	June 2010	55,736
Italy	July 2003	20,089
France	August 2003	19,490
Spain	August 2003	15,090
Germany	August 2003	9355
Portugal	August 2003	2696
France	July 2006	1388

2. DATA

For this study case we used the maximum daytime from Iasi weather station located in the urban area of Iasi municipality. The meteorological station used in this work reflects both urban and suburban conditions. The analysis is based on the maximum daytime air temperatures data series available for Iasi weather station in Romania, obtained from the ECA&D project database, which covers continuous measurements over a period of 55 years (1961-2016) (http://eca.knmi.nl/), and Meteomanz data base (http://www.meteomanz.com).

3. METHODOLOGY

Heat waves can be defined in various ways and detection methods. There are many definitions and some of them may be very ambiguous, but almost all of the definitions consider a threshold and a minimum number of consecutive days when the specific threshold is exceeded. One way to define heat waves is based on the concept of establishing specific thresholds by analyzing the persistence and frequency of heat waves. Another definition, of World Meteorological Organization is "when the daily maximum temperature in more than five consecutive days exceeds the average maximum number of consecutive days (larger than 5) during which the maximum temperature surpasses the average over 1961-1990 with at least 5 degrees.

In order to evaluate the heat waves risks, it's recommended to take into consideration both the probability of occurrence of the phenomenon and its consequences. However, because is very difficult to focus on the consequences because it requires a considerable amount of detailed data which are not available due to privacy and data protection reasons, in the current study case we aimed to detect and analyze the frequency and duration of the heat waves for the past decades in the metropolitan area of Iasi city, based on daily observation data over the period 1961 -2016 and to continues with another research in order to study the amplitude and magnitude.

For this study case we used the maximum daytime from Iasi weather station located in the urban area of Iasi municipality. The meteorological station used in this work reflects both urban and suburban conditions. Data processing was performed by the method of

percentiles, provided by Microsoft Excel software through the pre-defined functions PERCENTILE. We applied the method of 95th percentile as it allows detection of the heat waves all around the year and under each weather station without location and season problem (Perkins & Alexander, 2013; Croitoru, 2014).

In the first stage, the method involves choosing a benchmark, in our case 95th percentile, and placing percentile function, in the formula bar of the program, and highlighting the probability of occurrence of the phenomenon of 95%. The identification, of exceeded percentile was achieved by using a comparison function that indicates whether through one annual value was exceeded and zero if no value was exceeded. In the second stage using a macro command, the maximum temperature values were extracted for the exceed situations as percentile values. To study the frequency of massive heating phases were used only periods longer than three consecutive days witch exceed the percentile value.

Table 2.

Model to calculate the daily percentile

	1961	**1962**	**1963**	**1964**	**……**	**2015**	**2016**	**95th Percentile**
	Maximum temperature (OC)							
January, 1	3	2	-4	2	……	1	-6.1	7.77
January, 2	1.5	2.2	-1.2	-1.6	…..	5.9	-8.5	8.62
January, 3	6	2	-2.9	1.7	…..	6.1	-11.1	6.90
……..	……	……	…….	…….	…..	…….	……	……..
July, 1	24.6	24	32.4	17	…..	28.8	32.5	32.42
July, 2	28.4	24.1	27.8	18.9	…..	26.3	32.3	33.1
……..	……..	……..	……	……	…..	……	……..	…….
December, 29	1.2	-5.6	2.2	11	……	0.8	1.9	11.15
December, 30	2	5.5	1.5	6.5	……	-1	-0.3	12.12
December, 31	2.2	0.8	-1	1.6	……	-2.1	3.1	9.57

For the next stage, we created the frequency graphs through which evolution in time and space was highlighted. Below, is presented an example of a model of detecting heat waves (**Table 3**).

Table 3.

Model of detecting a heat wave based on the 95th percentile method at Iasi Weather Station

Data in the range	Maximum temperature	Test *	95th percentile value	Heat waves
14.07.2007	28,2	0	33,27	No
15.07.2007	30,9	0	33,97	No
16.7.2007	35,2	1	33,85	Yes
17.7.2007	37	1	34,95	Yes
18.7.2007	38,3	1	34,9	Yes
19.7.2007	39,8	1	34,87	Yes
20.7.2007	39,8	1	34,73	Yes
21.7.2007	39,7	1	33,82	Yes
22.7.2007	40,1	1	33,77	Yes
23.7.2007	34,3	1	33,88	Yes

4. RESULTS AND DISCUSSION

This type of analysis of daytime temperature data series recorded between 1961-2016 for Iasi weather station in Romania highlighted that during this time 1118 days with heat waves were found and a total of 98 heat waves of various lengths. The production of heat waves that exceed 10 days is exceptional. Such exceptions have a very low frequency of occurrence between 1961 and 2016. Regarding the duration of the heat waves, the most frequent are those between 3 and 5 days (**Fig. 2**). Those longer than three days are the most frequent, as expected and have a relative frequency of 41.7 %. They are followed by heat waves 4-days long (35.4 %), 5-days long (11.5 %) and 8-days long (5.2 %).

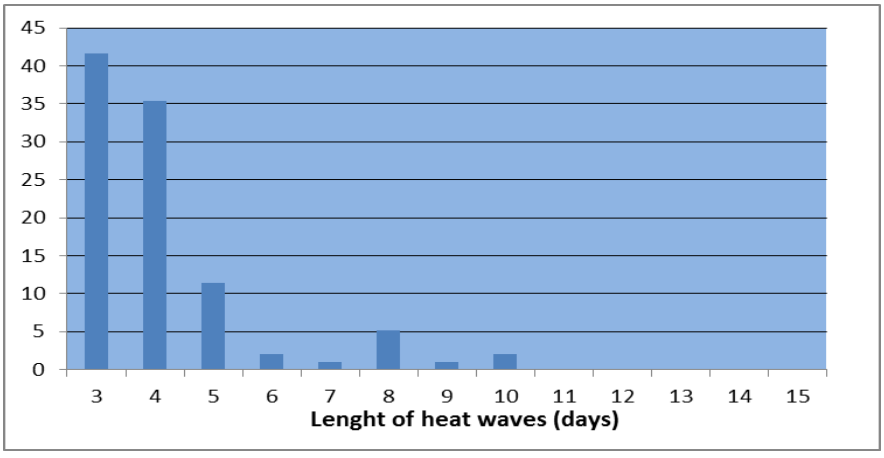

Fig. 2. Relative frequency (%) of heat waves period in Iasi (1961-2016)

The two longest intervals of heat waves were recorded both in 2007, between 20th and 29th of May and 16th and 25th of July, when the average of maximum temperature in Iasi was 32.79 °C and 37.82 °C (**Fig. 3** and **Fig. 4**).

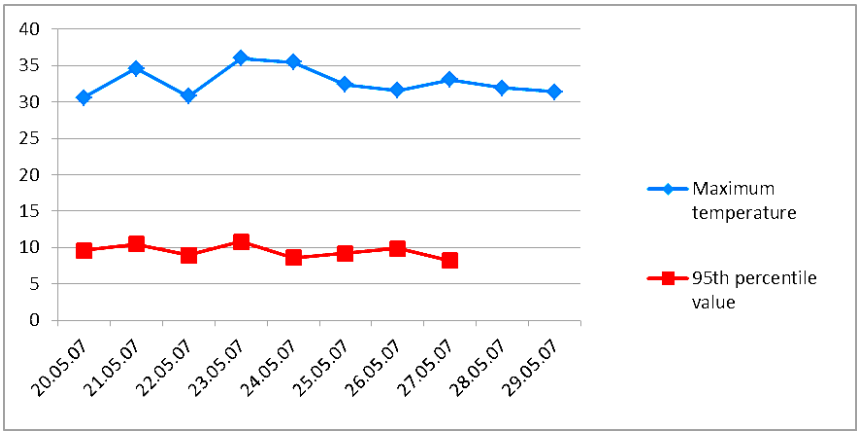

Fig. 3. Maximum temperature during one of the longest heat wave in Iasi, between 1961-2016

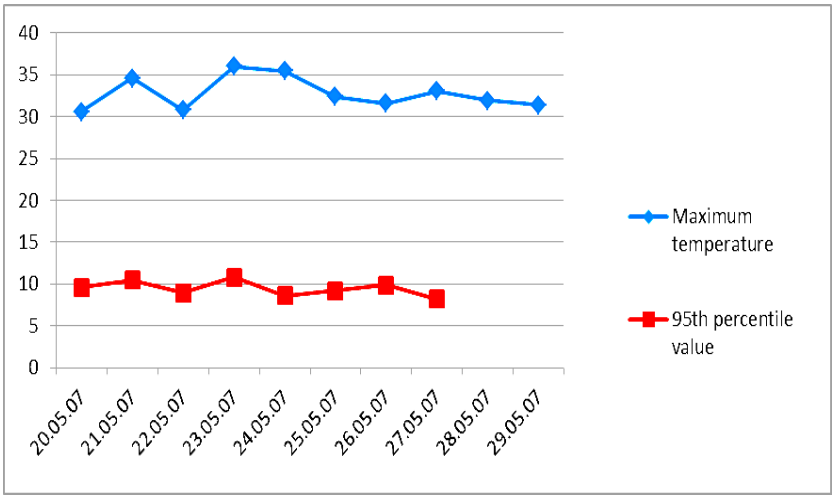

Fig. 4. Maximum temperature during one of the longest wave in Iasi, between 1961-2016.

Responsible for this is the severe heat wave which affected a large portion of Russia (western and central parts), as well the southeastern Europe during May, June-July (WMO, 2007). The maximum temperature measured during this interval was 36 °C and 40.1°C.

One of the most important idicators of the heat waves reprezents the annual evolution. The graph shows an significant increasing trend of heat waves (**Fig.5**). During the last decade the number of 6 heat waves occurred, summer being the season with the most frequent heat waves.

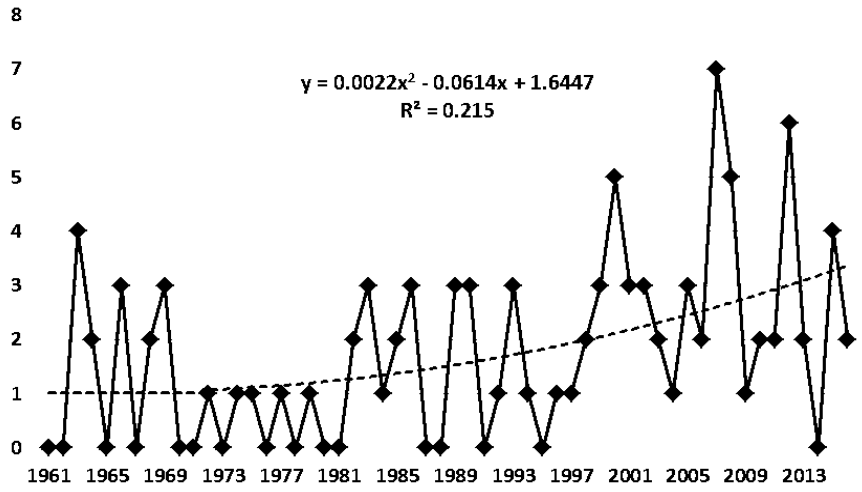

Fig. 5. The annual evolution of heat waves in Iasi municipality between 1961-2016

But the mere exploratory analysis of this series does not allow us to accept the growing parabolic trend just as easily. Even visually, there is a difference between growing and declining periods. That's why we applied the Haidu & Magyai-Saska (2009) method that make it possible to detect the sequential trend signal.

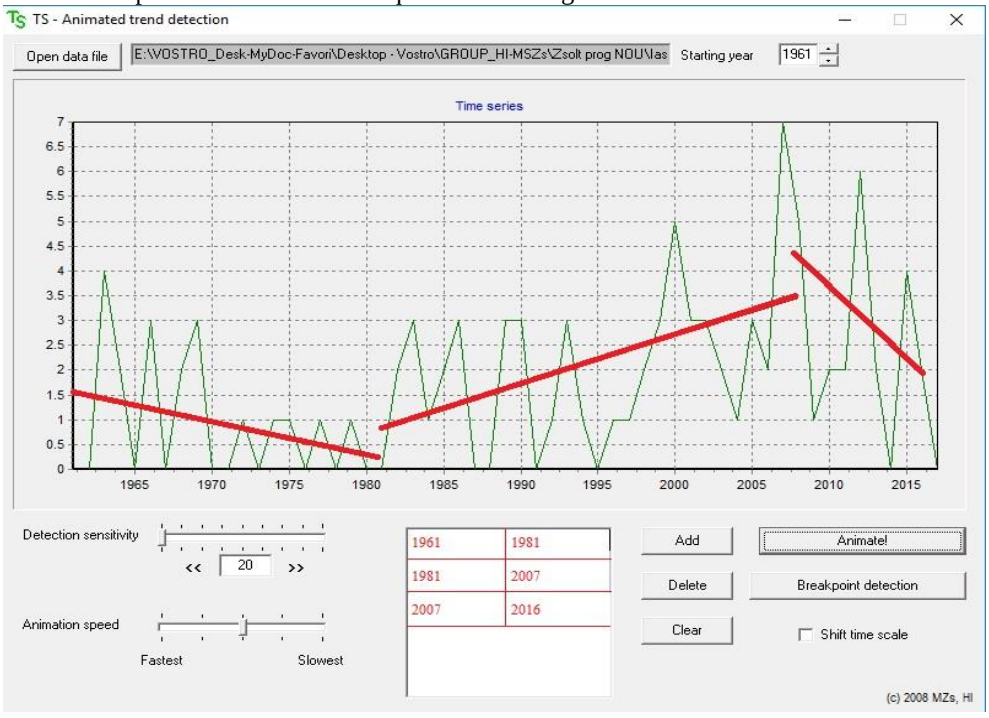

Fig. 6. Sequential trend signal detection (the method of Haidu & Magyari-Saska, 2009).

This investigation seems contrary to almost unanimous views of today that seek arguments of global warming but which actually support the idea of carefully examining the properties of time series (Haidu, 2016).

The result shows that the trend during 1961-2016 in Fig. 5, does not increase without limit, as would alarm the current theory of global climate change. The graph (**Fig. 6**) shows that after the year 2008 the number of annual waves tends to decrease, which does not, however, lead to the conclusion that in the future there could be no further increases or alternatives of opposite sequences.

Because our study has as its object the frequency analysis, obviously we need to call for more sophisticated methods suitable for the study of extremities. In hydrology, for example, the analysis of flash floods (the same several consecutive days of extreme values), can not be conceived without frequency analysis and probability computations (Győri et al., 2016). I have studied which of the specific statistical distributions for extreme data would be most suitable for the series of heat wave. Of course, we must first remove the global trend in order to achieve a residual stationary series. The processing of the time series, however, was not enough because the residual series had negative values. Therefore, we had to use a transformation of the residual series; the most suitable was the "absolute value" transform.

Good candidates were GEV, Gamma and Weibull, all three passed the χ^2 test. But the most appropriate, on the base of Bayesian information criterion and Akaike information criterion seems to be the Weibull distribution (**Fig. 7**).

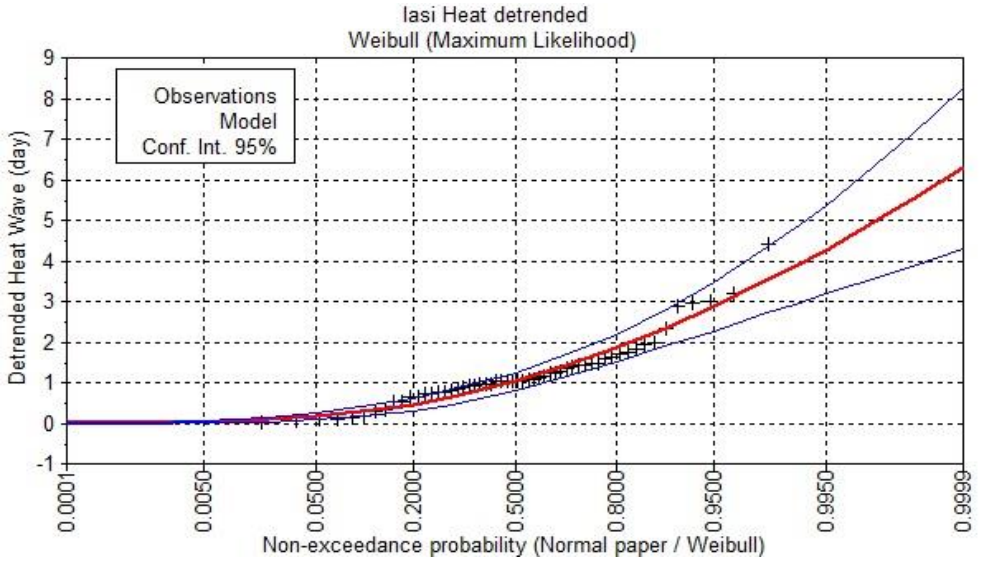

In this case, for a return period T = 100 the quintile XT = 3.87 days and for T = 1000, XT = 5.14. It should be noted that the above results are specific for the residual series, ie no global trend. In the hypothesis that the global trend remains in the future, we should add another 3 days to the results, and the consequences would be: XT_{100} = 7 days of heat wave, XT_{1000} = 8 days of heat wave. And if the global trend persists for the next decade then, around the year 2025, the crisis it would be even bigger because the results would have to be added for 1.5-2 days.

6. CONCLUSIONS

In our study changes in heat waves were analyzed over a period of 56-year (1961 2017). We have applied percentile-based method (95^{th}) on an amount of data and were calculated for each day of the year, from 1^{st} of December to 31^{st} of December. Based on our analysis we can conclude that most the most frequent heat waves are those lasting 3 and 4 days, but regarding the duration, the longest heat waves were considered during the summer of 2007, lasting 10 days, at Iasi meteorological station. From the first decade of the XXI century we can notice an increase in the annual frequency of the heat waves, due to the global warming and climate change.

As a consequence of increasing heat waves phenomena are the negative impact on economic activity, human health, the ecosystems, and infrastructure which put us in the situation to implement different strategies and emergency plans to reduce the impact. We consider that in the study must be done in the future, at a larger scale and vulnerability of different sectors must be studied, and also an amount of different variable of heat waves as magnitude and amplitude in order to conclude the real causes and impact.

REFERENCES

Bassil, K., D. C. Cole, K. Smoyer-Tomic, and M. Callaghan. 2007. *What is the Evidence on Applicability and Effectiveness of Public Health Interventions in Reducing Morbidity and Mortality during Heat Episodes?* Vancouver, BC: National Collaborating Centre for Environmental Health.

Croitoru, A.-E. (2014) Heat waves. Concept, definition and methods used to detect. *Riscuri și Catastrofe*, 15(2), 25–32.

Croitoru, A.-E.; Piticar, A.; Ciupertea, A.F.; Roșca, C.F. (2016) Changes in heat waves indices in Romania over the period 1961–2015. *Glob. Planet. Change*, *146*, 109–121

ECA&D, http://eca.knmi.nl/

Georgescu F., Andrei S., Stefan S., Stefanescu V., Barbu N. (2013) Heat waves in south-eastern Europe – identification of synoptic patterns using COST733 Catalogues. *Geophysical Research Abstract*, **15**:EGU2013-11834.

Győri M-M., Haidu I., Humbert J., (2016) *Deriving the floodplain in rural areas for high exceedance probability having limited data source*. Environmental Engineering and Management Journal, 15, (8), 1879-1887.

Haidu I., Magyari-Saska Z. (2009) *Animated Sequential Trend Signal Detection in Finite Samples*. Proceedings of the ITI 2009 31st Int. Conf. on Information Technology Interfaces, June 22-25, 2009, Cavtat, Croatia. Edited by: LuzarStiffler, V; Jarec, I; Bekic, Z. 249-254.

Haidu, I. (2016). What Is Technical Geography. *Geographia Technica*, 11(1), 1-5. DOI: 10.21163/GT_2016.111.01

Knowlton, K., M. Rotkin-Ellman, G. King, H. G. Margolis, D. Smith, G. Solomon, R. Trent, and P. English (2009), The 2006 California heat wave: Impacts on hospitalizations and emergency department visits. *Environ. Health Perspect*., 117, 61–67.

Meteomanz, http://www.meteomanz.com

Perkins, S.E., Alexander, L.V., 2013. On the measurement of heat waves. *J. Clim*. 26, 4500–4517. http://dx.doi.org/10.1175/JCLI-D-12-00383.1.

Sfîcă L., Croitoru A-E., Iordache I., Ciupertea A-F. (2017) Synoptic Conditions Generating Heat Waves and Warm Spells in Romania. Atmosphere, 8, 50; doi:10.3390/atmos8030050.

Spinoni, J.; Lakatos, M.; Szentimrey, T.; Bihari, Z.; Szalai, S.; Vogt, J.; Antofie, T. (2015) Heat and cold waves trends in Carpathian Region from 1961 to 2010. *Int. J. Climatol*, 35, 4197–4209.

Smoyer-Tomic K.S., Kuhn R., Hudson A. (2003) Heat Wave Hazards: An Overview of Heat Wave Impacts in Canada. *Natural Hazards*, 28(2-3), 463–485.

Wilhelmi O.V., Hayden M.H. (2010) Connecting people and place: a new framework for reducing urban vulnerability to extreme heat. Environ. Res. Lett. 5, DOI: 10.1088/1748-9326/5/1/014021.

MULTIRESOLUTION ANALYSIS IN THE VISIBLE SPECTRUM OF LANDSAT-TM IMAGES THROUGH WAVELET TRANSFORM

Marilyn CEPEDA [1], Iván PALACIOS [1], Alfonso TIERRA [2], Eduardo KIRBY [2]

DOI: 10.21163/GT_2018.131.03

ABSTRACT:
Multispectral satellite images are tools that allow the analysis of phenomena developed on the Earth's surface without being in contact. It is a raster model so it is possible to decompose it into a digital signal. There is a certain data that presents alterations (noise) due to errors caused by the sensors, atmospheric conditions, among others. Such examples affect its use and its derived products. Satellite images by their nature present difficulty in their processing and handling due to the considerable weight they have; whose problem justified the present work. The objective is to minimize white noise and to compress the image with the least possible loss of information through the Multiresolution Analysis (MRA) technique and Wavelet transformation. The images worked belong to the National Recreation Area "El Boliche" (Ecuador) that is next to the Cotopaxi volcano. Through a standard deviation evaluation of the obtained wavelet coefficients, the order of the "Discrete Wavelet Transform" (DWT) was established in the Daubechies (db) and Haar families. With db3 level 4, obtained a compression of 11.268% in respect to the original weight and with Haar level 4 11.288% as the best results. The wavelet db is more effective than the Haar type for the treatment of multispectral satellite images in the elimination of white noise and compression by means of the MRA, with a reconstruction of the signal without loss of information due to the type of wavelet used, which is evidenced in the image.
Key-words: *wavelets, MRA, satellite image, noise, compression.*

1. INTRODUCTION

Satellite technologies depend on using electromagnetic energy and its products such as satellite images or Global Positioning Systems depend on the wavelengths which are not equally effective for all remote sensing applications (González, 2014; Eastman, 2001; Tierra, 2016; Haidu, 2016). The images are captured by sensors; however, often present some type of distortion or redundancy in the data known. This distortion is known as noise which is stochastic variations that "contaminate an image" (Villegas, Puetamán & Salazar, 2007). Noise is produced by factors such as: atmospheric effects (selective and non-selective dispersion) and by the blur of the sensor, which limits its use (Fournier et al., 1997; Ergen, 2012). According to Miano (1999), and Chambolle et al., (1998) elimination of noise, as well as the compression of images are required to digital signals because problems related to information use and processing.

The wavelet is a technique used in the last decades for noise elimination and images compression. Wavelet has been used in different fields such as in medicine (Dalmiya et al., 2012; Weaver et al., 1991; Paz, 2001), in geology (Mohan & Poobal, 2017), natural

[1] *Ingeniería Geográfica y del Medio Ambiente. Universidad de las Fuerzas Armadas ESPE, Av. Gral Rumiñahui. Sangolquí, Ecuador, mvcepeda1@espe.edu.ec; ifpalacios@espe.edu.ec*
[2] *Grupo Geoespacial. Universidad de las Fuerzas Armadas ESPE, Av. Gral Rumiñahui Sangolquí, Ecuador, artierra@espe.edu.ec; epkirby@espe.edu.ec*

sciences (Rathinasamy et al., 2017; Bachour et al., 2016) and especially with remote sensors (Pipitone et al., 2018; Ansari & Buddhhiraju, 2016; Dheepa & Sukumaran, 2014), among others.

The wavelet technique analyzes image's content in each pixel decomposing the original signal into different scales with different levels of resolution (Eregen, 2012). Each level of resolution carries required information to reconstruct the original signal to the next level (Ballesteros, Renza & Rincon, 2015). In order to use the Multiresolution Analysis (MRA) we studied mathematical models as a function of signals behavior to reduce non-essential data from the original signal. The wavelet transform allows images processing of with reduced white noise and compression of information (Chambolle et al., 2015).

The objective of this study was to eliminate the white noise and compress a Landsat TM satellite image through the MRA technique and wavelet transform with a comparison between Haar and Daubechies (db) as an alternative for the use of images noise free and storage facility.

2. METHODS

2.1 Landsat TM multispectral images

Landsat TM is a multispectral scanning sensor created to obtain higher image resolution, its data are sensed in seven spectral bands (**Table 1**). When these bands are combined, they produce a range of tonalities and interpretations which greatly increase their applications. Depending on the satellite and the sensor, panchromatic and thermal multispectral channels can be included (NASA, 2017).

Table 1.

Characteristics of the Landsat TM sensor

TM Technical Specifications	
Spatial Resolution	30 meters
Spectral Range	0.45 – 12.5 µm
Number of Bands	7
Temporal Resolution	16 days
Image Size	185 km x 172 km

2.2 Noise

It is a defect of unwanted information due to data stochasticity which contaminates or degrades its use (Márquez, 2012). In the specific case of images, generally it represents the isolated pixels that take values other than the "real" ones. There are several types of noise in the treatment of signals such as: Gaussian or white that has reserved to the amplitude distribution with a function of normal probabilistic density, Brownian that has a maximum autocorrelation with increasing frequency and Flicker that decreases each time which doubles the frequency (Márquez, 2012). A recorded signal with corrupted noise can be represented as;

$$g(x,y) = f(x,y) + n(x,y) \quad (1)$$

Where $g(x,y)$ is the result of the original image distortion $f(x,y)$ by additive Gaussian noise $n(x,y)$.

The impulsive or Brownian is generated by digital (or even analog) transmission. It can be modeled as:

$$g(x,y) = (1-p) * f(x,y) + p * i(x,y) \quad (2)$$

Where $i(x,y)$ is the impulsive noise and p belongs to {0, 1}. The multiplicative or Flicker presents a granular appearance in the radar and ultrasound images. It is represented as:

$$g(x,y) = f(x,y) * m(x,y) \quad (3)$$

Where $m(x,y)$ is the multiplicative noise.

The present study focuses on the Gaussian noise which is usually produced by the sensor electronic components (Ballesteros, Renza & Rincon, 2015). The energy spectrum is constant for all frequencies, affects the entire image and the intensity of all pixels is altered and discontinuous (Villegas, Puetamán & Salazar, 2007). The final value of the pixel is the real value plus a certain amount of error. This can be described as a Gaussian variable following a normal distribution (Acevedo, 2011).

2.3 Wavelet transform

A Wavelet is a small wave whose energy is concentrated in time, its characteristic waveform is oscillating with a rapid attenuation that allows it to make analysis in time and frequency (Nieto & Orozco, 2008; Ballesteros, Renza & Rincon, 2015). It is based on the representation of a function in terms of a biparametric family of dilations and translations of a fixed function ψ, the mother wavelet is not sinusoidal, and it is represented as:

$$WT\big(f(x)\big) = f(x) * \Psi(x) = \frac{1}{a}\int_{-\infty}^{+\infty} f(t)\Psi\left(\frac{x-t}{a}\right)dt \quad (4)$$

Where "a" is the scale factor (dilation), "t" is the time (translation) and "x" is the position. The function ψ is called "mother wavelet"; first, wavelet because it is of an oscillating nature and of finite duration (compact support) and it is called mother for serving as the basis for the generation of the remaining window functions (Ballesteros, Renza & Rincon, 2015)

2.4 Discrete wavelet transform in 2D

The Multiresolution Analysis (MRA) method was used to calculate scaling coefficients of the wavelet transform. The data analyzed in the DWT are discrete and not stationary, therefore a methodology that manages to discretize the signals at specific levels is required. Mallat in 1988 proposed an algorithm based on sequence filters to obtain the wavelet transform instantaneously, which was called Mallat tree or decomposition wavelet tree (Mallat, 1989).

The MRA analyzes the content of images at different scales (resolutions) and at each level of resolution. MRA approach and detail signals carry all the information required to reconstruct the signal at the next level (Cadena & Cadena, 2016; Mallat, 1989). The wavelet coefficients calculation to reconstruction the signal should be performed quickly (Ballesteros, Renza & Rincon, 2015). High-pass and low-pass filters, which change the signal resolution, are used with high and low frequency components (Villegas, Puetamán & Salazar, 2007). The scale is changed through upsampling and downsampling (Daubechies,

1992). The MRA main feature is the ability to separate a signal into many components at different scales (resolutions) (Daubechies, 1992). The Haar system is not very appropriate to approximate soft functions, in fact any approximation of Haar is a discontinuous function (Villegas, Puetamán & Salazar, 2007).

The **Fig.1** shows how the DWT in each step (low and high) divides the image and continues to the next level with a new step and subdivides the signal to meet the level of discretization, which is assigned to the transformation. The result is to obtain the wavelet and scale coefficients in this case it is a level 3 discretization:

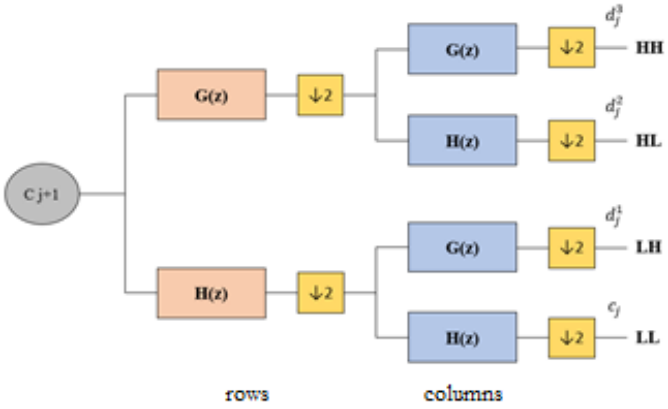

Fig. 1. Decomposition Wavelet tree of images.

Where dj are wavelet coefficients, cj are scaling coefficients that together reconstruct the original signal passing through the high pass filters G(z) and low pass H(z) (Pérez et al., 2002). The increase in number of samples (↑2) is called upsampling and the downsampling (↓2) removes samples of the signal, thus reducing the sample rate (Kingsbury, 2001; González, 2014; Mancero et al., 2017). The letters HH, HL, LH, LL, represent the filters high – high, high – low, low – high and low – low respectively.

For the selection of a wavelet type, following properties must be considered (Fournier et al., 1997):

Table 2.

Properties that must be considered for the selection of the wavelet

Properties	
Compact support	Filters must be FIR (finite impulse response), which are a type of digital filters whose response to a pulse input signal will have a finite number of non-zero terms.
Rational coefficients	It avoids floating-point operations
Smoothness	If the wavelet is not smooth, the error will be easy to detect visually
Length of filters	Preferably short filters. It is related to softness.

The filters that meet the condition are known as Quadrature Mirror Filters (QMF) González, 2014; Gómez et al., 2013). In multispectral images, the correlations between the bands are considerable, so this technique seeks to reduce spectral, spatial correlation and allow high compression radius (Ballesteros, Renza & Rincon, 2015). One step produces 4 subpictures or subbands, one is the approximation of the image, and the other 3 capture the vertical, horizontal and diagonal details of the image (Acevedo, 2011). **Figure 2** shows the larger sub-bands V1, H1 and D1 which capture the vertical, horizontal and diagonal details on the finer scale, these types of filters are known as Sobel, Roberts, Prewitt filters respectively (Shrivakshan & Chandrasekar, 2012). The sub-bands V2, H2 and D2 belong to the second fine scale. An approximation of the reconstructed image is the LL band in the upper left corner (Acevedo, 2011).

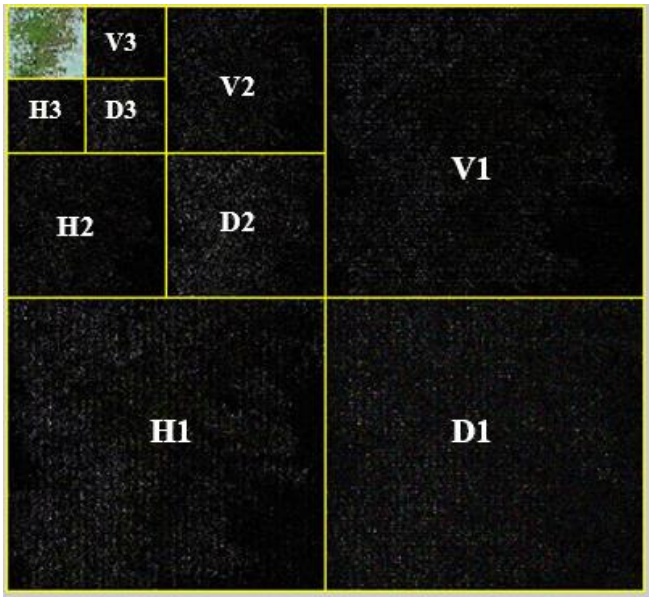

Fig. 2. Discretization of the image.

3. METHODOLOGY

The Landsat TM image of the National Recreation Area "El Boliche" - Ecuador was obtained from the official USGS (U.S. Geological Survey) website free of charge. The bands of the visible spectrum red, green and blue (RGB). Bands were separated and analyzed each one using the data and graphs obtained. Up to this moment, Haar approach is widely used in treatment of images as shown in the works of Talukder & Harada (2007), Porwik & Lisowska (2004), Raviraj & Sanavullah (2007) and Lai & Kuo (2000). In addition, the compression of information is lossy, while with another type of wavelet as db is lossless. For this reason, we decided to compare the results between the two approaches. Throughout an exploratory study of wavelet coefficients standard deviation of the image filtering which were obtained in the MATLAB wavelet toolbox package. Subsequently, the order of the wavelet and its level of discretization were determined according to the variation standard deviation in each level (**Table 3**). The optimal discretization level was

order 4 but 2, 3, 5 and 6 orders were worked with discretization levels 2, 3 and 4 for a better appreciation of results.

Table 3.

Standard deviation values for each wavelet order and their levels

Wavelet Type	Discretization Level	Standard deviation of the coefficients of the transform
db2	2	2.163
	3	2.350
	4	2.398
db3	2	2.118
	3	2.307
	4	2.356
db4	2	2.105
	3	2.297
	4	2.346
db5	2	2.103
	3	2.297
	4	2.346
db6	2	2.105
	3	2.298
	4	2.347

From the MRA, image filtering was performed with db and Haar wavelets for noise reduction, the statistics and percentage of energy retained were obtained. In the same way, the image was compressed with both wavelets. Once obtained the filtration and compression of the image, we proceeded to program an algorithm in the MATLAB software to graph the reconstructed signal in each band of the image. The best results were established for the elimination and compression.

4. RESULTS AND DISCUSSION

There is presence of noise in the Landsat TM images, determined by the visual analysis of the peaks in the signal expressed in digital levels values of each of the three bands of the visible spectrum (RGB). From the results of **Table 3**, it was determined that the standard deviation of the wavelet coefficients does not vary significantly from level 4, for this reason this level was chosen as the basis for the elimination and compression of the two wavelet families studied.

4.1 Noise filtering

The values of the wavelet coefficients were determined for db4, db3 and Haar with level of discretization 4 after filtering the image. The signal with db had a better reconstruction, due to the proximity to the original value of the frequency of the image in

the red and blue bands, unlike the green band that obtained a better approximation with Haar (**Table 4, 5 and 6**).

Table 4.

Comparison of frequency values in the red band

Red Band		
Filtered	**Digital level**	**Frequency value (Hz)**
db3_4	85	2.370E+05
db4_4		2.366E+05
haar_4		2.367E+05
Original image		2.320E+05

Table 5.

Comparison of frequency values in the green band

Green Band		
Filtered	**Digital level**	**Frequency value (Hz)**
db3_4	189	1.766E+05
db4_4		1.771E+05
haar_4		1.788E+05
Original image		1.781E+05

Table 6.

Comparison of frequency values in the blue band

Blue Band		
Filtered	**Digital level**	**Frequency value (Hz)**
db3_4	85	5.623E+05
db4_4		5.632E+05
haar_4		5.405E+05
Original image		5.840E+05

This is shown in signal obtained representation for each band in **Fig. 3, 4 and 5**, in which the 3 bands are represented separately with their frequency value and the digital level, where the noise removal is visually observed but also a notion of the loss of information that is obviously greater in Haar 4.

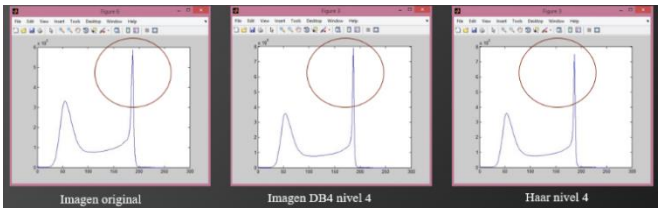

Fig. 3. Reconstructed signal of the blue band

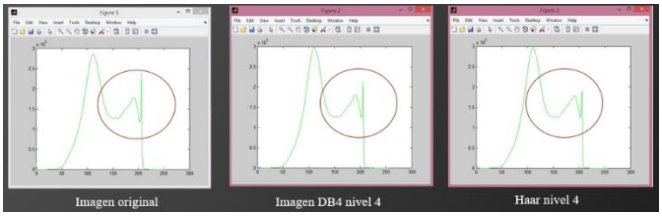

Fig. 4. Reconstructed signal of the green band

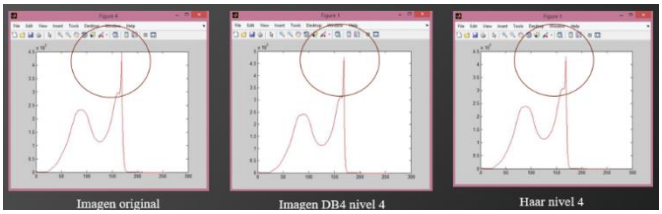

Fig. 5. Reconstructed signal of the red band

4.2 Compression

The maximum compressions were: Haar level 4 with 11,288% and db3 level of discretization 4 with 11,286% respect to the original weight. The compression had a minimum difference of 0.002% between Haar and db transforms. The percentage of energy retained for Haar 4 was 99.31% and for db3 level 4 it was 99.41%, which showed a better reconstruction of the image with the last transform. The filtered and compressed image with db3 discretization level 4 presented better spatial resolution than the image treated with Haar 4, because it had higher percentage of energy retained as evidenced in **Fig. 6**.

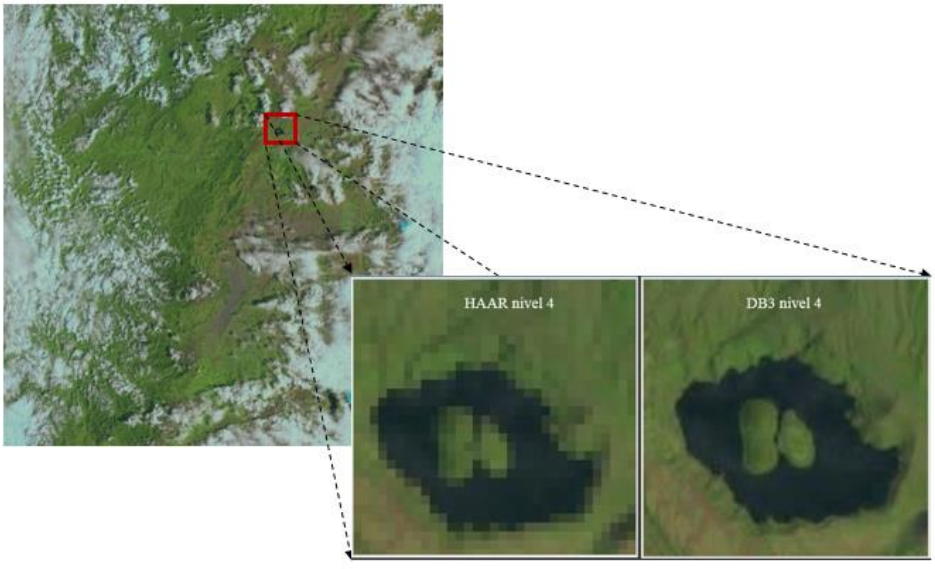

Fig. 6. Visual comparison between filtered and compressed images with Haar 4 and db3 level 4.

5. CONCLUSIONS

The level of discretization 4 was chosen as a basis for filtering and compression because from this level the standard deviation of the coefficients of the transform remained constant with respect to higher levels of discretization. The Landsat-TM images of the area of the National Recreation Area "El Boliche" - Ecuador, presented noise, evidenced visually in the "peaks" of the signals of the RGB spectral bands, which were diminished after the application of the transforms. The best result was obtained with db3 level of discretization 4, for noise filtering due to having a greater percentage of retained energy and for compression to be reduced by 11.286% in weight with respect to the original image without loss of information. The highest compression was with Haar 4 with 11.288% (minimum difference of 0.002% between Haar and db3 level 4), however, the spatial resolution with the Haar wavelet is low compared to the results with db3 level 4. The filtering and compression with db3 discretization level 4 is better for use in remote sensors, for conserving a radiometric resolution similar to the original and good spatial resolution.

R E F E R E N C E S

Ansari, R.A. & Buddhiraju, K.M. (2015). k-means based hybrid wavelet and curvelet transform approach for denoising of remotely sensed images. *Remote Sensing Letters*, 6(12), 982–991.

Ansari, R.A. & Buddhiraju, K.M. (2016). A Comparative Evaluation of Denoising of Remotely Sensed Images Using Wavelet, Curvelet and Contourlet Transforms. *Journal of the Indian Society of Remote Sensing*, 44(6), 843–853.

Bachour, R., Maslova, I., Ticlavilca, A.M., Walker, W.R. & McKee, M. (2016). Wavelet-multivariate relevance vector machine hybrid model for forecasting daily evapotranspiration. *Stochastic Environmental Research and Risk Assessment*, 30(1), 103–117.

Ballesteros, D.M., Renza, D. & Rincon, R. (2015). Gray-scale Images within Color Images using Similarity Histogram-Based Selection and Replacement Algorithm. *Journal Of Information Hiding And Multimedia Signal Processing*, 6, 1156–1166

Cadena, L. & Cadena, F. (2016). Análisis multiresolución en el procesamiento de imágenes satelitales. *Revista GEOESPACIAL*, 115–126.

Chambolle, A., De Vore, R.A., Lee, N.Y. & Lucier, B.J. (1998). Nonlinear wavelet image processing: variational problems, compression, and noise removal through wavelet shrinkage. *IEEE Transactions on Image Processing*, 7(3), 319–335.

Dalmiya, S., Dasgupta, A. & Kanti Datta, S. (2012). Application of Wavelet based K-means Algorithm in Mammogram Segmentation. *International Journal of Computer Applications*, 52(15), 15–19.

Daubechies, I. (1992). *Ten Lectures on Wavelets*, (1st ed.*)*. CBMC-NSF Regional Conference Series in Applied Mathematics, 254–257.

Dheepa, G. & Sukumaran, S. (2014). Hybrid Fusion Technique Using Dual Tree Complex Wavelet Transform for Satellite Remote Sensor Images. *International Review on Computers and Software (IRECOS)*, 9(9), 1560–1567.

Eastman, J.R. (2001). Idrisi 32 Release 2: Guide to GIS and Image Processing, Volume 1. Clark Labs: Worcester, MA, USA.

Ergen, B. (2012). Signal and Image Denoising Using Waveñet Transform. In: Baleanu, D. (Ed.) Advances in wavelet Theory and Their Appplications in Engineeering, Physics and Technooogy, InTech Europe, Rijeka, Croatia. Pp. 495-514.

Fournier, N., Castro, G., Russo, C., & Bria, O. (1997). Compresión de Imágenes fijas utilizando la Trasformada Wavelet. *Congreso Argentino de Ciencias de la Compuntación CACIC* 97, Universidad Nacional de La Plata, Argentina.

Gómez, E., Silva, E., Silva, D., & Aponte, G. (2013). Selection of a mother wavelet for frequency analysis of transient electrical signals using WPD. *Revista chilena de ingeniería*, 2, 262–270.

González, J. (2014). *Transformadas Wavelet impacto fundamental en procesamiento de señales y compresión de imágenes.* Master's Thesis, Technological University of Pereira, Colombia.

Haidu, I. (2016). What Is Technical Geography. *Geographia Technica,* 11(1), 1-5. DOI: 10.21163/GT_2016.111.01

Kingsbury, N. (2001). Complex wavelets for shift invariant analysis and filtering of signals. *Appl. Comput. Harmon. Anal*., 10(3), 234–253.

Lai, Y.K. & Kuo, C.J. (2000). A Haar Wavelet Approach to Compressed Image Quality Measurement. *Journal of Visual Communication and Image Representation*, 11(1), 17–40.

Mallat, S. (1989). A theory for multi-resolution signal decomposition: The wavelet representation. *IEEE Transaction on Pattern Analysis and Machine Intelligence*, 7, 674–693.

Mancero, H., Morales, B., Tierra, A. (2017). Estimación Del Coeficiente De Hurst De Las Series Temporales De Tráfico Vehicular En Zonas Urbanas Por Rango_Reescalado. *Revista Geoespacial*, 14(1), 103-120.

Márquez, J. (2012). *Ruido en datos, señales, imágenes*. [Online] Available from www.academicos.ccadet.unam.mx/jorge.marquez/cursos/imagenes_neurobiomed/Ruido.pdf [Accessed October 2017].

Miano, J. (1999). Compressed Image File Formats: JPEG, PNG, GIF, XBM, BMP. *Addison - Wesley*, 112–113.

Mohan, A. & Poobal, S. (2017). Crack detection using image processing: A critical review and analysis. *Alexandria Engineering Journal*, 1–12.

NASA (2017) National Aeronautics and Space Administration. [Online] Avaible from www.landsat.gsfc.nasa.gov/landsat-5-2/ [Accessed March 2017].

Nieto, N. & Orozco, D. (2008). The use of the discrete Wavelet transform in the reconstruction of sinusoidal signals. *Scientia et Technica Año XIV*, 38, 381–387.

Paz, J.E. (2001). Disminución del nivel de ruido en imágenes de Resonancia Magnética usando la Transformada Wavelet. La Habana, Cuba: *Memorias II Congreso Latinoamericano de Ingeniería Biomédica.*

Pérez A, La Mura, G., Piotrkowski, R. & Serrano, E. (2002). Procesamiento No Lineal con Wavelet para la Eliminación del Ruido en Imágenes Planares de medicina nuclear. *Revista Española de Medicina Nuclear*, 1, 15–21.

Pipitone, C., Maltese, A., Dardanelli, G., Lo Brutto, M. & La Loggia, G. (2018). Monitoring Water Surface and Level of a Reservoir Using Different Remote Sensing Approaches and Comparison with Dam Displacements Evaluated via GNSS. *Remote Sensing*, 10(71), 1–24.

Porwik, P. & Lisowska, A. (2004). The Haar–Wavelet Transform in Digital Image Processing: Its Status and Achievements. *Machine GRAPHICS & VISION*, 13(1,2), 79–98.

Rathinasamy, M., Bindhu, V.M., Adamowski, J., Narasimhan, B. & Khosa, R. (2017). Investigation of the scaling characteristics of LANDSAT temperature and vegetation data: a wavelet-based approach. *International Journal of Biometeorology*, 61(10), 1709–1721

Raviraj, P. & Sanavullah, M.Y. (2007). The Modified 2D-Haar Wavelet Transformation in Image Compression. *Middle-East Journal of Scientific Research*, 2(2), 73–78.

Shrivakshan, G.T. & Chandrasekar, C. (2012). A Comparison of various Edge Detection Techniques used in Image Processing. *IJCSI International Journal of Computer Science*, 9(5), 269–276.

Talukder, K.H. & Harada, K. (2007). Haar Wavelet Based Approach for Image Compression and Quality Assessment of Compressed Image. *IAENG International Journal of Applied Mathematics*, 36(1), 1–8.

Tierra, A. (2016). Nonlinear And Discontinuities Modeling Of Time Series Using Artificial Neural Network With Radial Basis Function. *Geographia Technica,* 11(2), 102-112. DOI: 10.21163/GT_2016.112.10

Villegas, J., Puetamán, G., & Salazar, H. (2007). Modelo de error en imágenes comprimidas con wavelets. *Revista de Ingeniería y Ciencias*, 3, 111–133.

Weaver, J.B., Xu,Y., Healy, D.M. & Cromwell, L.D. (1991). Filtering noise from images with wavelet transforms. *Magnetic Resonance in Medicine*, 21(2), 288–295.

THE CREATIVITY INDEX GROWTH RATE IN THE CZECH REPUBLIC: A SPATIAL APPROACH

Markéta CHALOUPKOVÁ[1], Josef KUNC[1], Zdeněk DVOŘÁK[1]

DOI: 10.21163/GT_2018.131.04

ABSTRACT:
The presented paper analyses the development of conditions for the development of a creative economy in the regions of the Czech Republic. Through the calculations of a number of sub-indicators in the area of talent, technology and tolerance (Florida´s 3T model), the development of the Creativity Index in 2011-2015 has been mapped in individual regions. In the next phase the development of the average growth rate of the Creativity Index was evaluated and graphically illustrated. At the end of the research, a situational and trending matrix of creativity was compiled, dividing the regions into four quadrants (leaders, up and coming, laggards, and losing ground). The results showed the dominant position of the capital city of Prague, which reached the highest score throughout the whole period and with great precedence surpassed all other regions. Only the South Moravian Region surpassed Prague in a specific way, in the value of the R & D indicator. In this region lies the second largest city of the Czech Republic in Brno, which has a very strong position in the field of research, development and innovation. The situational matrix captured the situation in which the leader's quadrant was only Prague, while the other regions were growing in the region quadrant. On the contrary, the trend matrix has suggested that Prague is losing its leading position as it is overtaken by the South Moravian region.

Key-words: *Creativity Index, 3T Model (Talent, Technology, Tolerance), Spatial Approach, Czech Republic*

1. INTRODUCTION

Since the end of the last century, the economies of developed countries (in the last decade and many transforming post-socialist countries) have undergone significant changes in connection with the growing importance of industries based on innovation, knowledge, information, digitization and creativity. There is a so-called knowledge-based economy, learning economy, creative economy, or digital economy (Lundvall & Johnson, 1994; OECD, 1996; Mackinnon & Cumbers, 2007; Veselá & Klimová, 2014; Carayannis et al., 2018). Most countries have great potential for developing a creative or knowledge-based economy that is based on its cultural, social and geographical context. Also, culture and, together with it, the so-called cultural and creative industries gain more and more attention as "engines of economic development", which are largely involved in creating prosperity and having a positive impact on the economy (Lampel & Germain, 2016; Liu, 2018). In the area of regional and urban development and planning, the cultural and creative industries are referred to as a new type of competitive advantage and source of innovation and competitiveness of companies, cities and regions (Bocella & Salerno, 2016).

[1] *Masaryk University, Faculty of Economics and Administration, 602 00 Brno, Czech Republic, marketa.chaloupkova@mail.muni.cz; kunc@econ.muni.cz; dvorak.zdenek@mail.muni.cz*

The term "cultural industry" was first used to criticize the commodification and unification of culture in 1944 by members of the Frankfurt School of Critical Theory by Theodor Adorn and Max Horkheimer in their book Dialectics of Enlightenment. During the 1960s and 1970s, the cultural industry was replaced by a plurality of cultural industries. Using a single number did not explain the complexity and diversity of the range of human activities that belong to this group (Hesmondhalgh, 2007). The boom of the cultural industries was largely related to the changes that society has undergone since the economic crisis of the 1970s. This is a period that is a typical shift from industrial to postindustrial, respectively information society, and based mainly on knowledge. Also, the production structure has changed significantly and industrial production has retreated to services. Consumers have begun to put much more pressure on modernization, quality, diversity and added value, a change that the culture sector has also had to react to (Power & Scott, 2004). The cultural sector has been seen as a potential means of economic development, especially in cities and metropolitan areas (Markusen et al., 2008).

European academics, urban planners and politicians began promoting the development of cultural sites and activities in the late 1980s as an appropriate way of revitalizing especially deprived post-industrial cities (Markusen et al., 2008). Investments in cultural industries were therefore included among local and regional development policy tools to regenerate cities and create job. (Selwood, 2006; Cikánek, 2013). Since the early 1990s, the growing influence of intangible corporate assets, particularly the value of brand names, has gained momentum. (Coyle, 1999). Social scientists from various disciplines (cultural studies, economics, sociology, or geography) have begun to emphasize the growing importance of culture, meaning, and symbols in the development of modern capitalism. (Leriche & Daviet, 2010).

The beginnings of the Creative Cities Concept are linked to the British Comedia Consultancy Group, which in the 1990s began to push the emphasis on incorporating art and culture into urban development strategies, which in turn will lead to economic growth that will depend on Creativity and Innovation in the 21st century (Hesmondhalgh, 2007). The idea of creative clusters draws on the theory of Michael Porter's industrial clusters, as local concentrations of interconnected companies and institutions in a particular field (Porter, 1990). Once cities and regions have had music festivals, galleries, or theatres, thanks to strategies for the development of culture and creativity, they have moved to the next stage of local development in which they have moved on to the creative class and those involved in the creative industries. (Florida, 2002; Hesmondhalgh, 2007; Cikánek, 2013).

At present, there is still no uniform view of the creative / cultural industries. Disagreements lie in the very designation of this area (cultural industries, creative industries, copyright industries and others) as well as in the definitions and enumerations of industries falling between the creative industries. Experts have gradually introduced and defined other key concepts such as creative cities (Landry, 2000; Scott, 2000), core creative arts a core creative industries (Throsby, 2001), patent and copyright industries (Howkins, 2001), creative class as a motor of urban regeneration (Florida, 2002), or model applications through the creativity index (Florida, 2002) and its modification of the creativity city index (Landry, 2011).

A number of newer works are not primarily theoretically and methodological, but they focus on case studies from selected cities and regions on creativity, smart and innovative practices in urban politics and planning, often geographic, spatial context (Rumpel et al., 2010; Angelidou, 2014; Tafel-Viia et al., 2015; Dörry, 2016). Spatial and planning studies

from rapidly growing Asian cities and metropolitan areas are also topical (Tang, 2016; Zhong, 2016; Fahmi et al., 2016 and many others).

Conditions for developing a creative economy at the state, region, or city level can be measured using different models and indexes. The above-mentioned Creativity Index is a new statistical indicator for the assessment and interpretation of the regions' growth determinants. The original Creativity Index was compiled by Florida (2002), using the 3T - talent, technology and tolerance model. This model was further expanded by other indicators within the next Euro-creativity index (Florida & Tinagli, 2004). The aim of our contribution is to analyse the development of conditions for the development of a creative economy in the regions of the Czech Republic by modifying and applying the 3T Model to the specifics of the Czech Republic, in particular by analysing the average rate of growth of the Creativity Index. To capture the development and the possibility of data interpretation, a five-year time period (2011-2015) was chosen.

2. METHODS AND DATA

In order to achieve the set goal, it was first necessary to calculate the overall Creativity Index. The methodology for calculating the overall Creativity index was inspired, in particular, by Florida (2002) and Kloudová (2009). The calculation of the index has been modified for research purposes in the Czech Republic. The overall index was calculated using six sub-indicators divided into three areas (talent, technology and tolerance).The data for the calculation of the individual indicators were mainly derived from the Czech Statistical Office, the Industrial Property Office of the Czech Republic, and the migration portal of the Ministry of the Interior. The calculation of these sub-indexes is shown in **Table 1** below.

Table 1.

Method of Creative index sub-indexes calculation.

Talent	**Human capital index (HCI)**	Ratio of population with university education in the region to the total population of the region
	Creative class index (CCI)	Ratio of creative professionals in the region to the total employment of the region
Technology	**Research and development index (R&D)**	Ratio of research and development spending to the GDP of the region
	Innovation index (INI)	Number of patent applications per inhabitant of the region
Tolerance	**Gay index (GI)**	Share of registered partnerships in the region on the total population of the region
	Immigration index (IMI)	The share of foreign migrants in the region on the total population of the region

Source: Florida (2002), edited

The aggregate Creativity index calculation was based on the average value of its sub-indexes. The order of individual regions was determined by the results of the Creativity index calculation. The values of the calculated indexes were converted to values between 0 and 1 using the standardized Min-Max method (OECD, 2008) for all regions of the Czech Republic, which allows to capture the distance between regions.

$$N_i = \frac{X_i - MIN(\forall_i X_i)}{MAX(\forall_i X_i) - MIN(\forall_i X_i)}$$

The calculation of the Creativity index was necessary for a follow-up analysis of the average growth rate of the Creativity index, which was calculated as the average growth coefficient multiplied by a hundred. The average growth coefficient for the time series (2011–2015) was calculated as the geometric average of the individual growth coefficients. The calculation of the average growth rate was therefore based on the following formula:

$$\bar{k} = \sqrt[n-1]{\prod_{t=2}^{n} k_t} = \sqrt[n-1]{\frac{y_n}{y_1}}$$

The average increment rate was calculated as the average increment coefficient multiplied by hundred. The average increment coefficient was calculated as the average growth rate minus one. The negative result of the measured indicator can be more precisely interpreted as a decrease. The final step of the Creativity index analysis was to build a situational and trend matrix of creativity (Creativity Matrix). The situational matrix capturing the state of the Czech Republic's regions in 2015 is not suitable for the interpretation of development (although it is commonly used in practice), as it cannot capture the development over time (Kloudová, 2009).

To identify a positive or negative shift regarding the past (or baseline of 2011), a trend matrix was developed to capture the evolution of the average growth rate in 2011–2015. To build this matrix, it was necessary to calculate the Creativity trend index first. This indicator is limited to the areas of talent and technology (i.e. 2T). The reason for omitting the tolerance indicator is a great difficulty to measure the development of human attitudes (Kloudová, 2009). Thus, the Creativity trend index is the sum of the average values of R&D, innovation, human capital, and creative class. Average of these values should reduce the distortion that could occur in the event of unexpected or cyclical fluctuations. The Creativity Matrix is constructed by plotting the Creativity index on the x-axis and the trend values of the Creativity index on the y-axis. The obtained graph is therefore divided into 4 quadrants (leaders, growth, lagging and land-losing) in which the regions are assigned.

3. RESULTS AND DISCUSSION

Based on the above-mentioned methodology, the Creativity index was measured for all regions of the Czech Republic (see **Table 2**). In the surveyed period (2011-2015), the capital city of Prague, which is a separate region with a concentration of offices of multinational companies, foreign capital, research and development centres. Its dominant position is also supported by the low values of the Creativity index measured in the Central Bohemia region, which can be regarded as a backdrop of Prague and is largely "vacuumed". After the partial indicators analysis, we can state that South Moravian region surpassed Prague in the value of the R&D indicator, probably due to higher subsidies, which is probably due to higher subsidies flowing to the region from EU funds and to which Prague did not have access in earlier years. The South Moravian region shows the

second highest values of the Creativity index over the entire monitored period, which is primarily the second largest city of the Czech Republic in Brno, where the R & D, innovation and knowledge economy sectors are concentrated. The third position is held by the Liberec region, which reaches high values especially in the Creative class index, respectively that is the share of creative employment to total employment in the region, and R&D index (maximum in 2012). It is a region with good connections to Prague, where industrial enterprises, nowadays tied to hi-tech, innovative technologies and foreign capital, concentrate in the context of the historical tradition. The region also houses the largest industrial enterprise in the country - Škoda Mladá Boleslav (automotive industry) with a large research and development base. On the other hand, the Vysočina Region consistently shows the lowest values which can be described as probably the most rural.

Table 2.

Creativity index in the regions of the Czech Republic.

Name of the region	Abbreviation	2011	2012	2013	2014	2015
Prague	PHA	0.98	0.95	0.95	0.96	0.98
Central Bohemia	STC	0.26	0.25	0.26	0.23	0.24
South Bohemia	JHC	0.25	0.19	0.18	0.21	0.25
Plzeň	PLK	0.36	0.28	0.23	0.28	0.34
Karlovy Vary	KVK	0.21	0.24	0.15	0.16	0.24
Ústí nad Labem	ULK	0.19	0.22	0.11	0.24	0.22
Liberec	LBK	0.39	0.31	0.32	0.34	0.40
Hradec Králové	HKK	0.21	0.18	0.24	0.19	0.24
Pardubice	PAK	0.20	0.24	0.17	0.18	0.21
Vysočina	VYS	0.06	0.06	0.05	0.04	0.05
South Moravia	JMK	0.48	0.46	0.47	0.46	0.49
Olomouc	OLK	0.18	0.22	0.19	0.19	0.22
Zlín	ZLK	0.20	0.17	0.20	0.18	0.19
Moravia-Silesia	MSK	0.22	0.25	0.23	0.24	0.24

Source: own calculations

It is also interesting to keep track of development in the last two years of measurement, as between 2014 and 2015; there was a significant positive shift in the South Bohemia, Plzeň, Karlovy Vary, Hradec Králové, South Moravian, and Liberec regions. The reason for this significant shift is a strong increase in the creative class that is in the talent field, which supports Florida's idea regardingthe existence of so-called creative centres. Florida (2002) considers creative centres as diverse, tolerant, and open places for new ideas, leading to concentration of creative capital, and consequently to greater pressure to innovation, development of high-tech technologies and to economic, social, and environmental growth.

The next phase of the survey was to compare the growth rate of the Creativity index. The highest average growth rate of the Creativity index was measured in the Olomouc region (1.05), followed by Karlovy Vary (1.04) and Ústí nad Labem (1.04) regions. On the contrary, the lowest average growth rate was recorded in Vysočina (0.95), Central Bohemian (0.98), and Plzeň (0.98) regions. For all regions of the Czech Republic, the average increment rate of the Creativity index was also measured. **Table 3** and **Fig. 1**,

shows regions that have been shifted upwards (shown by yellow shades) and regions that have experienced a decrease (shown by blue shades). The highest values of the average increment rate were recorded in the Olomouc region (5.10) and the lowest values in the Vysočina region (-5.37).

Table 3.

Average increment rate of the Creativity index in the regions of the Czech Republic.

Name of the region	Abbre-viation	Growth rate 2011	Growth rate 2012	Growth rate 2013	Growth rate 2014	Growth rate 2015	Average growth rate	Average rate of increment
Prague	PHA	-	0.97	1.00	1.01	1.02	1.00	0.00
Central Bohemia	STC	-	0.94	1.06	0.88	1.05	0.98	-1.93
South Bohemia	JHC	-	0.78	0.93	1.15	1.21	1.00	0.37
Plzeň	PLK	-	0.78	0.82	1.19	1.22	0.98	-1.68
Karlovy Vary	KVK	-	1.15	0.62	1.10	1.47	1.04	3.91
Ústí nad Labem	ULK	-	1.16	0.52	2.15	0.92	1.04	4.34
Liberec	LBK	-	0.78	1.03	1.08	1.17	1.00	0.47
Hradec Králové	HKK	-	0.85	1.33	0.77	1.29	1.03	2.79
Pardubice	PAK	-	1.16	0.70	1.08	1.18	1.01	0.91
Vysočina	VYS	-	0.90	0.82	0.90	1.21	0.95	-5.37
South Moravia	JMK	-	0.94	1.03	0.98	1.07	1.00	0.35
Olomouc	OLK	-	1.24	0.83	1.04	1.14	1.05	5.10
Zlín	ZLK	-	0.86	1.16	0.90	1.08	0.99	-0.86
Moravia-Silesia	MSK	-	1.11	0.94	1.03	1.01	1.02	2.10

Source: own calculations

Fig. 1. Average increment rate of the Creativity index in the regions of the Czech Republic. (Source: own processing)

The obtained values of the aggregate Creativity index measured for individual regions of the Czech Republic were subsequently used in the last step of the analysis, in which the situational and trend matrix of creativity was created (**Fig. 2**). The situation matrix shows that only Prague is in the quadrant of leaders, while the other regions are growing region quadrant. Based on the results, it is expected that the South Moravian region and the Liberec region will continue in catching up Prague region. On the contrary, the Vysočina Region is very close to the quadrant of the lagging regions, which may signal another weakening of the region's position in the future.

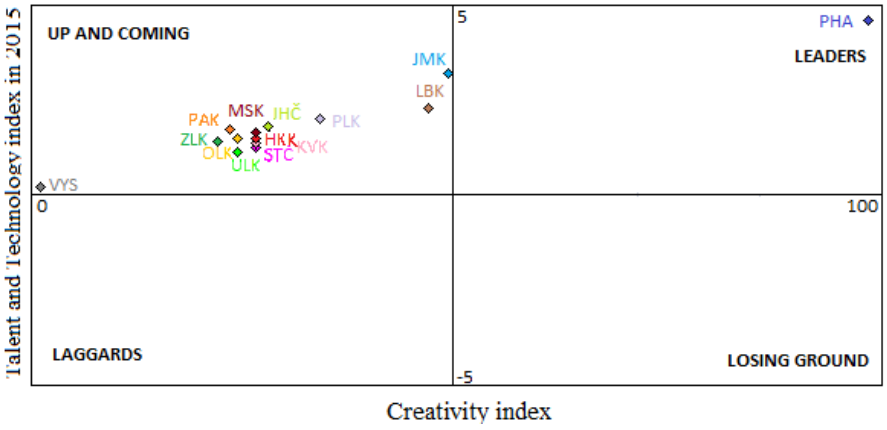

Fig. 2. Situational creativity matrix for the regions of the Czech Republic. (Source: own calculations)

Based on the results shown in the trend matrix (see below, **Fig. 3**), it can be said that Prague region is slightly losing its leading position because the South Moravian region, positioned in the growth quadrant, is catching up. All other regions are also positioned in the growth quadrant, which is a significant positive shift than the one found in the Kloudová (2009), which included a trend matrix for the period 2001 to 2007. Ústí nad Labem, Karlovy Vary, and Plzeň regions experienced the greatest improvement. They were positioned in the lagging quadrant during 2001–2007. The reason for the upward trend is an investment increase into the development of the region, the effort of the region to attract the creative class and, consequently, to increase the economic prosperity of the region, as could be for example seen in studies (Leriche and Daviet, 2010; Rumpel et al., 2010; Tafel-Viia et al., 2015; Krzysztofik et al., 2016).

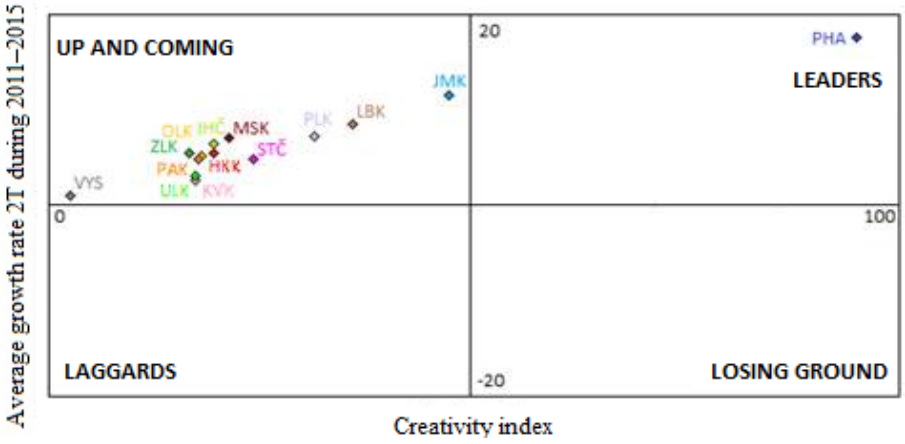

Fig. 3. Trend creativity matrix for regions of the Czech Republic (2011–2015).
(Source: own calculations)

4. CONCLUSIONS

In today's era of globalization, it is confirmed that creativity and innovation are the driving force of a creative economy. Organizations, regions, cities and urban agglomerations use creativity to generate significantly higher revenues and ensure greater stability in the future (Tonev et al., 2017). Creative economics (including various sustainable and smart aspects) is unique in that it relies on an unlimited resource, ie human creativity, which also gives rise to a significant multidimensional approach to studying changes in the context of economic, geographical, demographic, cultural or social (Van der Pol, 2007; Ponzini & Rossi, 2010; Turón & Gomis, 2016).

Although Landry (2011), as one of the leading representatives of creative research, speaks in his theoretical contribution of 25 years of research and defines, for example, ten key indicators to assess creative urban dynamics, statistical coverage of creative sectors at international level is still a problem, challenge. This is mainly due to the fact that creativity has fairly clear inputs, but not uniform and easily quantifiable outputs. The manifestations

of creativity can be found in all economic spheres or sectors (primary, secondary, tertiary) which makes it very difficult to identify them (Kloudová, 2009).

One of the basic methodological approaches to measuring creativity is the 3T Model-based Creativity Index (see above), which was compiled by Florida (2002) and later modified to the Euro-creativity index (Florida & Tinagli, 2004). Consequently, Hui et al. (2004) created the so-called "5Cs Model" Creativity Index, which extends Florida's indicators, especially in the area of non-economic factors (human, institutional / structural, cultural and social capital). However, any modification or extension entails increased demands on the base and comparable data available. Therefore, most studies using the original 3T model or modified version of Florida are geared to assessing creativity at the level of one state, region or city (Tinagli et al., 2007; Rumpel et al., 2010; Tinagli et al., 2012; Fahmi et al., 2016; Dörry et al., 2016). The comparison of creative potential and human capital in the EU-27 was attempted by Bobirca & Draghici (2011), while their modification was called the European Creativity Trend Index. Leading Scandinavia and Benelux countries have been at the forefront, on the other hand, the last countries of South East Europe and the Baltic States. However, research by Romanian scientists uses data from the period 10-15 years ago, and the upward movement of post-socialist Europe can be expected today.

The results of our research in the regions of the Czech Republic showed the dominant position of the City of Prague, which reached the highest score over the whole period and prevailed with great predominance over all other regions. Only the South Moravian Region surpassed Prague in a specific way, in the value of the R & D indicator. In this region lies the second largest city of the Czech Republic in Brno, which has a very strong position in the field of research, development and innovation. The situational matrix captured the situation where only the Prague was in the quadrant of leaders, while the other regions were growing in the region quadrant, which is a significant shift compared to the methodically similarly designed study Kloudová (2009). On the contrary, the trend matrix has suggested that Prague is losing its leading position as it is overtaken by the South Moravian region. However, the other regions also saw a shift in the growth quadrant of the regions.

In conclusion, it is possible to generalize, as many authors quote in their works, that if regions are to continue to improve and to be more competitive in the "creative age" they should continue to invest in research, development and innovation, which would subsequently contribute to increasing the potential of human capital and upward movement. Similarly, as in the past 10 years, the regions in the Czech Republic have succeeded.

ACKNOWLEDGEMENTS

This contribution was supported by an internal grant of the Faculty of Economics and Administration, Masaryk University, entitled “Cities, municipalities, regions: management, processes and interactions in theory and practice“ (MUNI/A/0994/2017).

REFERENCES

Angelidou, M. (2014) Smart city policies: A spatial approach. *Cities*, 41, S3-S11.

Bobirca, A., Draghici, A. (2011) Creativity and economic development. *International Journal of Economics and Management Engineering*, 5(11), 1447-1452.

Boccella, N., Salerno, I. (2016) Creative Economy, Cultural Industries and Local Development. *Procedia - Social and Behavioral Sciences*, 223, 291-296.

Carayannis, E.G., Ferreira, J.J.M., Jalali, M.S., Ferreira, F.A.F. (2018) MCDA in knowledge-based economies: Methodological developments and real world applications. *Technological Forecasting and Social Change*, (In Press).

Cikánek, M. (2013) *Kreativní průmysly: příležitost pro novou ekonomiku*. II. nové, rozšířené a revidované vydání. Praha: Institut umění, 2013

Coyle, D. (1999) *The weightless world: strategies for managing the digital economy*. Cambridge, MA: MIT Press.

Dörry, S., Rosol, M., Thissen, F. (2016) The significance of creative industry policy narratives for Zurich's transformation toward a post-industrial city. *Cities*, 58, 137-142.

Fahmi, F.Z., Koster, S., van Dijk, J. (2016) The location of creative industries in a developing country: The case of Indonesia. *Cities*, 59, 66-79.

Florida, R. (2002) *The Rise of the Creative Class–and how it's transforming work, leisure, community and everyday life*. New York: Basic Books.

Florida, R., Tinagli, I. (2004) *Europe in the Creative Age.* London: Carnegie Mellon Software Industry Center/DEMOS.

Howkins, J. (2001) *The creative economy: how people make money from ideas*. London: Penguin.

Hesmondhalgh, D. (2007) *The cultural industries*. Los Angeles: Sage.

Hui, D., NG, Ch-H., Mok, P. (2004) A Study on Creativity Index. Retrieved from http://www.hab.gov.hk/file_manager/en/documents/policy_responsibilities/arts_culture_recreation_and_sport/HKCI-InteriReport-printed.pdf [Accessed 9th February 2018].

Kloudová, J. (2009) Kreativní ekonomika a její měření. *Ekonomický časopis*, 57(3), 247-262.

Krzysztofik, R., Tkocz, M., Spórna, T., Kantor-Pietraga, I. (2016): Some dilemmas of post-industrialism in a region of traditional industry: The case of the Katowice conurbation, Poland. *Moravian Geographical Reports*, 24(1), 42–54.

Lampel, J., Germain, O. (2016) Creative industries as hubs of new organizational and business practices. *Journal of Business Research*, 69(7), 2327-2333.

Landry, Ch. (2011) The creativity city index. *City, Culture and Society*, 2, 173-176.

Leriche, F., Daviet, S. (2010) Cultural Economy: An Opportunity to Boost Employment and Regional Development? *Regional Studies*. 44(7), 807-811.

Liu, Ch-H.S. (2018) Examining social capital, organizational learning and knowledge transfer in cultural and creative industries of practice. *Tourism Management*, 64, 258-270.

Lundvall, B-A., Johnson, B. (1994) The learning economy. *Journal of Industry Studies*, 1, 23-43.

Mackinnon, D., Cumbers, A. (2007) *An Introduction to economic geography. Globalization, uneven development and place*. Harlow: Pearson Education Limited.

Markusen, A., Wassall, G.H., Denatale, D., Cohen, R. (2008) Defining the Creative Economy: Industry and Occupational Approaches. *Economic Development Quarterly*, 22(1), 24-45.

OECD (1996) The Knowledge-based economy. Paris: OECD/GD. Retrieved from https://www.oecd.org/sti/sci-tech/1913021.pdf. [Accessed 5th February 2018].

OECD and European Commission (2008). Handbook on Constructing Composite Indicators: Methodology and User Guide, by Nardo, M. M. Saisana, A. Saltelli and S. Tarantola (EC/JRC), A. Hoffman and E. Giovannini (OECD).

Ponzini, D., Rossi, U. (2010) Becoming a creative city: The entrepreneurial mayor, network politics and the promise of an urban renaissance. *Urban Studies*, 47(5), 1037-1057.

Power, D. and Scott, A.J. (2004) *Cultural industries and the production of culture*. New York: Routledge.

Rumpel, P., Slach, O., Koutský, J. (2010) Creative industries in spatial perspective in the old industrial Moravian-Silesian Region. *E&M Economics and Management*, 4/2010, 30-46.

Scott, A.J. (2000) *The cultural economy of cities: essays on the geography of image-producing industries*. Thousand Oaks, California: SAGE Publications.

Selwood, S. (2006) A part to play? International Journal of Cultural Policy, 12(1), 35-53.

Tafel-Viia, K., Terk, E., Lassur, S., Viia, A. (2015) Creative industries in the capital cities of the Baltic States: Are there innovations in urban policy? *Moravian Geographical Reports*, 23(4), 47–58.

Tang, W-S. (2016) Creative industries, public engagement and urban redevelopment in Hong Kong: Cultural regeneration as another dose of isotopia? *Cities*, 56, 156-164.

Tinagli, I. (2012) Norway in the creative age. Report 2012. Retrieved from https://www.vegvesen.no/_attachment/408714/binary/704251. [Accessed 14th February 2018].

Tinagli, I., Florida, R., Ström, P., Wahlquist, E. (2007) Sweden in the creative age. Göteborg University & CreativityGroupeEurope: School of Business, Economics and Law. Retrieved from http://creativeclassgroup.com/rfcgdb/articles/Sweden%20in%20the%20Creative%20Age.pdf. [Accessed 14th February 2018].

Throsby, C. (2001) *Economics and culture: essays on the geography of image-producing industries*. York: Cambridge University Press.

Tonev, P., Dvořák, Z., Šašinka, P., Kunc, J., Chaloupková, M., Šilhan, Z. (2017). Different approaches to defining metropolitan areas (Case study: cities of Brno and Ostrava, Czech Republic). *Geographia Technica*, 12(1), 108-120.

Turón, C., Gomis, J. (2016) Implementation of elements of sustainability applied to the urbanization of productive areas. *Geographia Technica*, 11(2), 113-124.

Van der Pol, H. (2007) Key role of cultural and creative industries in the economy. Canada: UNESCO Institute for Statistics. Retrieved from https://www.oecd.org/site/worldforum06/38703999.pdf [Accessed 14th February 2018].

Veselá, D., Klimová, K. (2014) Knowledge-based Economy vs. Creative Economy. *Procedia - Social and Behavioral Sciences*, 141, 413-417.

Zhong, S. (2016) Artists and Shanghai's culture-led urban regeneration: *Cities*, 56, 165-171.

GEOMEDIA ROLE FOR MOUNTAIN ROUTES DEVELOPMENT. MESEHE AND PISOIU WATERFALL COMPARATIVE STUDY

Ni Made ERNAWATI[1], Adrian TORPAN[2], Mihai VODA[3]

DOI: 10.21163/GT_2018.131.05

ABSTRACT:
This study discusses a tropical and a temperate forest route development to Mesehe and Pisoiu Waterfall supporting sustainable tourism development in Pohsanten Community, Bali, Indonesia and Bistra, Romania. It is a qualitative study using a combination of observation, direct participation and non- structured interviews as data collecting methods. Geo-data was collected during forest expeditions, interactions and interviews with local community members who participate in tourism. Re-establishing the geo-heritage supports sustainability to the people in terms of socio economic wellbeing, promotes legal use of forest and conservation. The study suggests 3 types of products: Village off road vehicle (ORV) recreation, mountain biking, and forest trekking. It concludes tourism could be a solution to the misuse of natural environment, brings about socio cultural and economic benefits to the members of the village; thus, sustainable tourism development for Pohsanten and Bistra communities.
Key-words: *geomedia, ORV, community-based tourism, geo-tagging, recreation.*

1. INTRODUCTION

Technology evolution is reflected in every aspect of people's life, challenging continuous learning and fast adaptation. Considering humans as the central component of surrounding Geosystem, the use of geographical techniques for location referencing progressed from paper maps to mobile phones map applications (Voda, 2013). How to place a specific location in space represented a question that has generated a range of different specialized responses. Coordinates calculation, correct position determination constitute the privilege of geospatial tools manipulators (Luo et al., 2009).

Direct on field measurements transition to satellite imagery interpretation, GIS advancements to open source maps enabled geographical creativity and unexpected visualization opportunities of world local environments. Web-based GIS and interactive digital cartography are representing the new geospatial technologies in the location-aware future (Wilson, 2012; 2014). The visualization of diverse digital geo-information coming from different media sources represents Geomedia (Voda, 2015; Digital Earth, 2014). Geographical location related details are provided by Geomedia tools like Google Maps, Google Earth, Facebook, Flickr, Instagram, online and offline maps or navigation geo-applications developed for mobile phones (Jin et al., 2010; Google Earth, 2017).

Wilson (2014) observed the increasing diversity of interfaces that are using geospatial data, underlining the importance of GIScience in the process of communities' culture comprehension. The worldwide availability of smartphone devices has opened new opportunities for the future use of geospatial technologies.

[1] *Politeknik Negeri Bali University, Jimabaran, Bali, Indonesia, madeernawati@pnb.ac.id;*
[2] *Folkuniversitetet, Jönköping, Sweden, adriantorpan@yahoo.com;*
[3] *Dimitrie Cantemir University, 540545, Targu Mures, Romania, mihaivoda@cantemir.ro;*

Luo et al. (2010) analyzed important modalities of geo-information useful in multimedia and vision research stating that geo-tagging has contributed to communities' geo-awareness. Their research shows how digital photography geo-tagging reveals place and position information, adding geographical recognition metadata to a variety of images, videos or photos taken with GPS incorporated devices.

Geo-information in multimedia could assist in developing tourism attractions particularly: trekking, Off Road Vehicle (ORV) recreation, mountain biking, mountain climbing. As the information technology could provide hand on information needed by geotourists, while in the middle of wilderness, it is worth examining its impact on local communities which already are beneficiaries of mobile devices and internet access. Smartphones can provide directions based on geo-tagged photos, indications on the surrounding human or natural environments, cultural resources and various sharing opportunities for information distribution or validation by other online world wide travellers.

Various investigations have explored the subject, especially Schwanen and Kwan (2008), Wang et al. (2012), Dickinson et al. (2014), Meng et al. (2014), Martínez-Graña et al. (2017), Sidali et al. (2017), showing that modern geomedia, particularly smartphones applications are offering information, protecting and promoting the local natural and cultural potential. Geomedia enables the visualizing process of a diversity of places geographical realities in a different way. The best example is Airbnb platform, which has a powerful impact on travellers' decisiveness to select destinations, based on locations accurate maps, directions, photos, reviews and rating system (Voda & Negru, 2015).

Inal et al. (2017) presented the technological evolution of the smartphones in archaeological applications, in the acquiring process of the coordinates system with mobile phones instead of GPS devices, outlining the visual representation importance of the results on Google Earth Program. Baiocchi et al. (2017), stated that the single point positioning receivers advance was represented by the new Global Navigation Satellite Systems (GNSS) techniques introduced for Samsung Galaxy III and recent IPhone models. A legend could build a strong brand for tourist destinations (Robinson & Wiltshier, 2011; Ernawati, 2015). In Transylvania- Romania, for example, the legend of Dracula may become the main tourism attraction with the support of Geomedia tools. This kind of legends, connected to local angels, also exists in Bali, Indonesia (Ernawati, 2015).

This article intends to discuss the use of Geomedia tools in the establishment process of sustainable tourism activities that could bring benefits to the local Transylvanian and Balinese communities, as well as present off road vehicle, mountain-biking and trekking options along the Pisoiu and Mesehe waterfall routes. The results of the study could be used as a reference to assist communities in developing tourism in the analyzed villages of Pohsanten and Bistra that could provide social and economic benefits, promote conservation, and prevent the misuse of the mountain wild areas as described by Voda, Torpan & Moldovan (2017), Voda, Moldovan, Torpan & Henning (2014).

2. RESEARCH METHODOLOGY

This is a qualitative study using observation, direct participation and non-structured interviews as data collecting methods. Data was collected during the forest trekking, interactions with locals who participate in tourism, and interviews that were conducted with the head of farmer organization, local guides and other tourism related service providers in the village.

Google Earth and Google Maps™ datasets of Transylvania and Bali were used for maps elaboration. Mountain routes were firstly explored for GPS tracking by ORV, motorbike and pedestrian means. The tracks were charted on orthophoto maps and topographic profile graphs were created in ArcGIS 10 using digital elevation models and Interpolation Line from 3D Analyst toolbar (Google Earth, 2017; ArcGIS Server, 2017).

Smartphones technology was used for the geotagging process of images taken along the identified routes, recording the compas direction of Iphone8+ incorporated camera and automatically embedding GPS location. Location data and comprehensive metadata were procured from GPS trajectories identifying the exact longer stops positions where photos were taken. Invert geo-coding was executed to get or provide a semantic connotation of the places correlated to the GPS coordinates. The method was expanded to envisage the semantic position typology based on site geographical observations (Liu et al., 2006).

Considerable Android applications were tested for coordinate's identification and mapping purposes but location accuracy of GSM providers is approximately 3 and a half meters. Inal et al. (2017), observed that this precision is sufficient for Archaeological sites.

The Pic2Map exchangeable image file (EXIF) data viewer methodology was used for location determination based on analysis of iPhone8 and Xiaomi Redmi 3S image data. The photo coordinates were extracted from the interchange information digital files and located on Google Maps™ (Pic2Map, 2018).

3. MESEHE AND PISOIU MOUNTAIN ROUTES

Mesehe Waterfall is located near Pohsanten village 120 km from Jimbaran. The exit point from Bali main road Denpasar – Gilimanuk is located at the Obelisk monument – Tugu. The Pasatan temple is about 10 km distance from the exit point that could be easily reached by ORV or motorcycle.

Pisoiu Waterfall is placed upstream Cofu Valley, located in Calimani Mountains with Bistra village as the mountain route entry point at 66 km from Targu Mures. Motor-bike and ORV constitute reasonable options to reach the waterfall. Both tracks are running through the villagers households as the routes are going deeper into the natural scenery that becomes more picturesque as entering the forests. Airbnb platform offers genuine local accommodation options in both analyzed locations. Motor bike, mountain bike and ORV tours around scenic Pasatan area using the temple outer section as a break point could represent moderate options before accessing the tropical forest trail in Bali. In Transylvania, the mountain gravel road that stretches from Bistra village to Donca, Mijlocu and Stegii valley is often used for motorbike, mountain bike and ORV recreational activities.

Pasatan temple is the center of spirituality in Pohsanten village; moreover, the temple is not only worshiped by Pohsanten community members but also by Balinese community. Many people feel having a close connection and being blessed by the Water Goddess abodes the temple. The nearby Subak (s) which are the traditional farming organizations pray in Pasatan temple for a successful planting season; as practiced by the Subak of rice farming organization praying in Bedugul temple (Norken, Suputra & Arsana, 2017). A legend told that the temple is spiritually related to the Mesehe waterfall located in the mountain at the upper edge of the area. The waterfall is said to be an angel bathing and a purification place for the Goddess before resides in the temple. In the old-time people in the village conducted a pilgrimage: Pasatan temple to Mesehe angel-bath waterfall, nowadays the practice ceased and even the track across a tropical forest to the waterfall has lost.

Currently the villagers want to re-establish the practice and combine it with tourism activities. The Goddess legend could become a theme for Pohsanten tourism as argued by House (1997). In order to be successful, a mountain rural area needs to have geomedia representation based a strong distinctive tourist attractions theme. The difficult trail from Pasatan temple to Mesehe Angel-bath Waterfall stretches through a tropical forest consisting of 4.4 km pathways which takes about 4 hours trekking. This whole route is for well trained, adventure trekkers (**Fig. 1**).

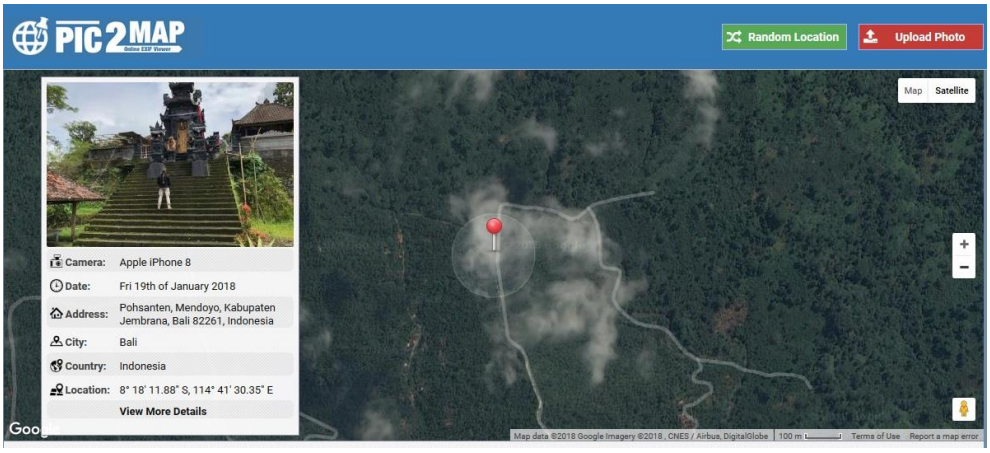

Fig. 1. Pasatan Temple study area in Bali, Indonesia.

There are few posts along the route wherein each has its own highlight of activities and point of interest. Semantic connotation of the stopping places (Stony River crossing) were correlated to the GPS coordinates. (**Fig. 2**). Pasatan Temple is the starting point, which is the spiritual center where in Dewi Danu the Lake Goddess is worshipped. Archeological artifacts were found in Pasatan temple area and categorized based on Android GeoApp photo identification process (Inal et al., 2017). There is a central stone with 7 orbiting rocky artifacts with different carved symbols. For the Pohsanten village people, apart from praying place the temple constitutes a meditation quarter.

Fig. 2. Geo-tagged Iphone8 photo from Stony River crossing.

Stony River crossing represents the place where tourist could rest and have clear water. This post can be the first terminating point for the trekkers (Magyari-Saska & Dombay, 2016). Location determination was done based on the analysis of iPhone8 image data interpretation and incorporated GPS sensor. Proposed tourist activities in the area can include river-bathing, fishing or river canyoning along its clear water-flow. The distance is 1 km from Pasatan Temple forest entrance.

The tropical forest resting point placement was decided during the common expedition organized with Pohsanten representants, being located half way from the temple to the waterfall (**Fig. 3**). Reaching this Banyan tree (*Ficus Benghalensis*) location requires more physical effort, being considered a challenging section because of the steep mountain climb. This was an eco-spot where various old grow forest trees were identified and described for the Pohsanten Geomedia platform. It is the viewing point from the mountain top and the last resting area before reaching the Mesehe waterfall.

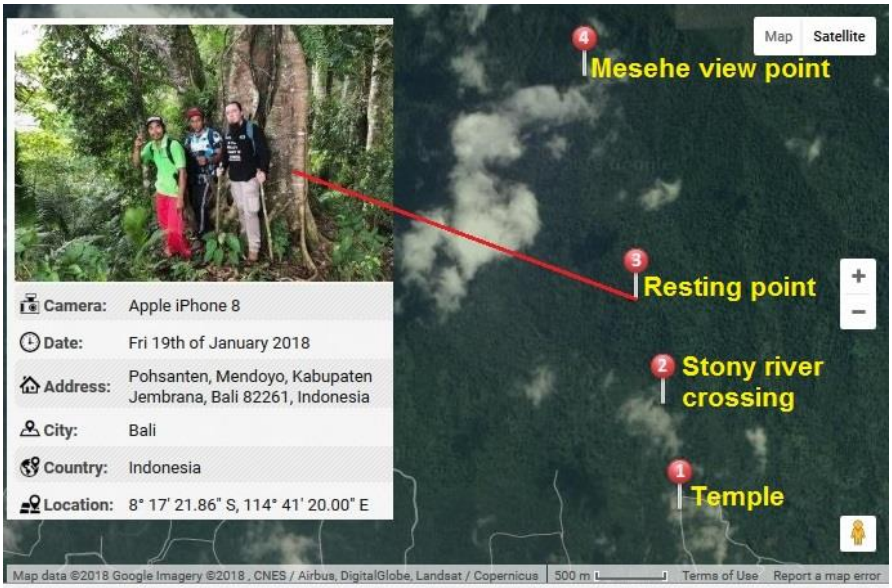

Fig. 3. Pic2MAP photo location determination on Mesehe route (Pic2Map, 2018).

The terminating point of the Mesehe forest trail is the waterfall, which has two platforms. The first platform host the viewing and the resting area and the second represents a sacred space with restricted access unless for praying purposes. Mesehe Waterfall suggested route options development for tourist activities could include Pohsanten Village motor bike tours, recreational trekking using the Stony River as a terminating point, and the Mesehe Waterfall tropical forest adventure for professionals. Pisoiu Waterfall from Cofu Valley is located in Caliman Mountains along a temperate zone forest exploitation route that follows Bistra River and Cofu tributary. Transylvanian mountain routes were explored for GPS tracking by ORV (Suzuki Grand Vitara 4x4) and motorbike (DRZ 400E).

The importance of local legends as House (1997) argued can be valorized on Geomedia platform for Bistra Village. Compared to Pohsanten Goddess legend from Bali, the Dracula myth has better international visibility but no geospatial coordinates.

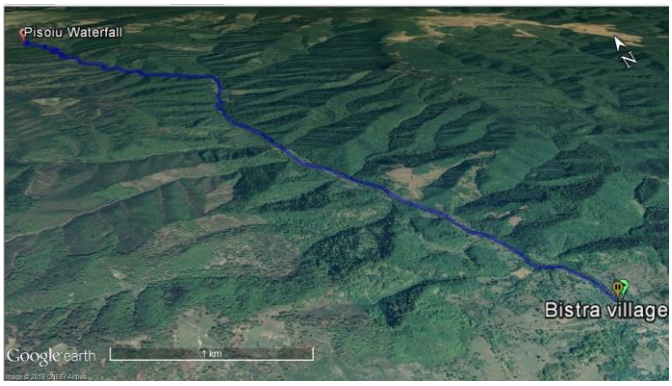

Fig. 4. Pisoiu Waterfall route to Dracula Castle in Transylvania.

As Bram Stoker described the black horses-drawn carriage journey through the Transylvanian Mountains in his Dracula book, our research identified the geographical locations of Jonathan Harker`s passage on the Dracula Castle way (Stoker, 1897, Negru et al., 2015). Our studies are indicating the Iszten Szek mountain top as the Caliman Range entrance reference related to Dracula Castle access. In order to clarify the Borgo Pass contradiction, the mountain range crossing options were determined, taking into account the Iszten Szek peak restricted visibility from the South direction. Further research has demonstrated that Bistra River with the right hand tributary Cofu constitutes the first passage alternative to Colibita Lake and Borgo Pass, where Dracula Castle was built (**Fig.** 4). Caliman range gravel roads topographic profile graphs were created for mountain gravel roads, using collected informations and Google Earth datasets. The most spectacular route is represented by Luca Bradului Village- Negoiu Saddle- Toplita Monument gravel road, which can easily cross the 2000 m altitude volcanic mountains to reach the legendary Dracula Castle (Fig. 5).

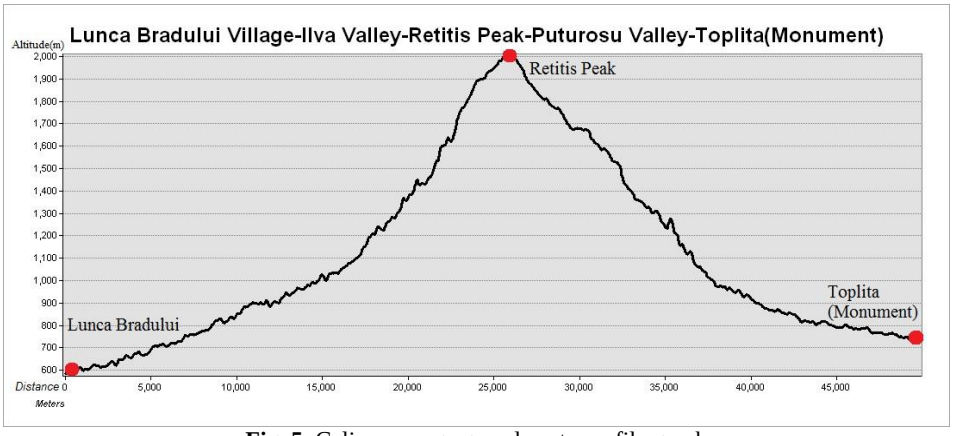

Fig. 5. Caliman range gravel route profile graph

Google Maps™ datasets of Transylvania and Bali were used for Geomedia platforms elaboration. The geotagging process of photos taken along the identified routes was initiated based on available smartphones technology of iPhone8 and Redmi 3 S Xiaomi digital cameras.

Our research is recommending three recreational activities for potential tourists, based on local community's decision makers' interviews: gravel roads ORV tours, mountain biking, and forest adventure trekking. Semantic nomination of the resting locations, significant crossing spots and terminal points were done using smartphones GeoApps correlated to the GPS provided directions. Redmi 3S Xiaomi Android software technology proved to be more accurate than iPhone 8 Apple (**Fig. 6**).

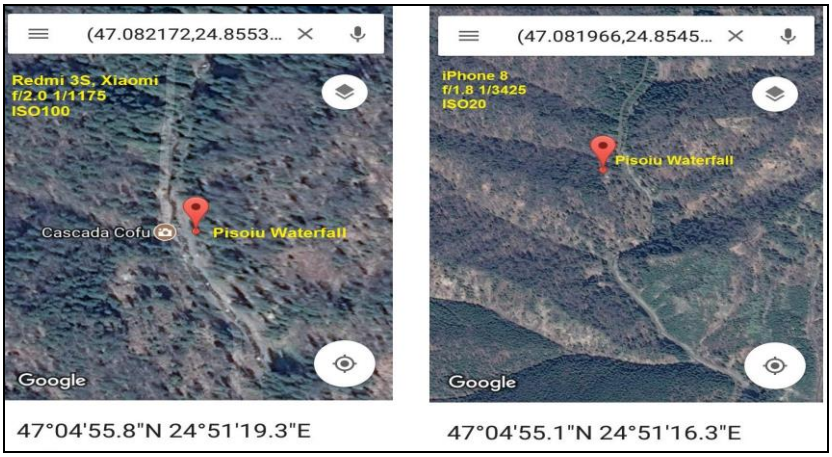

Fig. 6. Pisoiu Waterfall comparative geo-location. Redmi 3S Xiaomi vs iPhone8.

Geo-tagged media represented by specific community members photos (from Bali or Transylvania) or blogger sites (local or international) are offering particular details for numerous location-based utilities such as Airbnb local homes near Pohsanten in Bali, Indonesia or Bistra in Transylvania, Romania (**Fig. 7)**. Tourist can choose what to visit based on social media images, travel blogs or Airbnb type platforms (Luo et al., 2010; Voda & Negru, 2015).

Mesehe and Pisoiu Waterfall mountainous routes are both connected to protected areas, being situated in the vicinity of West Bali National Park and Calimani National Park. The access roads are located in rural communities of Pohsanten, Bali and Bistra, Transylvania with poor inhabitants but various cultural resources that can be valorized using the new Geomedia technological advances. Our research integrated field photography and online mapping techniques encouraging locals to share their geo-tagged photos for the project scientific database (USGS, 2017). Smartphones diverse applications with geo-tagged photos and social media sharing options, mobile networks wider coverage and continuously growing internet availability are transforming people's life. Remote villages are offering exquisite rural home stays and the villagers become real experiences providers on Airbnb. The use of Geomedia tools can directly influence the economic development of Pohsanten and Bistra specific chosen regions, providing instant online access to Facebook, Instagram or Airbnb.

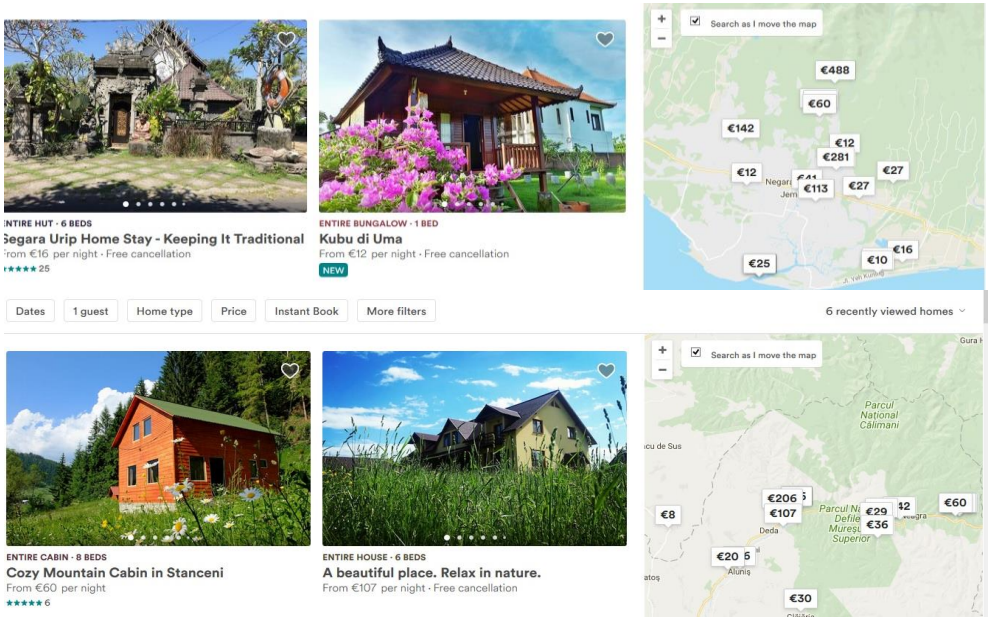

Fig. 7. Local homes accommodation offers near Pohsanten, Bali (up) and Bistra (bottom), Transylvania (Airbnb, 2018).

The sharing of Bali or Transylvania idle attractions via tech platforms can generate economic benefits. Sharing economy is helping the villagers to earn extra income and boost their community (Rinne, 2018).

4. DISCUSSION

Sustainable tourism involves and assesses three elements: economic, socio-cultural and natural environment (UNWTO, 2013). Village tourism or community-based tourism (CBT) represents a form of sustainable tourism called alternative tourism at its earlier stage. Eadington and Smith (1992) argue that alternative tourism attempts to develop a more meaningful 'host and guest' relationship, and is more sensitive to local people and the environment (Loker-Murphy & Pearce, 1995), based on community values and environmental ethics (House, 1997). Weaver (2006) argues the characteristics of alternative tourism include: catering for special interest tourists; using pre-existing attraction of authentic culture, history, and natural environment; tourist and local orientation; small-scale and local community ownership businesses; observing the principles of dispersed pattern and low density; unobtrusive and vernacular style architecture features; economic features include low tourist receipts, linkage with local sectors, low leakage, high multiplier effect, and the role of tourism is a supplementary economic activity; regulation features comprise high local community control, public intervention, priority of public wellbeing, and a long-term time frame. Community-based tourism could be defined as a form of tourism development that prioritizes community participation during planning and operation while delivering quality tourist experiences; utilizes culture and natural environment as tourist attractions and is oriented to their conservation and for the prosperity and wellbeing of the

locals. Academics discuss the positive impacts of CBT, e.g. it supports cultural conservation (Picard, 2008); brings about positive economic benefits and is used as a catalyst for community development (Singh, 2012; Butcher, 1997). Apart from the benefits, some unfavorable impacts also envisioned, Beeton (2006) and Butcher (1997) summaries the possible negative impacts of tourism as natural environment destruction, economic dislocation and cultural degradation.

The World Tourism Organisation (WTO) defines sustainable tourism as '… *meeting the needs of present tourists and host regions while protecting and enhancing opportunities for the future*' (WTO, 1998, p. 21). Sustainable tourism is '*envisaged as leading to the management of all resources in such a way that economic, social and aesthetic needs can be fulfilled while maintaining cultural integrity, essential ecological processes, biological diversity and life support systems*' (Lu & Nepal, 2009, p. 6).

Further research is needed for the re-establishing of the traditional pilgrimage from Pasatan temple to the Mesehe Waterfall and for Dracula legend search from Bistra Village to the Pisoiu Waterfall. Tourism development will support sustainability to the Bali and Transylvania villagers in terms of socio economic wellbeing, promotes legal use of forest and conservation. This also provides a legal admission from the local government for the village people to pass through the forest to reach the waterfall legally. Activities in the forest will be exposed and monitored through sustainable tourism practice; thus, reduce illegal and detrimental forest activities. For the development and operation of tourism in Pohsanten and Bistra communities, is vital to permanently observe the principles of sustainable tourism and CBT. Pohsanten Village is a farming area where *cacao* is the main produce and Bistra area is mainly orientated on foresting activities. Mountain routes tourism development is expected to provide an additional source of income for the local inhabitants, to influence the local socio-culture in a positive way, to increase people's awareness and to promote forest conservation actions (Voda, Torpan & Moldovan, 2017).

6. CONCLUSIONS

The use of Geomedia to valorize mountain resources using specific geosites as the highlight and designated routes for connection, contributes to the practice of sustainable living particularly sustainable tourism in villages situated in mountainous regions. The results would be applicable to all mountain communities because Geomedia tools are free to use and widely available. The positive Geomedia impacts could be in a form of: provision of an alternative source of income; broaden the horizon and the perspective of the village people; the conservation of the natural environment particularly the forest, which in turn promotes a better function of natural cycles, maintaining a dynamic equilibrium of existing ecosystems. Geomedia also provides an opportunity for visitors to know more about nature and forest, whilst enjoy quality natural tourism experiences.

Pohsanten community determined the Indonesian Directorate of Higher Education to fund preparation activities for community based tourism development: human resources buildout, brochures and website creation, sing boards along the Mesehe Route forest trail with information panels about natural habitats and ecosystems. But the obtained grant scheme is significantly smaller than expected and there are many challenges: the outer quarter of the temple needs to be considered representable as a visitor reception area. Paving the track up to the River crossing is recommended, restrooms, guests' rooms and restaurant facilities attached to the temple vicinity are envisioned. The Pohsanten village has public land where these facilities could be built. The village authorities at all level from

Bali, formal and traditional leaders, the community members and a considerable number of farmers are enthusiast about developing tourism perspective. Online available GeoApps for travellers' smartphones with incorporated GPS sensor will contribute to the mountain routes accuracy maintenance and minimum impact on natural ecosystems. Mobile phone geo-applications will provide necessary details about the surrounding habitats which are following the forest trails with photos for different species, resting areas and available accommodation options in the mountain proximity. Community members will be encouraged to present their households and favourite activities as experiences, based on Airbnb homes and experiences models developed for the new generation of sharing economy tourists.

REFERENCES

Airbnb, (2018). *Airbnb platform* [Online]. Available from: http://www.airbnb.com, [Jan. 2018].

ArcGIS Server, (2017). *Website of ArcGIS Server* [Online]. Environmental Systems Research Institute, Available from: www.esri.com/software/arcgis/arcgisserver/, [Accessed Dec. 2017].

Baiocchi, V., Constantino, D. & Vatore, F. (2017). Suitability of Averaging GPS/GNSS Paths to Build Geometrically Correct Digital Road. *Geographia Technica*, 12 (2), 1-9.

Beeton, S. (2006). Community development through tourism. Collingwood, Australia: Landlinks Press.

Butcher, J. (1997). Sustainable development or development?. In M. J. Stabler (Ed.), Tourism & sustainability principles to practice (pp. 27-38). Oxon, UK: Biddles ltd.

Dickinson, J.E., Ghali, K., Cherrett, T., Speed, C., Davies, N., Norgate, S. (2014). Tourism and the smartphone app: capabilities, emerging practice and scope in the travel domain. *Current Issues in Tourism*. 17(1), 84-101.

Eadington, W. R., & Smith, V. L. (1992). Introduction: The emergence of alternative form of tourism. In V. L. Smith & W. R. Eadington (Eds.), Tourism alternatives: Potential and problem in the development of tourism (pp.1-12). Phyladelphia, US: University of Pennsylvania Press.

Ernawati, N. M. (2015). Producer–market orientation of community-based tourism (CBT) products: A case study in Bali, Indonesia. Unpublished thesis. Perth: Edith Cowan University.

Google Earth (2017) *Google Earth Image*. [Online] Available from www.google.com/earth/ [Accessed December 2017].

House, J. (1997). Redefining sustainability: A structural approach to sustainable tourism. In M. J. Stabler (Ed.), Tourism & sustainability principle to practice (pp. 89-104). Oxon, UK: Biddles ltd.

Inal, C., Kocak, O., Esen, O., Bulbul, S. & Kizgut, R. (2017). Surveying and Mapping using Mobile Phone in Archaeological Settlements. *Geographia Technica*, 12 (2), 82-96.

Jin X., Gallagher A., Cao L., Luo J. & Han J. (2010) The wisdom of social multimedia: using Flickr for prediction and forecast. In Proceedings of ACM Multimedia.

Liu L., Wolfson O. & Yin H. (2006) Extracting semantic location from outdoor positioning systems. In Proceedings of the IEEE International Conference on Mobile Data Management.

Locker-Murphy, L. & Pearce, P. (1995). Young budget travellers: Backpackers in Australia. *Annals of Tourism Research*, 22(4), 819-843.

Lu, J., & Nepal, S. K. (2009). Sustainable tourism research: An analysis of papers published in the Journal of Sustainable Tourism. *Journal of Sustainable Tourism*, 17(1), 5–16. doi:10.108/09669580802582480.

Luo Z, Li H, Tang J, Hong R, & Chua T-S (2009) ViewFocus: explore places of interests on Google maps using photos with view direction filtering. In Proceedings of ACM Multimedia.

Magyari-Saska Z., & Dombay I. (2016). Mixed Group Hikers optimal resting place location along trails. Test Area at Lacu-Rosu Region (Romania). *Geographia Technica*, 11 (2), 69-77.

Martínez-Graña, A.M., Serrano, L., González-Delgado, J. A., Dabrio, C. J. & Legoinha, P. (2017) Sustainable geotourism using digital technologies along a rural georoute in Monsagro (Salamanca, Spain), *Int.J.Dig.Earth*, 10:2, 121-138, DOI: 10.1080/17538947.2016.1209582.

Meng, B., Min-Hyung, K. & Yeong-Hyeon, H. (2014). Users and Non-users of Smartphones for Travel: Differences in Factors Influencing the Adoption Decision, *A.Pac.Jour.Tour.Res.*, DOI: 10.1080/10941665.2014.958508.

Negru, R., Voda, M. & Dumitrache, N.D. (2015). Geodiversity assessment as a tool for Geotourism in the Istenszeke Natural Park. *Academica Science Journal, Geographica Series*, 1(6), 13-21.

Norken, I N., Suputra, I K. & Arsana, I G. N. K. 2017. Institutional and Regulatory Roles in Maintaining Sustainability of Subak as a World Cultural Heritage in Bali. *Asian Agri-History*, 21(4), pp. 245-254

Picard, M. (2008). Balinese identity as tourist attraction from 'cultural tourism' (pariwisata budaya) to 'Bali erect' (ajeg Bali). *Tourist Studies*, 8(2), 155-173. doi: 10.1177/1468797608099246

Pic2Map (2018) Photo Location Viewer [Online]. Available from: https://www.pic2map.com/ [Accessed January 2018].

Rinne, A. (2018), The dark side of the sharing economy [Online]. Available from: https://www.weforum.org/agenda/2018/01/the-dark-side-of-the-sharing-economy/ [Accessed January 2018].

Robinson, P. & Wiltshier, P. (2011). Community tourism. In P. Robinson, S. Heitmann, & P. Dieke (Eds.), Research themes for tourism (pp. 87-99). Wallingford, UK: Cabi. Available from http://www.cabi.org.ezproxy.ecu.edu.au/CABeBooks/ShowPDF.aspx?PAN=20113005506

Schwanen, T. & Kwan, M-P. (2008). The Internet, Mobile-phone and Space-time Constraints, *Geoforum*, 39 (3) 1362-1377.

Sidali, K. L., Huber, D., & Schamel, G. (2017). Long-Term Sustainable Development of Tourism in South Tyrol: An Analysis of Tourists' Perception. *Sustainability*, 9(10), 1791.

Singh, S. (2012). Community participation – in need of a fresh perspective. In T. V. Singh (Ed.), Aspects of tourism: Critical debates in tourism (pp. 113-117). Bristol, UK: Channel View Publications.

Stoker, B. (1897), *Dracula*, Westminister Archibald Constable and Company a Whitehall Gardens, London.

UNWTO (2016) *United Nations World Tourism Organisation* [Online]. Sustainable development of tourism. Available from: http://sdt.unwto.org/en/content/about-us-5 [Accessed September 2016].

USGS (2017) *The United States Geological Survey* [Online]. Land Cover Trends Geotagged Photography. Available from: https://lta.cr.usgs.gov/lct_photos [Accessed December 2017].

Voda, M., Torpan, A. & Moldovan, L. (2017). Wild Carpathia Future Development: From Illegal Deforestation to ORV Sustainable Recreation. *Sustainability*, 9(2254), 1-11.

Voda, M. & Negru, R. (2015). Geomedia role in Mures Valley Castles Tourism Development between Ogra and Brancovenesti. *Academica Science Journal, Geographica Series*, 1(6), 63-70.

Voda, M., Moldovan, L. Torpan, A. & Henning, H. (2014). Using Gis for Mountain Wild Routes Assessment in Order to Qualify Them for Tourism Valorisation. *Geographia Technica*, 09 (1), 101-108.

Voda, M. (2013). The role of Geospatial Technologies, Geographic Information and ICT in promoting rural communities sustainable development in Transylvania. *Academica Science Journal, Geographica Series*, 3, 90-95.

Wang, D., Park, S., & Fesenmaier, D.R. (2012). The Role of Smartphones in Mediating the Tourism Experience. *Journ. of Trav. Res.*, 51(4), 371-387.

Weaver, D. (2006). Sustainable tourism theory and practice. Oxford, UK: Elsevier.

Wilson, M.W. (2012). Location-based services, conspicuous mobility, and the location-aware future. Geoforum 43, 1266–1275.

Wilson, M.W. (2014). Geospatial technologies in the location-aware future. *Journal of Transport Geography*, 34, 297–299.

World Tourism Organization [WTO]. (1998). Guide for local authorities on developing sustainable tourism. Madrid, Spain: World Tourism Organization.

THE "BASE MAP" FOR URBAN PLANNING: CARTOGRAPHIC REPRESENTATION AS A FUNDAMENTAL TOOL FOR THE REPRESENTATION OF THE TOWN PLAN

Jordi GOMIS [1], Carlos TURÓN [1]

DOI: 10.21163/GT_2018.131.06

ABSTRACT:
Topographic information of the territory is essential in many areas of the sciences, especially in those involving the discipline of Geography in its broadest sense and aspects. However, the cartographic representation of the territory can be considered the 'first' drawing of the long process of the urban planning project. Without this 'first' drawing, the town planner is unable to deal with this task of planning satisfactorily. The proper representation of the morphology, or if you prefer, the geomorphology of the territory and of the elements and objects it 'supports and contains', is manifested in the cartographic representation that the architect or urban planner needs to define their proposed planning. This article discusses 'the graphic evolution' of these first and necessary 'base maps', from a purely instrumental point of view and from one of the visual perception of the solutions adopted, focusing on urban plans drafted in the last four decades.

Key-words: *Graphic representation, Technical drawing, Urban Planning, City drawing, Urbanism, Cartography.*

1. INTRODUCTION

It is a requirement and a need for all planning work to dispose of enough knowledge of the place where it is to be implemented. For the same reason, for their performance, urban and spatial planning will require knowledge that should cover all the factors involved in the process of the growth and extension of the city, and how the territory is used in general (Esteban, 2007). Often as a basis for intervention, the map, whether it is of networked relationships or a geographically precise location, precedes the plan (Desimini & Waldheim, 2016). The base map, with its corresponding representation of the topography of the territory, shows the physical reality of the area where the new city plan is to be implemented. This physical reality is expressed through cartography, an absolutely essential component and probably the most important of all those comprising the information necessary for carrying out urban planning (Bosselman, 1997).

The effectiveness of this cartography will depend, primarily, on the quality, scale and type of plans that are used (Aradillas & Cabezas, 1992). It should be noted that the quality of cartography varies depending on the amount of information contained in the maps, the reliability of this information and, of course, the graphic quality of the drawing. Regarding the scales of the maps, they depend specifically on the nature and scope of each particular task (École national des sciences geographiques, 1999). In the study of our concern, the scale is determined mainly by the choice made by the technician when commissioning the base map on which s/he has to work. In the case of the sample analysed, the scales are, basically,

[1] *Universitat Rovira i Virgili, Tarragona, Spain, jordi.gomis@urv.cat,carlos.turon@urv.cat*

1:5,000 and 1:1,000. In most cases, these scales allow one to appreciate the whole urban centre and its physical relationship with its immediate surroundings and deal precisely with the urban fabric in order to refine and adjust specific urban planning actions. In urban planning, the city plan is defined by means of zonal delimitations that must be appropriately accurate according to the different sense of each of the urban development systems. In this case, the assessment of cartographic precision is absolutely essential. However, we also find authors that specify the need and requirement that nowadays, and with the means that are available, the imprecisions in the representation of the base map affected by urban planning are not acceptable under any circumstances, and can only lead to unwanted conflicts that slow down the implementation of plans. In any case, it is clear that the precise and unambiguous definition of the territory where the urban development is to take place or of its various scopes is a strictly necessary element of any planning and that, of course, it must be rigorously represented in the planning drawings manifestly and clearly (Dondis & Gonzalez, 1976). In this case, cartography and its representation becomes a fundamental tool for planners and architects. In fact, several most interesting theoretical studies, such as for example the one by Cattor and Perkins (Cattor & Perkins, 2014), look in depth at the study of alternative spatial models applied to a wide range of scales and in very different contexts of representation, often even, a long way from the normal scales of representation of common urban development plans.

However, too often the real problems of the graphic coding and of the visual perception of the plan are forgotten and a great deal of attention is given to aspects that are too instrumental and that diverge from pure graphic representation and its visual result (Deforge, 1975). All too often, the real problems of town planning drawings that are really executed and put at the disposal of the citizens who consult them, and/or the municipal technical services that develop them, are ignored. Often, too much attention and debate are given to plans that, published in books and journals due to their intrinsic disciplinary interest, their special territorial dimension or, why not, the pure brilliance of the urban planner, digress from the ordinary and common task of urban planning and its daily management. It is, therefore, this specific language, this particular graphic representation that is used by so many 'non-theoretical' architects and urban planners, that is to say, those who finally draw up and sign planning works that mostly become tangible realities, which is what this paper aims to explore. The present study aims to analyse the graphic systems that planners have used to represent the cartography of planning areas from an especially visual point of view, through an evolutionary and historical review of the different graphic solutions used by technicians. Unfortunately, and given the logical limited length of this article, it is not possible to present either the methodology or the detailed results obtained in the research, believing it far more interesting to relate the findings with which the research has provided its authors. It should be pointed out, however, that that the study sample of maps spans from the last decades of the 19th century until 2015.

2. THE REPRESENTATION OF TOPOGRAPHY AND THE BASE MAP

The representation of the topography and the base map has remained constant especially since the beginning of so-called 'modern urbanism'. The processes of representing the territory, which logically have served as the basis for drawing the new arrangements and designed planning, have undergone few graphic modifications, although they have improved substantially in terms of technical execution, end results and accuracy. Descriptive plans of the city and its surroundings, with a more accurate representation of the territory, had been

developed and began to be present in many representations of cities in the 18th century, where even buildings within the blocks of the cities and also properties and suburban properties and fields were represented (**Fig. 1**).

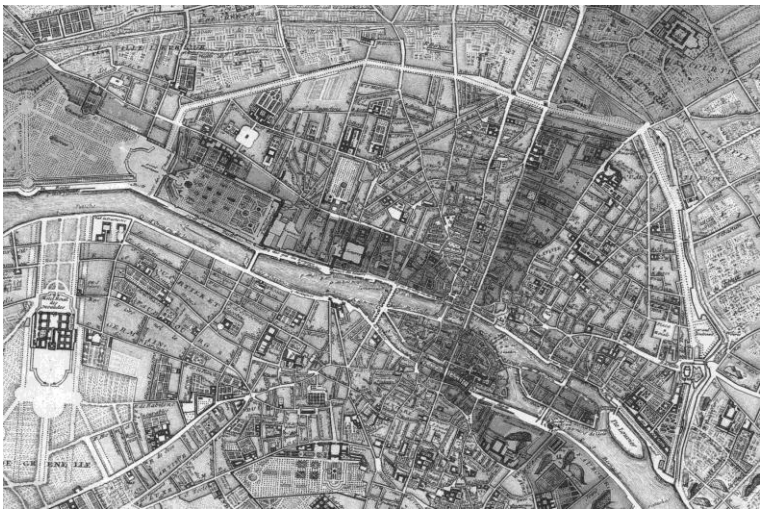

Fig. 1. Part of the map of Paris in 1740, by Jean Delagrive (1689-1757) (Sambrico, 1990).

However, for the purposes of their graphic analysis, it must be borne in mind that these historical maps often suffered geometric deformations and other degradations during their conservation and others caused by acquisition (scanning) (Baiocchi & Maurizio, 2000). But also, the rigorous georeferencing of historical cartography allows for the spatial comparison with current cartographies and with very high resolution satellite images, and the consequent analysis of the urban structure and its formal and functional contents (Baiocchi et al, 2013).

Topography, as we understand it today, with the representation of contours and auxiliary data on survey points and heights, appeared in the late 19th and early 20th century. In earlier plans, the geographical aspects were limited to indicating coasts, gullies, rivers, marsh areas, significant elevations, etc. It was after the development of photographic surveying that, with the help of primitive aerial photos assisted and completed with data from specific tachymetric surveys, topographic maps of large areas of the territory became generalized. These maps are perfectly suitable for technicians to approach new growth and urban development projects with greater accuracy and reliability. They are maps in which the topography of the region is shown by contours, thus becoming an especially valuable tool for the technician. Maps that, on semi-transparent or opaque paper, were used either as a basis, using various techniques, for superimposing the new proposals put forward. Graphic techniques to modify and add new planning to base maps ranged from the use of coloured pencil or tempera paints, and 'gouache', if drawn on opaque copies of the base map (**Fig. 2**), to the use of conventional ink, if the plan was presented in black and white on transparent or semi-transparent paper (Zell, 2008).

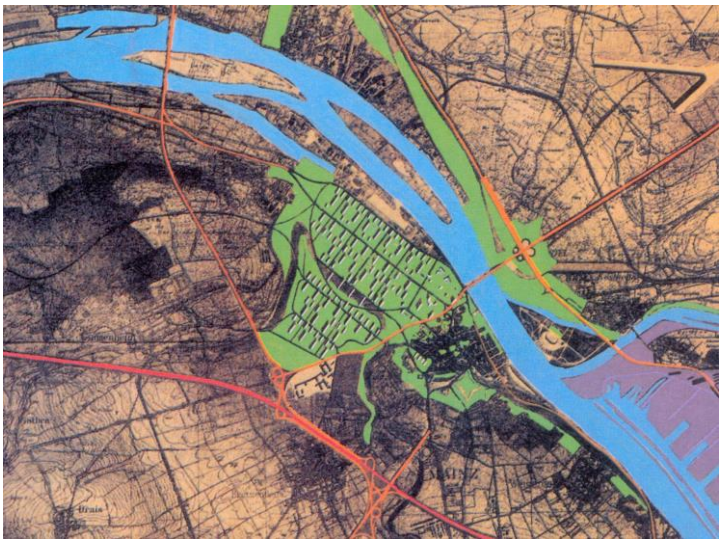

Fig. 2. Project of the Mainz reconstruction plan (Germany) - by means of linear apartment blocks, designed by the architect M. Lods in 1947. 'Gouaches' on map printed on cardboard (Bosma & Hellinga 1997).

As for cadastral maps, in which topographical issues are often of secondary nature, the tachymetric survey was the usual technique, and the use of blueprints on paper of different transparency was chosen to work on in preference due to being easy to modify. It should not be overlooked that cadastral maps are often made to a scale at which the degree of detail is greater and, therefore, it is common that, if a photographic survey exists, it is checked, complementing it with a cadastral study. Graphically, the base map and topography are generally drawn using fine lines. It can be seen how at the end of the 19th century and until after the first half of the 20th century there was a tendency to use types of thicknesses closer to the group or range of 0.8mm and of 1.2mm (Corbella 1983). This feature, applicable, as we shall see, to many of the aspects analysed, probably is more closely related to the drawing utensils and tools that existed at the time of drawing than the conscious decision of the designer or draughtsman (Piedmont-Palladino, 2007).

We will see how, as drawing tools and techniques evolved the thickness with which the graphic resources finally applied decrease visibly. As the map and the representation of the topography are essentially to help with the final representation of the planned design, graphically it is usually approached with fine lines and small text size so as not to 'dirty' and clutter the drawing. Only the lines used to represent the 'principal contours' are usually drawn more thickly, but never exceeding a thickness of more than 0.4 or 0.5 mm. Naturally, to say that the base map provides 'additional' information does not mean that it does not involve some transcendent and necessary data that the technician must analyse and assess for consideration in the definition of the proposed city plan. It is also clear that due to the drawing techniques and tools available at the time, every attempt was made to avoid dashes and/or dots to save time and avoid errors. Only a few technicians use topographic representation as a sufficiently significant graphic instrument, which makes its presence and notoriety deliberate in the representation of the idea of the planning they have created (**Fig. 3**).

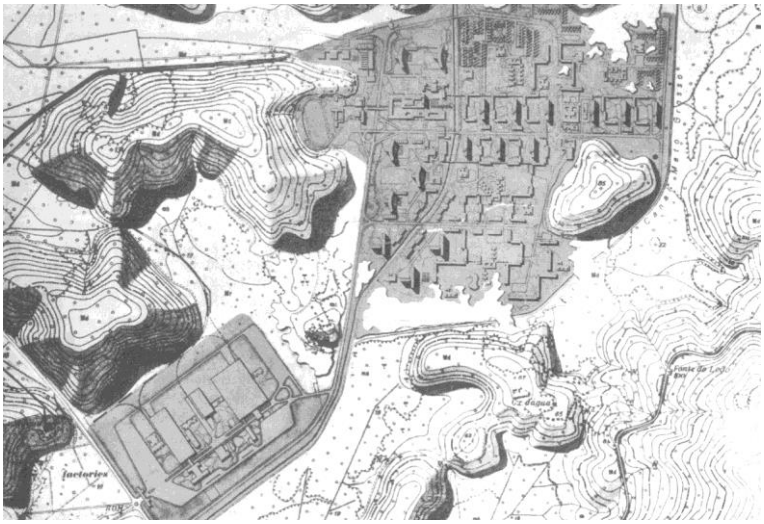

Fig. 3. Ground plan of 'Cidade dos Motores' in Brazil. This new city was designed by J.L. Sert in 1945. It is a city between Rio de Janeiro and Petropolis which was planned for 25,000 people. Intentionally J.L. Sert sought to leave the hills surrounding the city full of vegetation, concentrating the construction in the flat regions of the land and this is what he wanted to show with the excessively highlighted representation of the topography of the hills (Freixa & Rosolia, 1981).

3. GRAPHYC DEVELOPMENT

3.1 Period 1980-1989

Main graphic characteristics of the period 1980-1989:

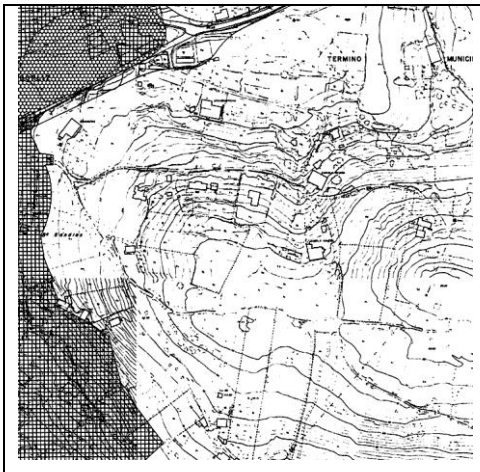

Cartographic base: Conventional topography based on topographic surveys completed with tachymetric surveys.

Lines:
Predominant thickness: 0.2 mm.
Range of thicknesses: Group 0.8/1.2
Types of lines used: Continuous
Colour: Black and white

Patterns and textures: Not available

Text:
Predominant thickness: 0.2 mm.
Typography: ISO

Colour: Black and white
Reproduction technique: Heliographic
Delineation technique: Manual

Fig. 4. Representative example of the graphic font of the period 1980-1989 (Author's file).

3.2 Period 1990-1999

Main graphic characteristics of the period 1990-1999:

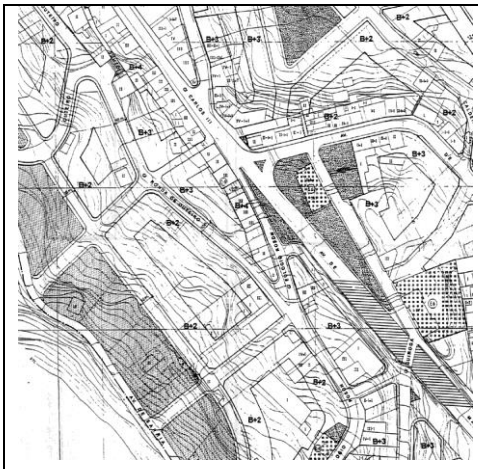	**Cartographic base:** Conventional topography based on topographic surveys. **Lines:** Predominant thickness: 0.1 mm. Range of thicknesses: Group 0.3/0.5 Types of lines used: Continuous Colour: Black and white **Patterns and textures:** Not available **Text:** Predominant thickness: 0.1 mm. Typography: ISO **Colour:** Black and white **Reproduction technique:** Heliographic **Delineation technique:** CAD tools

Fig. 5. Representative example of the graphic font of the period 1990-1999 (Author's file).

3.3 Period 2000-2015

Main graphic characteristics of the period 2000-2015:

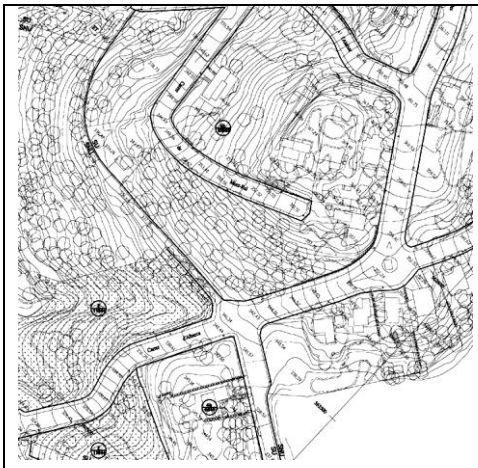	**Cartographic base:** Conventional topography based on topographic surveys. **Lines:** Predominant thickness: 0.1 mm. Range of thicknesses: Group 0.3/0.5 Types of lines used: Continuous Colour: Black and white **Patterns and textures:** Not available **Text:** Predominant thickness: 0.1 mm. Typography: ISO **Colour:** Black and white **Reproduction technique:** Heliographic **Delineation technique:** CAD tools

Fig. 6. Representative example of the graphic font of the period 1990-1999 (Author's file).

4. FINAL CONCLUSIONS: FROM THE 1990s TO THE LASTEST TRENDS

During the 1990s, CAD tools were to make delineation easier but would also be limited by the systems for printing and reproducing the maps made. While the use of CAD tools facilitated the recovery and the addition of colour to base maps and planning drawings, they were extremely limited, on the one hand, by the existing printing devices, which still worked with varieties of technical pen tips, and, especially, due to the maintenance of the blueprint process of generating copies. These limitations meant that, despite the availability of new drawing tools that allowed enhancing the quality of the work and incorporating colour, it was this latter issue that was sacrificed, due to the limitations that still existed when transferring the drawing onto a 'paper medium'. It should be mentioned, however, that during this period, the drawing tools hitherto used to draw plans disappeared. The templates of letters and symbols or decals of patterns and textures are elements that were quickly eliminated, since the CAD engines and their utilities would render them completely unnecessary.

From the end of the 1990s the use of large format inkjet printers started to become generalized. In this case, generalization meant that their price allowed the incorporation of these printing tools a reasonable cost. Thus, planners could no longer incorporate colour into their plans. And this happened for two reasons: firstly because computer-assisted design programmes have allowed this since some time ago, and secondly, and in this case more decisively, because machines were available that enabled colour printing and copying of the plans that had been drafted, and at a more than acceptable cost. Copying was now replaced by the printing of as many originals as required.

Changes in the fonts used to annotate the various aspects of the plans, the use of several types of lines, the progressive reduction of the general thickness of the lines that provided the precision and clarity of the drawing, the use of colours or thicknesses that keep the base map on a visual second level, etc., are variations on the use of graphic resources that have been implemented and that, seen in their entirety, have brought clear graphic and visual benefits to urban planning drawings. This introduction of changes in instrumental techniques seems not to have finished. Today, consulting on paper has been replaced with consulting on computer screens as well as the use of photoplans. Doubtless there will be new changes in the graphic approach to new urban planning documents. Referring to the new trends observed, it must be stated that the progressive incorporation of colour in urban planning plans has facilitated the inclusion of a great deal of data, especially in base maps, that sensibly, were previously disregarded or ignored in order simplify the map visually.

The help that the nuance of colour may infer in these data now allows its incorporation. The use of the colour grey, which relieves contour lines of their visual impact, even allows the inclusion of data such as 'dot clouds', which now can be added in order topographically and altimetrically to specify concrete and specific areas of the territory, in view of the need for a more accurate study (**Fig. 7**). This is because the categorization of the land, which is achieved with the addition of colour, makes reading the document and the hierarchy of graphical aspects easier over the topographic and cadastral elements represented.

Maps in which the topographic representation of the terrain is not too important are usually those of rather built-up areas. In these cases, the importance of the base map lies mainly in the sub-divisory or cadastral aspect, with the orography of the territory losing much of its importance and, generally, avoiding its representation.

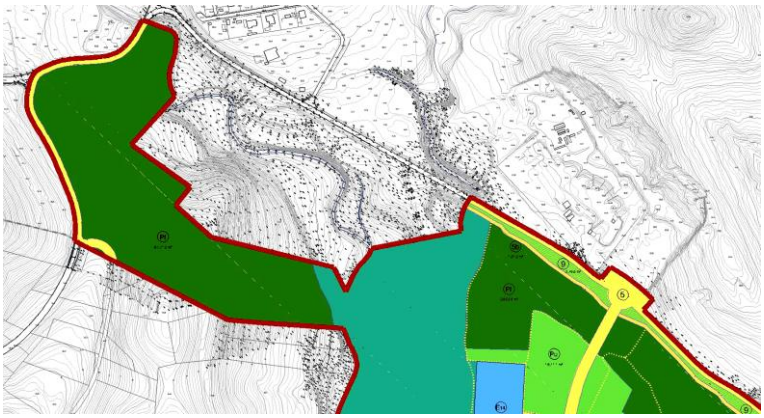

Fig. 7. Part of the land classification map of the Sector 'Pla de Ponent' – Gavà Town Council (Catalonia-Spain)- 2008. Observe how the base map includes data –in this case dot clouds- in order topographically to specify certain areas of the territory (Gavà Town Council, 2008).

The mechanisms of representing cadastral and plot data are usually similar to those are used to represent topographic base maps. The addition of colour in maps and drawings clearly shows the planned areas and at the same time categorizes them. The base data are usually represented with very thin lines, or by using the range of greys to reduce their visual importance and not to disturb the observer in their reading and understanding of the map (**Fig. 8**).

Fig. 8: Plan to renew the district of 'Kanaaloevers' in the Dutch city of 'Apeldoorn', 2008. The base map, basically cadastral and sub-divisory, is drawn using fine lines and in the range of greys (Apeldoorn Town Hall, 2008).

More recently work has also been performed using orthophotoscopic maps as their base map maps, which give a very clear picture of the terrain and, at the same time, of how the project will be superimposed.

The advantage of this type of drawing is that it shows the viewer very clearly the implementation of what has been planned and how it will be organized on a real image of the territory. For the 'layperson' it is an especially useful resource since it allows visually identifying the region for the future arrangement and, at the same time, enables getting a clear idea, a bird's eye view, of the final outcome of the foreseen planning. However, this type of graphic representation is not, a priori, a widely used tool for the performance of urban planning projects in the development phase, but is rather used as a base map of final plans for presentation or 'layouts'.

To conclude this section, there must be mention of the incorporation of photoplans as base maps. Photoplans are aerial photographs enlarged to the desired size and are basically used to make interpretations of conventional topographic maps.

Recently, it has started to become commonplace for both zoning plans as well as floor plans –Layouts or Master Plans-, to be rendered on the basis of photoplans where, by means of more or less opaque colours, the zonifications, roadways, plots, etc. that have been planned are superimposed. Thus, the town planner will draw on the photograph of the territory all that he wishes to be represented, thus replacing the traditional layout.

Certainly, from a purely technical point of view, the drawing can be considered to lose the clarity and precision that should always be maintained, and it is rather an image intended for the non-specialist that does not allow upholding the necessary level of technical rigour. We must consider that the use of photoplans may pose certain problems in the management of 'extensive graphic information' involved in this 'new' base map Studying in detail the adaptation of the photoplan as a new graphic resource applicable to new ways of presentation, publication and consultation of urban planning work appears to be a field of clear interest to the urban planner (Gomis & Turón, 2017). Nevertheless, it is a resource that we are seeing increasingly, especially on the urban planning information pages that can be found on the internet. Far more common and available in this new medium than on paper, this type of representation is beginning to set the trend in the new presentations of regional planning.

REFERENCES

Apeldoorn Town Hall, 2008. *Cultural Heritage: Apeldoorn (The Netherlands)* [online] Available at: http://www.planum.net/cultural-heritage-the-netherlands [Accessed 23 March 2017]

Aradillas, M. & Cabezas, F. (1992). *Dibujo y sistemas de representación: Planos acotados y dibujo topográfico*. Universidad de Sevilla: Escuela universitaria de Ingeniería Técnica Agrícola ed.

Baiocchi V. & Maurizio C. (2000). Problemi dei calibrazioni di file raster e vettoriali in un sistema informativo territoriale. *Bolletino della società italiana di topografia e fotometria*. Vol. 1, pp. 23-32.

Baiocchi V., Lelo K., Milone M.V., Mormille M. & Tanga E. (2013). Knowing the past for managing the present: a comparison between historical cartography and satellite images for the study of Rome's city centre. *Geographia Technica*, Cluj University Press. Issue 8 No. 1, pp. 17-27.

Bosselmann, P. (1997*). Representation of places: Reality and realism in city design*. Berkeley, University of California Press.

Bosma, K. & Hellinga, H. (1997). *Mastering the city: North-European city planning 1900-2000.* Rotterdam: NAi Publications.

Cattor, B. & Perkins, C. (2014). Re-cartographies of Landscape: New Narratives in Architectural Atlases. *The Cartographic Journal*. Volume 51, Issue 2: Cartography and Narratives.

Corbella, D. (1983). *Dibujo Técnico. Elementos de normalización*. Madrid: Corbella Barrios, David.

Deforge, Y. (1975). *Le graphisme technique*. Paris: Université René Descartes.
Desimini, J. & Waldheim, C. (2016). *Cartographic Grounds: Projecting the Landscape Imaginary*. New York NY: Princeton Architectural Press.
Dondis D. & González J. (1976). La sintaxis de la imagen: Introducción al alfabeto *visual*. Barcelona: Gustavo Gili.
École nationale des sciencies geographiques (1999). *Cartographie -Volume 1- Sémiologie graphique et conception cartographique*. Cité Descartes, Champs-sur-Marne: École nationale des sciencies geographiques.
Esteban, J. (2007*). L'ordenació urbanística: Conceptes, eines i pràctiques*. Barcelona: Diputació Barcelona.
Freixa, J. & Rosolia, O. (1981). *Josep Ll. Sert*. Barcelona: Gustavo Gili.
Gavà Town Council (2006). Modifiació del Pla General Municipal/Pla de Ponent. Available at: http://www.gavaciutat.cat/documents/1694232/1730163/04.+Zonificaciomodiplaponent.pdf/7275230f-fce1-43ad-a5ff-e6efc34929ff [Accessed 23 March 2017]
Gomis, J. & Turón C. (2017). From layout to photoplan: reflections on the "rePRESENTATION" of urban planning. *Geographia Technica*, 12 (1), pp 57-63.
Piedmont-Palladino, S. (2007). *Tools of the Imagination: Drawing tools and technologies from the eighteenth century to the present*. New York NY: Princeton Architectural Press.
Sambrico, C. (1990). El "Límite" de la ciudad ilustrada: La ordenación de un espacio urbano. *ARQUITECTURA (Revista del Colegio Oficial de Arquitectos de Madrid)*. Issue September-December 1990, No. 286-287 pp. 168-183.
Zell, M. (2008). *The architectural drawing course: Understand the principles and master the practices*. London: Thames & Hudson.

ASSESSMENT OF EFFECTIVENESS OF COASTAL PROTECTION STRUCTURES FOR ENSURING A CONSTANT LAGOON-SEA WATER EXCHANGE IN THE NORTH-WESTERN BLACK SEA REGION

Dmytro KUSHNIR[1], Yuri TUCHKOVENKO[1]

DOI: 10.21163/GT_2018.131.07

ABSTRACT:
Coastal lagoons of the Northern-Western Black Sea region show a long-term tendency in decreasing their water volume while increasing in water salinity as well as in nutrient and pollutant concentration. This occurs due to a limited connection between the lagoons and the sea, on the one hand, and the significant negative freshwater balance, on the other hand. To compensate this, a constant multi-directional water exchange with the sea through connecting canals is needed for the lagoons. However, the connecting canals require marine engineering, ensuring the protection from the sand deposition at their sea parts, in order to guarantee a year-round bidirectional 'sea-lagoon' water exchange. In the present work, a case study has been implemented to the Tylihulskyi Lyman lagoon, for which the existing canal has been reconstructed. A coupled numerical model for currents, waves and sediment transport has been used to estimate the efficiency of various engineering options of hydroengineering protective structure, which is being constructed at the sea part of the restored artificial canal, connecting the Tylihulskyi Lyman Lagoon with the Black Sea. A real storm pattern with maximum sediment transport has been simulated. Four variants of the engineering design of hydroengineering structure for wave and sediment protection were considered. Results have shown that the optimal solution for the hydroengineering structure is the variant comprised of parabolic-shaped groynes and the underwater breakwater. Reduction in the intake of sediments into the canal is achieved by sedimentation at the entrance to the protective structure. Therefore, under a long-term operation of the 'sea-lagoon' connecting canal, measures for removing the depositions accumulated in the inner sections of the protective structure should be implemented. The results of this study can be generalized to other lagoons of the Azov-Black Sea basin.

Key-words: *North-Western Black Sea Region, lagoons, canals, sediment deposition, modelling.*

1. INTRODUCTION

Coastal lagoons have an important socio-economic significance, providing a substantial natural-resource potential (fisheries and aquaculture, tourism and recreation, agricultural developments etc.), that serves the respective needs of the society (Gönenç & Wolflin, 2005). One of the intrinsic features of coastal lagoons is their connection with the sea via one or more inlets in the barrier (bar) between the lagoon and the sea. The marine part of these inlets can be clogged down with sediment, which is getting transported by the waves, tides, storm surges, and nearshore currents.

There are 16 coastal lagoons situated in the Ukrainian North-Western Black Sea region. Most of the lagoons, or 'the lymans', as they are called locally, have a man-induced and intermitted connection with the Black Sea due to climate changes and anthropogenic transformation of the sandy barriers (bars), which separate lagoons from the sea.

[1] *Odessa State Environmental University, 15 Lvivska str., Odessa, Ukraine, 65016, dkush@ukr.net.*

Small artificial inlets (canals) have traditionally been laid in the sandy bars, functioning only for a few months a year: to let young fish pass into the lagoon from the sea in spring for fattening and to catch fish that leave the lagoon in autumn. The regular cessation of the water transmission through the canals is implicated from the sand accretion on their marine part. Under continuing absence of the conjunction with the sea, the lagoons demonstrate a long-term tendency of water volume decrease and consequent shallowing, as well as increased water salinity and concentration of nutrients and pollutants in their water (Brito et al., 2016).

Significant deficiency in the annual freshwater balance has been formed in the lagoons in recent decades as a result of climate changes: increase of air temperature and growth of evaporation rates, reduction of atmospheric precipitation and freshwater inflow from tributaries (Loboda & Bozhok, 2015). Current operational mode of the 'sea-lagoon' interconnecting canals and their low water-transmitting capability make it possible to compensate the deficiency in the water balance of the lagoons, although do not ensure their complete flushing (Viero & Defina, 2016). Bielecka et al. (2015) showed that the effective solution to the problem of stabilization of hydro-ecological regime of the lagoons lies in ensuring the constant intra-annual multi-directional water exchange with the sea through the canals with a higher water-carrying capacity.

During the winter-spring period of high water, initiated by rivers and streams flowing into the lagoons, the excess of the monthly average water level in the lagoons over the sea level takes place under minimal evaporation rate from the lagoons' water surface. Along with the wind-induced water level variations in the sea and in the lagoons, this excess is expected to provide the multi-directionality of the 'sea-lagoon' water exchange (Tuchkovenko, Kushnir & Loboda, 2015).

The multidirectional water exchange with the sea will lower the rates of salt accumulation in the lagoons and decrease the trophicity of their water, since the sea water typically has much lower salinity and nutrient concentration than the water within the lagoons (Tuchkovenko, Bogatova & Tuchkovenko, 2015). For guaranteeing a year-round operational mode of the canals, it is necessary to protect them from shoaling, resulted from the deposition of sand, which is being transported at the sea side (Tuchkovenko & Loboda, 2014).

The objective of this work is to estimate, on the basis of the results of numerical modelling, the efficiency of different variants of the engineering design of hydroengineering structure, located in the sea part of the reconstructed artificial canal, connecting the Tylihulskyi Lyman Lagoon (TLL) with the sea, in terms of minimizing the deposition of sediment.

2. MATERIAL AND METHODS

2.1 Study site

The Tylihulskyi Lyman Lagoon (46.65833-47.08833° N, 30.955-31.21167° E) is situated on the Ukrainian part of the North-Western Black Sea coast (Fig. 1). It has a surface area of 129 million m^2 and a water volume of 693 million m^3. The length of the lagoon is now 52 km and the width varies from 0.2 to 5.4 km in particular sections. The mean depth in the lagoon is 5.4 m and the maximum depth is 22.2 m in the southern part. The northern part of the lagoon is shallow, with depths less than 4 m (Tuchkovenko, Loboda & Khokhlov, 2015).

The lagoon is separated from the Black Sea with a natural sand bar. In the late 1950s, in an effort to connect the lagoon with the sea, an artificial canal for fishery purposes was laid across in the bar. The canal is 3.3 km long and 3 m deep. The southern part of the canal, which is adjacent to the sea, has become much shallower over the years (**Fig. 1**). The bottom depth there averages a few dozen of centimeters only.

Since 2001, the canal has been in unsteady operation, functioning merely for several months in a year. For instance, in 2013 the canal was opened for 40 days in spring and approximately for 30 days in autumn. In spring and autumn 2014 the canal functioned for 26 and 35 days respectively. As a result of the weak water exchange with the sea, insufficient to compensate for the deficit of fresh water balance, the water level in the lagoon has decreased by 1.5 m in 5 years, compared to the sea level. Water salinity in the lagoon has increased from 19-20 ppt to 27-35 ppt over this period.

The Tylihulskyi Lyman Lagoon along with the territories adjacent to its coast is included to the Natural Reserve Fund of Ukraine and to the network of sites of Important Bird and Biodiversity Area (IBAs) Programme. It is designated as a Wetland of International Importance according to the Convention on Wetlands, called the Ramsar Convention (Gubanova et al., 2015).

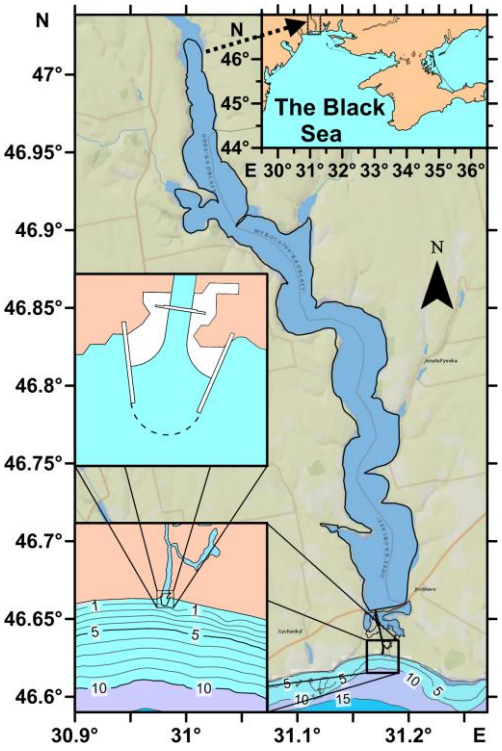

Fig. 1 Map showing the Tylihulskyi Lyman Lagoon (TLL) with adjacent coastal area. Insets: locations of the TLL on the North-Western Black Sea coast, the 'sea-lagoon' interconnecting channel and the constructed hydroengineering structure for wave and sediment protection.

For stabilizing the hydro-ecological regime of the lagoon, a project of the reconstruction of the 'sea-lagoon' connecting canal has been developed. The project involves the canal deepening to 2 m relative to the mean annual sea level mark and construction of a hydroengineering structure for wave and sediment protection on the sea end of the canal. The problem of choosing the most effective embodiment of this hydroengineering structure is considered in this article.

2.2 The Delft3D modelling suite

For this case study, a 2D version of the Delft3D-FLOW numerical hydrodynamic model, coupled online with the Delft3D-WAVE module for calculating the propagation and transformation of wind wave parameters (based on the third generation SWAN spectral model, version 40.72ABCDE) was applied (http://oss.deltares.nl/web/delft3d).

This integrated modelling suite can simulate the stirring, movement and deposition of the set of different sediment fractions under the influence of wind-wave currents. The Delft3D-FLOW hydrodynamic module solves two- and three-dimensional Navier-Stokes and transport equations for an incompressible fluid under the shallow water and Boussinesq assumption on the curvilinear or rectilinear grid. The Delft3D-WAVE module simulates the propagation, breaking and transformation of the wind waves at a distance from the shore and in the shallow water, assimilating input information about the water level and currents, modelled by the Delft3D-FLOW module. Simultaneously, the sediment transport and morphology module Delft3D-MOR calculates bed load and suspended sediment transport and bottom deformations at each flow time step.

The overall mathematic structure of the Delft3D morphodynamic model is described by Lesser et al. (2004). The model was used for direct application at the Frisian Inlet, located in the Dutch Wadden Sea, to investigate the long-term development of the bathymetry of tidal inlet systems (Van Leeuwen, Van der Vegt & de Swart, 2003).

Using 2DH and 3D hydro-morphodynamic models, which were applied to the Patos Lagoon, a coastal lagoon connected to the inner Shelf of Cassino Beach, South Brazil, Vinzon et al. (2009) concluded that the remote wind has the most influence on the lagoon's water exchange with the sea.

The first simulation scenario with multiple sediment fraction settings applied to hindcast the morphologic change in San Pablo Bay, a subembayment of the San Francisco Estuary, California, USA, on a decadal time scale by means of a 3-D numerical model (Delft3D), was presented in the work (Van der Wegen, Jaffe & Roelvink, 2011).

Transport of a mixture of cohesive sediments and sand in the Paranagua Estuarine Complex in the south of Brazil, which houses a navigation canal from the Atlantic Ocean to a busy harbor, was simulated by means of a 3-D numerical model (Delft3D) for sediment transport coupled with wave-current models (Mayerle et al., 2015).

2.3 Model set-up

In the present study, both the bedload and suspended load transport of sediments were computed according to Bijker formulation, which is often used for coastal areas and takes into account the combined effect of the nearshore currents and wave stirring on the transport of sediment fractions (Smit, Reniers & Stive, 2012).

A domain-decomposition technique (Deltares, 2016) was used for the detailed spatial discretization in the marine area of the 'sea-lagoon' interconnecting canal. The Tylihulskyi Lyman lagoon and the adjoining sea water area of 50 km2 were schematized using a curvilinear grid with varying cell size from about 75 m at the coast to 300 m near the open

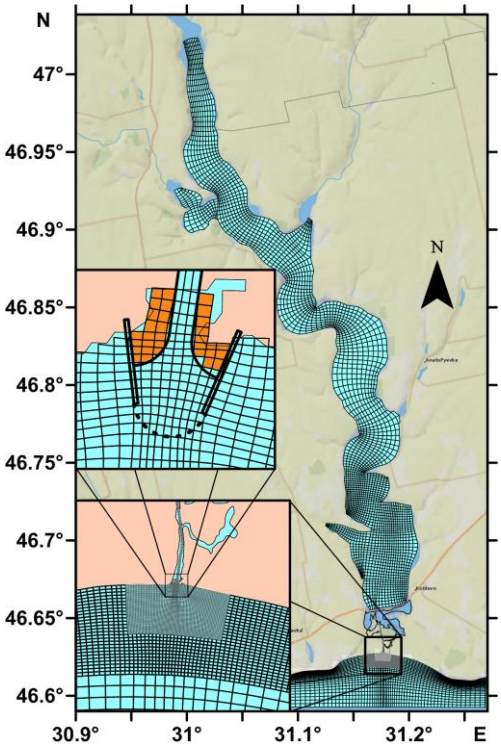

Fig. 2. Modelling grid with insets showing domain decomposition domains at the sea area near the 'sea-lagoon' interconnecting canal.

sea boundaries. Inside the main grid, two refined sub-grids were created with sequentially increasing cell sizes of 35-55 m and 7-16 m, respectively (**Fig. 2**).

Initial bathymetry of the sea area adopted in the model was based on navigational charts issued by Ukrmorcartographia branch of State Hydrographic Service of Ukraine (http://charts.gov.ua/index_en.htm). Bathymetry of the lagoon was composed of the measurements data, taken between 2010 and 2012.

Four fractions of non-cohesive sediment with different particle sizes were considered in the simulations, in accordance with the engineering and geological survey data. These fractions, conventionally named as 'pulverescent sand', 'fine sand-1', 'fine sand-2' and 'medium sand', were characterized by different median particle diameter D_{50} of 0.167 $\times 10^{-3}$ m, 0.192 $\times 10^{-3}$ m, 0.214 $\times 10^{-3}$ m and 0.217 $\times 10^{-3}$ m, respectively.

In the bed, three layers of sediments with different spatially varying thickness and composition were specified.

A real storm situation of 3.5 days duration, caused by a southern wind with a speed up to 12 m s-1, was simulated. The storm was observed from 12.00 on May 15 2010 to 00.00 on May 19 2010 at the nearest to the lagoon hydro-meteorological station 'Port 'Yuzhny'.

Observational data from this station about water level, wind speed and direction, and wind waves parameters (**Fig. 3**), were used to set the boundary conditions at vertical (water-air) and lateral (sea) open boundaries of the computational domain.

The following variants of the engineering design of hydroengineering structure located in the marine part of the 'sea-lagoon' canal were simulated:

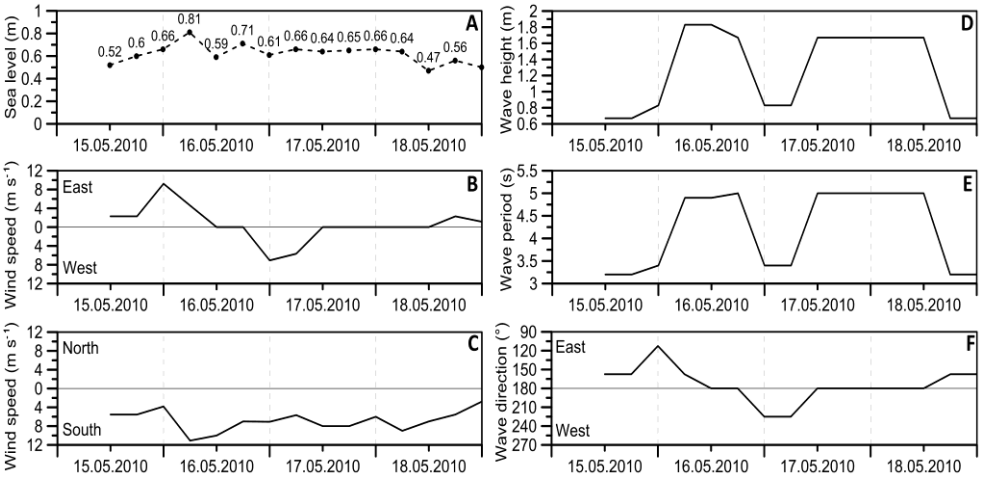

Fig. 3 Input hydro-meteorological data, used in simulations: sea level (A), wind speed at 10 meter in the East-West direction (B) and North-South direction (C), significant wave height (D), wave speed (E) and wave direction (F) recorded at the hydro-meteorological station 'Port 'Yuzhny'.

- Variant 0: the canal without the hydroengineering structure for wave and sediment protection;
- Variant 1: the canal with the hydroengineering structure in the shape of two groynes 90 m long, placed at ±75 angle to the shore and connected by an arched underwater breakwater 98 m long. A distance between the groynes at the structure entrance is 65 m, the bottom mark inside the structure is minus 2.6 m in the Baltic Height System 1977 (BHS-77);
- Variant 2: the canal with the hydroengineering structure in the shape of two groynes 125 m long with curved extreme ends without the underwater breakwater. The distance between the groynes at the structure entrance is 25 m, the bottom mark inside the structure is minus 2.6 m in BHS-77;
- Variant 3: the hydroengineering structure on the canal sea part is constructed in the shape of a spur dyke: two parallel cross-shore groynes 250 m long, with a distance of 32 m between them. The bottom mark inside the structure is minus 2.11 m in BHS-77.

A reconstructed interconnecting canal with a bottom mark of minus 2.11 m in BHS-77 and a width of 23 m was considered for all above-mentioned variants.

A computational time step was set to 9 seconds to all domain decomposition domains. Propagation and transformation of wind wave parameters were modelled online with hydro-morphodynamic simulations, with a 30-minute interval. The initial conditions for water level in all modelling domains matched together with boundary conditions at the start time of the simulation and were set to a uniform value of plus 0.12 meters in BHS-77.

3. RESULTS AND DISCUSSION

The efficiency of different variants of hydroengineering structure for wave and sediment protection in the sea part of the 'sea-lagoon' interconnecting canal was evaluated on the basis of sediment transport intensity near the canal entrance.

Fig. 4 shows modelled significant wave heights in meters and mean wave directions. The depth averaged currents for different options of the 'sea-lagoon' canal reconstruction are shown in **Fig. 5**. The passing of waves to the sea part of the connecting canal is being blocked most successfully under variant 1 of the structure, which includes the construction of the underwater breakwater (Fig. 4B). Without the underwater breakwater (variants 2 and 3), waves are passing inside the protective structure that leads to the formation of a jet directed from the entrance of the sea part of the structure towards the sea end of the canal (see **Figs. 5C, 5D**).

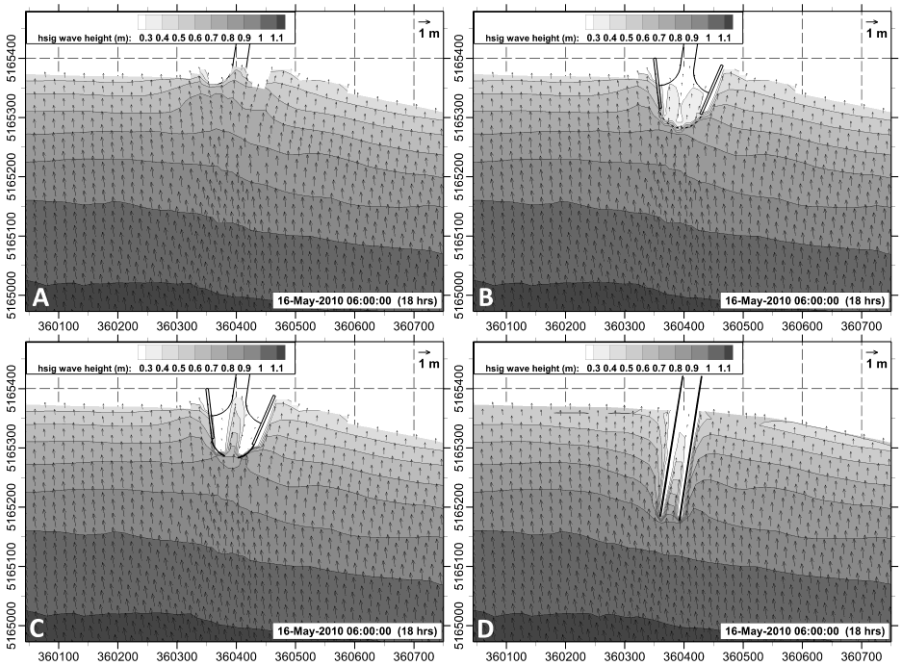

Fig. 4. Computed significant wave heights and mean wave directions after 18 hours from the start of the simulation under different variants of the 'sea-lagoon' canal reconstruction: variant 0 (A), variant 1 (B), variant 2 (C), variant 3 (D).

Fields of total sediment unit flux are shown in **Fig. 6**. When implementing variant 1 of the hydroengineering structure, the intensity of sediment transport in the interior of the structure and at the entrance to the 'sea-lagoon' canal reaches to its minimum. The maximum sediment transport directed towards the channel corresponds to simulated variant 0 without the protective hydroengineering structure. The area of intensive sediment transport with explicit directionality from the entrance of the structure towards the sea end of the canal is being formed in the simulations with variants 2 and 3 (**Figs. 6C, 6D**).

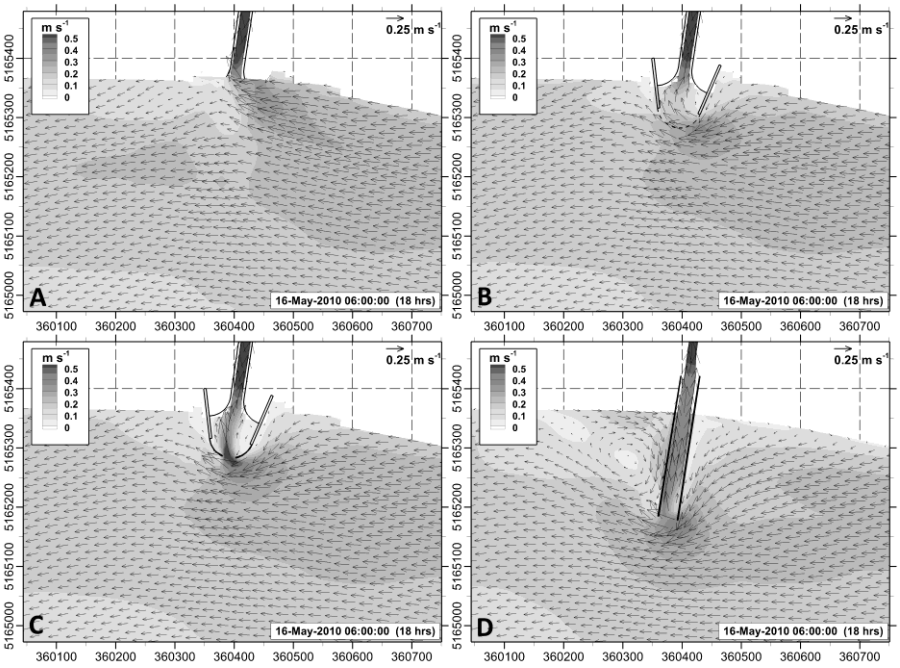

Fig. 5. Depth averaged currents after 18 hours from the start of the simulation under different variants of the 'sea-lagoon' canal reconstruction: variant 0 (A), variant 1 (B), variant 2 (C), variant 3 (D).

The results above support the conclusion that the most effective variant of the hydroengineering protective structure in terms of minimizing the sediment transport into the canal is the variant 1. The variant 3 of the protective structure is the second in effectiveness amongst the modelled variants.

In **Fig. 7** are shown the final depth changes at the end of the modelling period in meters, obtained from simulations under different variants of the 'sea-lagoon' canal reconstruction. Reduction in the intake of sediments into the canal is achieved by sedimentation at the entrance to the protective structure caused by the decrease in transporting capability of the hydrodynamic flow. Essentially, protective structures are the traps for suspended sediment coming from the open sea part of the modelling domain. Therefore, under a long-term operation of the protective structures, measures for removing the depositions accumulated in their inner sections should be implemented. It is seen that bands of erosion are formed inside the protective structure in the variants 2 and 3 (**Figs. 7C, 7D**), which increases the transport of sediments into the connecting channel.

The considered variants of hydroengineering structures for wave and sediment protection were analyzed additionally for compliance with the fishery requirements imposed on the activity in the lagoon and in the canal. Under the variant 3 of the protective structure (the spur dyke), dykes 250 m long completely block the shoreline area, preventing the migration of fish from the sea to the canal. The spurs also block a longshore sediment transport, which will lead to the development of such phenomenon as downstream scour and other adverse morpho-lithodynamic processes.

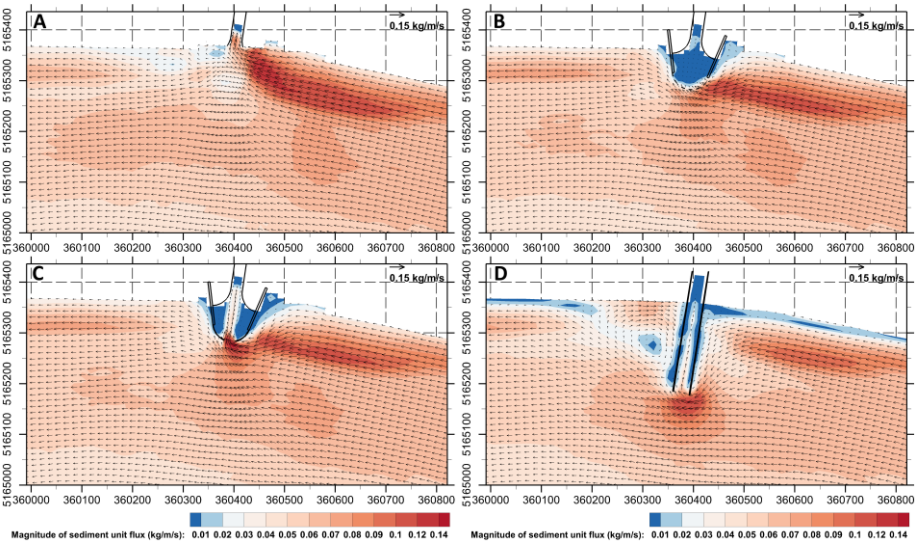

Fig. 6. Computed patterns of total sediment unit flux after 18 hours from the start of the simulation under different variants of the 'sea-lagoon' canal reconstruction: variant 0 (A), variant 1 (B), variant 2 (C), variant 3 (D).

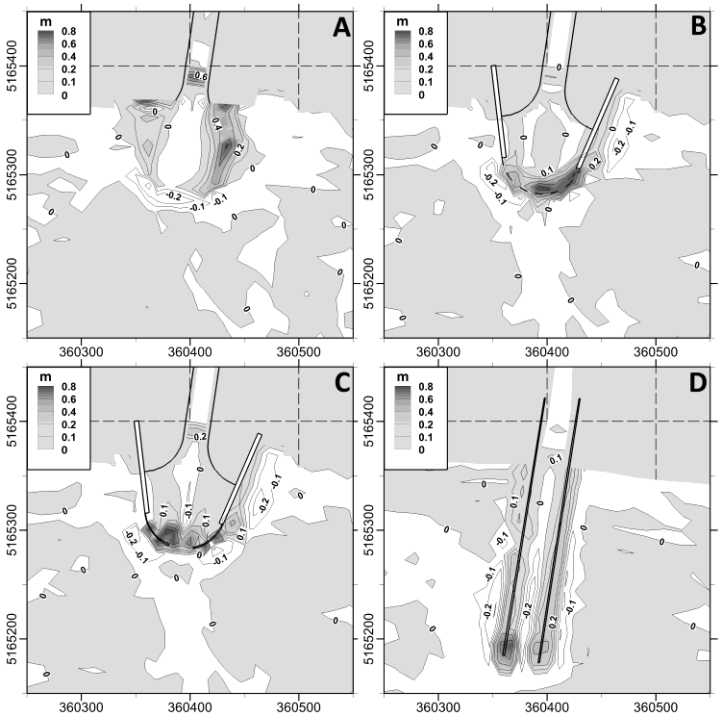

Fig. 7. Calculated depth change at the 'sea-lagoon' canal entrance under different variants of its reconstruction: variant 0 (A), variant 1 (B), variant 2 (C), variant 3 (D).

At the same time, variant 1 (a parabolic arrangement of dykes with the underwater breakwater) is perfectly adequate for fishery purposes in its parameters and intended mode of operation.

4. CONCLUSIONS

The most effective variant of the hydroengineering structure for wave and sediment protection in the sea part of the 'Black Sea-Tylihulskyi Lyman Lagoon' interconnecting canal was chosen, based on the results of the modelling of wave and wind induced currents and sediment transport using the suite of process-based numerical models.

This variant, which ensures a minimal deposition of sediment, represents two groynes 90 m long, placed at ±75 angle to the shore and connected by the arc-shaped underwater breakwater 98 m long at their sea ends. A long term operation of the structure presumes a recurring removal of the sediment accumulated in its interior.

Due to the significant increase in the deficit of the annual fresh water balance in the lagoons of the North-Western Black Sea caused by climate changes, the problem of ensuring the regular operation of artificial canals connecting the lagoons with the sea is still to be solved for a number of lagoons of the Azov-Black Sea basin: Molochny Lagoon, Budak Lagoon, Dofinovsky Lagoon, Tuzlov group of lagoons, etc. Therefore, the findings of this study can be generalized to other lagoons of the Azov-Black Sea basin.

REFERENCES

Bielecka, M., Robakiewicz, M., Zalevwski, M., Khokhlov, V., Tuchkovenko, Yu. & Lloret, J. (2015) Lagoons impact integrated scenarios. In: Lillebø, A.I., Stålnacke, P. & Gooch, G.D. (eds.) Coastal Lagoons in Europe: Integrated Water Resource Strategies. London, IWA Publishing. pp. 211-216.

Brito, A.C, Newton, A., Tett, P. & Fernandes, T.F. (2012) How will shallow coastal lagoons respond to climate change? A modelling investigation. Estuarine, Coastal and Shelf Science, 112, 98-104.

Deltares (2017). Delft3D-FLOW – Simulation of multi-dimensional hydrodynamic flows and transport phenomena, including sediments – User Manual. Hydro-Morphodynamics. Deltares Systems, Delft, the Netherlands. Available at: http://content.oss.deltares.nl/delft3d/manuals/Delft3D-FLOW_User_Manual.pdf.

Gönenç, I.E. & Wolflin, J.P. (eds.) (2005). Coastal Lagoons: Ecosystem Processes and Modeling for Sustainable Use and Development. CRC Press, Boca Raton, Florida, USA.

Gubanova, O.R., Tuchkovenko, Yu.S, Khokhlov, V.M., Stepanenko, S.M., Baggett, S. (2015) The management story of Tyligulskyi Liman Lagoon. In: Lillebø, A.I., Stålnacke, P., Gooch, G.D. (eds.) Coastal Lagoons in Europe: Integrated Water Resource Strategies. London, IWA Publishing. pp. 87-95.

Lesser, G.R., Roelvink, J.A., van Kester, J.A.T.M. & Stelling, G.S. (2004). Development and validation of a three-dimensional morphological model. Coastal Engineering, 51, 883–915.

Loboda, N. & Bozhok, Yu. (2015) Impact of climate change on water resources of North-Western Black Sea region. International Journal of Research in Earth and Environmental Sciences, 2, 1-6.

Mayerle, R., Narayanan, R., Etri, T. & Abd Wahab, A.K. (2015). A case study of sediment transport in the Paranagua Estuary Complex in Brazil. Ocean Engineering, 106, 161–174.

Smit, M.W.J., Reniers, A.J.H.M. & Stive, M.J.F. (2012). Role of morphological variability in the evolution of nearshore sandbars. Coastal Engineering, 69, 19–28.

Tuchkovenko, Yu.S., Bogatova, Yu.I. & Tuchkovenko, O.A. (2015) Hydrochemical regime of Tylihulskiy Lyman Lagoon in modern period. Vìsn. Odes. derž. ekol. unìv. – Bull. of OSENU, 19, 126-133 (In Russian).

Tuchkovenko, Yu.S., Loboda, N.S. & Khokhlov, V.M. (2015) The physio-geographical background and ecology of Tyligulskyi Liman Lagoon. In: Lillebø, A.I., Stålnacke, P., Gooch, G.D. (eds.) Coastal Lagoons in Europe: Integrated Water Resource Strategies. London, IWA Publishing. pp. 77-85.

Tuchkovenko, Yu.S., Kushnir, D.V. & Loboda, N.S. (2015) Estimation of the influence of water exchange with the sea conditions on the water level and salinity variability in the Tylihulskyi Lyman Lagoon. Ukr. gìdrometeorol. ž. – Ukr. hydrometeor. J., 16, 232-241. (in Russian).

Tuchkovenko, Yu.S. & Loboda, N.S. (eds.) (2014) Water resources and hydroecological conditions of the Tylihulskyi Lyman lagoon. TES, Odessa, Ukraine (in Ukrainian).

Van der Wegen, M., Jaffe, B.E. & Roelvink, J.A. (2011). Process-based, morphodynamic hindcast of decadal deposition patterns in San Pablo Bay, California, 1856–1887. J. Geophys. Res., 116, 1–22.

Van Leeuwen, S.M., Van der Vegt, M. & de Swart, H.E. (2003). Morphodynamics of ebb-tidal deltas: a model approach. Estuarine, Coastal and Shelf Science, 57, 899–907.

Viero, D.P., Defina, A. (2016) Water age, exposure time, and local flushing time in semi-enclosed, tidal basins with negligible freshwater inflow. Journal of Marine Systems,156, 16-29.

Vinzon, S.B., Winterwerp, J.C., Nogueira, R. & de Boer, G.J. (2009). Mud deposit formation on the open coast of the larger Patos Lagoon–Cassino Beach system. Continental Shelf Research, 29, 572–588.

BALANCING SOIL PARAMETERS AND FARMERS BUDGET BY FEATURE SELECTION AND ORDERED WEIGHTED AVERAGING

Marzieh MOKARRAM [1], Mehran SHAYGAN [2]*, George Ch. MILIARESIS [3]

DOI: 10.21163/GT_2018.131.08

ABSTRACT:
A method is presented allowing farmers at Shiraz in the Fars province of Iran to balance in between their budget and the soil parameters. First, the three alternatives (Best-First, Greedy-Stepwise and Ranker) of the Feature Selection Method identify the most critical soil fertility parameters. Training data model evaluation indicate that the Greedy-Stepwise feature selection algorithm (with attribute evaluator of CFS-Subset-Eval) presents the highest accuracy for the particular study area. Soil fertility is found to highly depends on Potassium, Phosphor, and Organic Carbon while Copper, Iron, Manganese, and Zinc dependencies are rejected. Finally, by utilizing Ordered Weighted Averaging, six maps with different risk levels in terms of the soil fertility are constructed allowing alternative management options according to the farmers budget. The major scientific contributions are summarized to a) the identification of soil fertility parameters, and the b) construction of maps modeling soil fertility for various degrees of uncertainty allowing agricultural cost effective planning in the study area.

Key words: *Ordered weighted averaging (OWA); feature selection algorithm; fuzzy; Soil fertility.*

1. INTRODUCTION

Crop nutrition and soil fertility elevations are important for sustainable productivity in agricultural lands. There are different methods for determination of soil fertility such as Xie et al. (2015) used principal component analysis for elevation of soil fertility. The results showed that the succession of rocky desertification (RD) had different impacts on soil fertility indicators. Nagaraja et al. (2016) used Generalized soil mass (GSM), Bulk-density-based soil mass (BDSM) and Fine-earth-volume-based (FEV) method for estimations of soil fertility in physically degraded agricultural soils. The results show that the best method for prediction of soil fertility is GSM and BDSM methods. One of the methods for determination of soil fertility is multi-criteria evaluation. The multi-criteria evaluation may be used to develop and evaluate alternative plans which may facilitate a compromise between interested parties (Malczewski, 1996).

Incorporation Multi Criteria Decision Analysis (MCDA) methods and GIS makes a strong tool for spatial planning (Asproth et al., 1999; Belkhiri et al., 2011; Haidu, 2016; Makropoulos et al., 2003; Malczewski & Rinner, 2005; Mohammad et al., 2013).

[1] *Department of Range and Watershed Management, College of Agriculture and Natural Resources of Darab, Shiraz University, Iran, Email: m.mokarram@shirazu.ac.ir*
[*2] *K. N. Toosi University of Technology, 19967-15433 Tehran, Iran, Email: mehranshaygan@gmail.com*
[3] *Open University of Cyprus, 38, Tripoleos Str., 104-42 Athens, Greece, e-mail: miliaresis.g@gmail.com*

The aim of the present study is to prepare the soil fertility maps based on the OWA operators of GIS-based multi-criteria evaluation procedures and feature selection west of Shiraz city, in the Fars province that is one of the most important centers of agriculture in Iran. Such a research effort is expected to provide the framework for cost effective agricultural planning in the particular study area. First, the factors determining soil fertility in the study area should be quantified, and then OWA method is expected to specify soil fertility at different risk levels.

2. METHODOLOGY

In order to prepare the soil fertility maps training data at 45 test sites were collected. Then Feature Selection Algorithm is expected to identify the most significant soils properties specifying soil fertility. Then maps will be constructed by spatial interpolation per significant soil property while fuzzy parameter maps should allow the definition of different risk levels with OWA. The methods description follows here under.

2.1. Feature selection

In order to select the most significant soil properties for soil fertility, the feature selection method is implemented. Feature selection has four steps (**Fig. 1**): a) Generation procedure, b) Elevation subset, c) Stopping criterion and d) Validation procedure. The feature selection implementation is shown in **Fig. 1**.

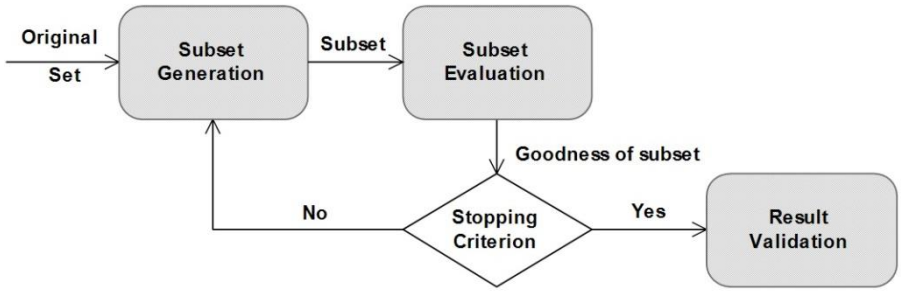

Fig. 1. The feature selection implementation.

Weka v.3.8 as learning machine (Waikato University, 2015) is used for Feature Selection. Three search methods which include Best-First, GreedyStepwis and Ranker as search method are tested as attribute evaluators. More specifically: a)for Best-First method, the CFS-Subset-Eval is used, b) For Greedy-Stepwise method, the CFS-Subset-Eval is used, and c)for Ranker method, the Info-Gain-Attribute-Eval, Gain-Ratio-Attribute-Eval, Symmetricer-Attribute-Eval, Relife-FAttribute-Eval, and Principal-Components are used.

Best-First: In the search method using Greedyhill Climbing augmented with a backtracking facility performs space of attribute subsets. In the search method starts with the empty set or full set of attributes and search forward or backward respectively. Also it start at any point and search in two directions.

GreedyStepwis: Using the space of attribute subsets performs a greedy forward or backward search. The search method starts with no, all attributes or from a free point in the space. Ranker: It ranks attributes by their individual evaluations.

In previous research efforts (Dash & Liu, 2003; Naseriparsa et al., 2013) the performance evaluation of the Feature Selection Algorithm is based on a) the Average Number of Misclassified Samples (AMS, see equation 1) and b) on the Average Relative Absolute Error (ARAE, see equation 2).

$$AMS = \frac{\sum_{i=1}^{n} MS_i}{N} \tag{1}$$

Where

MSi is the number of misclassified for each models and N is the sampling points.

$$ARAE = \frac{\sum_{i=1}^{n} RAE_i}{N} \tag{2}$$

Where

RAEi is the relative absolute error for the classification models and N is the sampling points.

2.2. Inverse Distance Weighted (IDW)

The IDW method (Burrough & McDonnell, 1998) was used for interpolating the effective data in order to determine the soil fertility at regular grid. The IDW method (see equation 3) is actually a distance-weighted average of the sampled points at a defined neighborhood.

$$\hat{z}(x_0) = \frac{\sum_{i=1}^{n} z(x_i)\, \mathrm{d}_{ij}^{-r}}{\sum_{i=1}^{n} \mathrm{d}_{ij}^{-r}} \tag{3}$$

Where x_0 is the estimation point and x_i are the data points within a chosen neighborhood. Weights (r) are related to the distance by d_{ij}.

2.3. Ordered Weight Average (OWA)

Based on the input data, the OWA combination operator associates with the i- th location of a set of order weights v = v1, v2, . . . , vn such that vj $\in$ [0, 1], j=1,2,..,n, $\sum_{j=1}^{N} v_j = 1$, and it is defined in equation 4 (Malczewski et al., 2003).

$$OWA_i = \sum_{j=1}^{N} \left(\frac{\mathrm{u}_j \mathrm{v}_j}{\sum_{j=1}^{n} \mathrm{u}_j \mathrm{v}_j}\right) z_{tf} \tag{4}$$

Where zi1 ≥ zi2 ≥ . . . ≥ zin are the sequences obtained by reordering the attribute values ai1, ai2, . . ., ain, and uj is the criterion weight reordered based on the attribute value, zij.

2.4. Study Area

The study area is located at latitude of N 29° 34′- 29° 36′and longitude of E 52° 49′ to 52° 57′ (**Fig. 2**) in the west of Shiraz, Iran. It is an area of about 44 km^2. The elevation of the study area ranges from 1,574 m to 1,722 m.

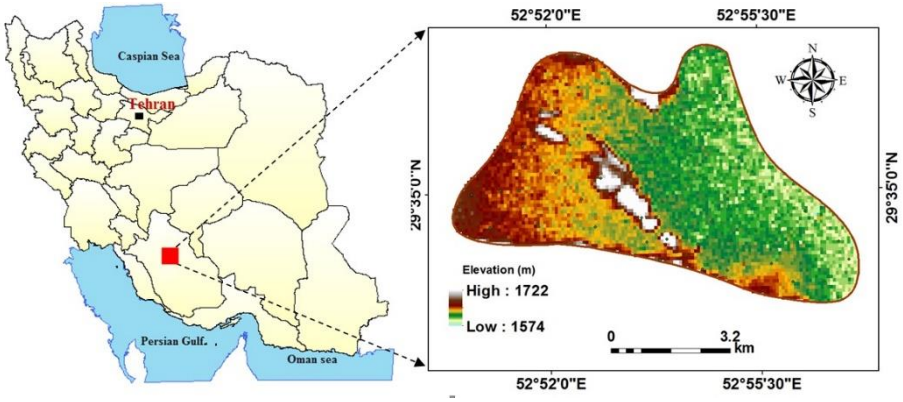

Fig. 2. Study Area and its location

The case study has a mid-latitude semi-arid cool climate (Köppen-Geiger classification: BSk). Based on the Holdridge life zones system of bioclimatic classification Shiraz is situated in or near the warm temperate thorn steppe biome. Details about climate of the study area such as temperature, precipitation are shown in **Fig. 3**.

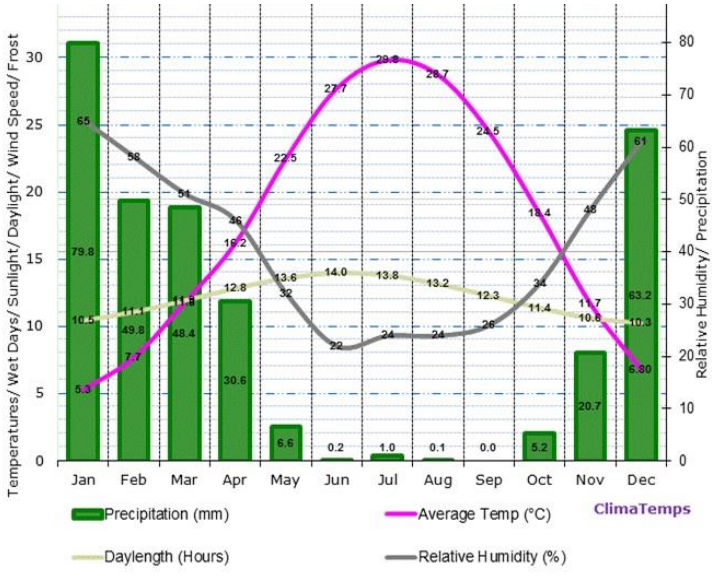

Fig. 3. Details about climate of the study area such as temperature, precipitation

3. RESULTS

In order to predict the variability of the soil fertility, some minerals were used which are named here as potassium (K), phosphor (P), copper (Cu), iron (Fe), manganese (Mn), organic carbon (OC) and zinc (Zn) (0-60 cm of soil surface); then, maps of each parameter were prepared (**Table 1**) (Organization of Agriculture, Jihad Fars province). In continue using feature selection algorithm, IDW, Fuzzy method, AHP were determined soil fertility maps with different risk levels.

Table 1.

Descriptive statistics of the data for the soil fertility (Organization of Agriculture, Jihad Fars province)

Statistic parameters	K (mg/kg)	P (mg/kg)	Cu (mg/kg)	Fe (mg/kg)	Mn (mg/kg)	OC (mg/kg)	Zn (mg/kg)
maximum	666.00	30.00	2.00	15.00	52.50	1.65	3.00
minimum	137.00	2.00	0.20	1.00	2.80	0.18	0.10
average	313.73	13.94	0.97	4.54	14.77	1.01	0.65
STDEV	104.28	6.49	0.36	2.84	10.71	0.35	0.50

3.1. Feature selection

In the study for selection of importance data using feature selection algorithm was used Weka v.3.8. In the study different combination of feature selection method are used such as: Best-First, GreedyStepwis and Ranker as search method. For Best-First used CFS-Subset-Eval as attribute evaluator. For Greedy-Stepwise used CFS-Subset-Eval as attribute evaluator. While Info-Gain-Attribute-Eval, Gain-Ratio-Attribute-Eval, Symmetricer-Attribute-Eval, Relife-FAttribute-Eval, Principal-Components used as attribute evaluator for ranker method. The more details of each methods with attribute evaluator show in **Table 2** and **Table 3**. According to **Table 2** the importance data for determination of soil fertility for Best-First (CFS-Subset-Eval) and Greedy-Stepwise (CFS-Subset-Eval) were Fe, Mn and Cu. Cu, Fe and Mn were as the importance data for Ranker (Gain-Ratio-Attribute-Eval). For Ranker (Symmetricer-Attribute-Eval), N, P and K was as importance data. For Ranker (Relife-FAttribute-Eval) the best data for determination of soil fertility were Cu, Fe and P. while for Ranker (Principal-Components), Cu, P and Mn was as importance data

Table 2.

Features selected by different feature selection methods

Search method	Attribute evaluator	Selected Features
Best-First	CFS-Subset-Eval	Fe, Mn, Cu
Greedy-Stepwise	CFS-Subset-Eval	Fe, Mn, Cu
Ranker	Info-Gain-Attribute-Eval	Cu, Fe, Mn
	Gain-Ratio-Attribute-Eval	Mn, P, Fe
	Symmetricer-Attribute-Eval	OC, P, K
	Relife-FAttribute-Eval	Cu, Fe, P
	Principal-Components	Cu, P, Mn

For analysis of feature selection algorithm and select the best methods and their performance are evaluated using C4.5 (J48) classifier. Information of the classifier show in **Table 3**. According to **Table 3** determined that the best method with the lowest number of incorrect and the highest correlation of coefficient was Ranker (Relife- squared error FAttribute-Eval).

Table 3.

Evaluation of classifiers based on J48

Search method	Attribute evaluator	Classifier model	Test mode	Correlation coefficient	Mean absolute error	Root mean squared error	Relative absolute error	Root relative	Number of correct	Correct
Best-First	CFS-Subset-Eval	Full training set	10 Fold class validates	75.29	0.105	0.229	46.77	68.62	64	21
Greedy-Stepwise	CFS-Subset-Eval	Full training set	10 Fold class validates	75.29	0.105	0.229	46.77	68.62	64	21
Ranker	Info-Gain-Attribute-Eval	Full training set	10 Fold class validates	75.29	0.105	0.229	46.77	68.62	64	21
	Gain-Ratio-Attribute-Eval	Full training set	10 Fold class validates	75.29	0.105	0.229	46.77	68.62	64	21
	Symmetricer-Attribute-Eval	Full training set	10 Fold class validates	75.29	0.105	0.229	46.77	68.62	64	21
	Relife-FAttribute-Eval	Full training set	10 Fold class validates	88	0.0706	0.15	32.89	57.11	80	5
	Principal-Components	Full training set	10 Fold class validates	75.29	0.105	0.229	46.77	68.62	64	21

Finally for determination of error and performance values used AMS and ARAE. The results of two methods show in **Table 4**. According to **Table 4** Ranker (Relife-FAttribute-Eval) had the lowest AMS (7.69) and ARAE (38.69) that selected as the best method for extraction of the importance data for determination of soil fertility.

Table 4.

Value of performance

Search method	Attribute evaluator	Performance method	
		ARAE	AMS
Best-First	CFS-Subset-Eval	55.02	32.31
Greedy-Stepwise	CFS-Subset-Eval	55.02	32.31
Ranker	Info-Gain-Attribute-Eval	55.02	32.31
	Gain-Ratio-Attribute-Eval	55.02	32.31
	Symmetricer-Attribute-Eval	55.02	32.31
	Relife-FAttribute-Eval	38.69	7.69
	Principal-Components	55.02	32.31

Finally OC, P and K from Ranker (Relife-FAttribute-Eval) was used for determination of soil fertility in OWA method.

3.2. Inverse Distance Weighted (IDW)

The IDW interpolation was used to predict K, P and OC values which are all shown in **Fig. 4**. According to **Fig. 4**, within the chosen study area, most elements in the north and parts of the south were determined to have lower amounts than other regions.

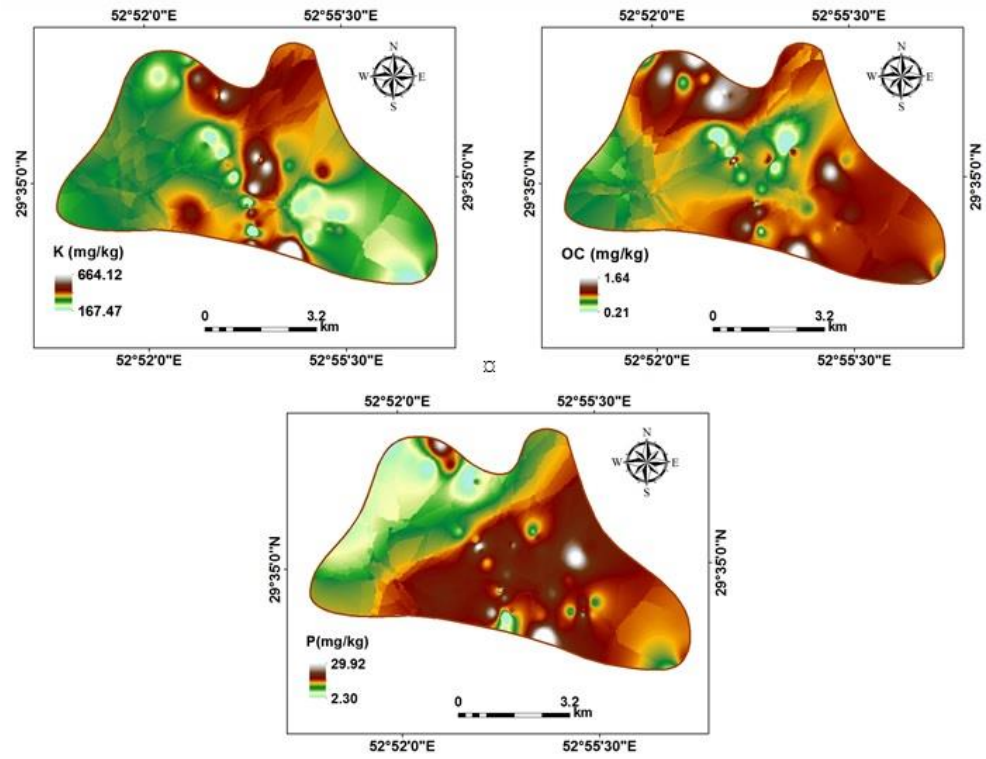

Fig. 4. Tha map of K, P and OC values which are interpolated by IDW

3.3. Fuzzy method

The membership function for each parameter (K, P and OC) was defined according to FAO (1983), and each fuzzy map was created with value range in between 0 and 1 (**Fig. 5**).

According to **Fig. 5**, the mainly east and southeast of the study area had suitable values for P parameter with fuzzy membership value close to 1, an exception being the parts in center and west of the study area. Also according to the K fuzzy map, some parts of the north, southeast and west were not suitable as well.

3.4. OWA method

In order to use OWA method was used IDRISI32 software. **Table 5** consist of six generic sets of order weights for seven factors: (1) an average level of the risk and a full trade-off, (2) a low level of the risk and no trade-off, (3) a high level of the risk and no trade- off, (4) a low level of the risk and an average trade-off, (5) a high level of the risk and an average trade-off, (6) an average level of the risk and no trade-off (**Table 5**).

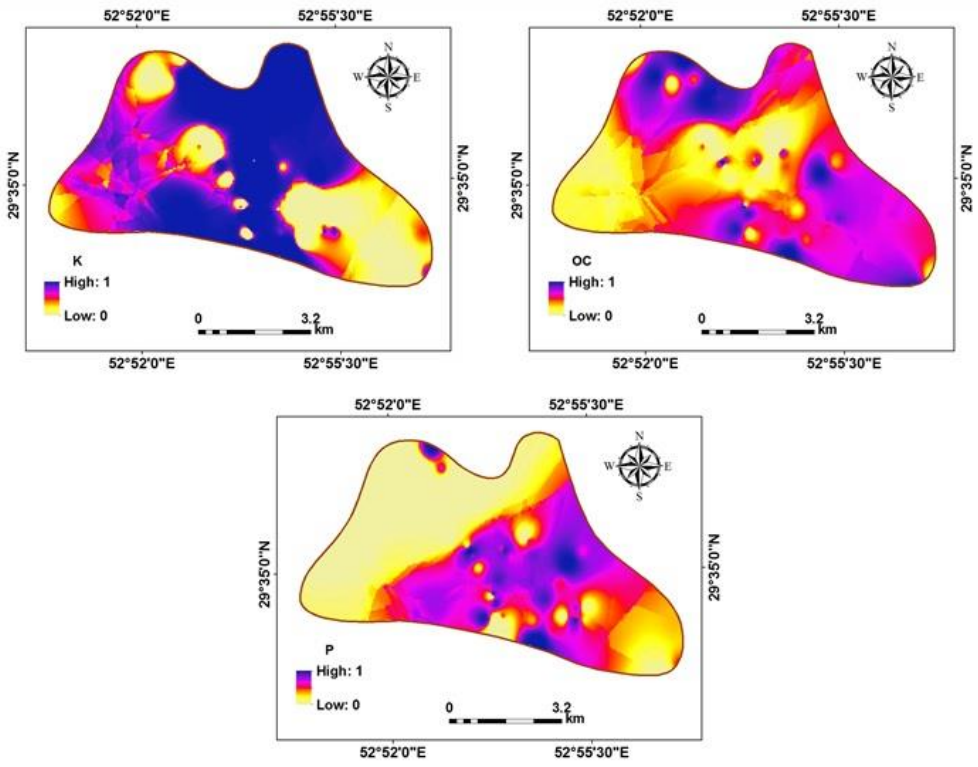

Fig. 5. Fuzzy Map for soil parameters including k, P and OC

According to **Fig. 6**, with decreasing risk (no trade-off) (**Fig. 6 (2)**), the area with high soil fertility was determined. So, that only the parts of center, south and southeast of the study area was suitable for soil fertility. Also with increasing risk (no trade-off) (**Fig. 6 (3)** all of the study had good soil fertility. According to **Fig. 6 (3)** almost the all of the study area had high soil fertility. With average risk (full trade-off) (**Fig. 6 (1)**) the all of effective parameters of soil fertility were received some weight (0.33). According to **Fig. 6 (1)** the parts of the study area had good value (except a parts of center and southwest of the study area). The **Fig. 6 (4)** showed low risk with average trade-off that in comparison of **Fig. 6 (2)** had more risk. The **Fig. 6 (5)** showed high risk with average trade-off that in comparison of **Fig. 6 (3)** had lower risk for determination of soil fertility. **Fig. 6 (6)** showed average risk with no trade-off that in comparison of **Fig. 6 (3)** had more risk.

Table 5.

Typical sets of order weights for three factors.

	(1) Average level of risk and full trade-off		
order weight	0.33	0.33	0.33
rank	1st	2nd	3rd
	(2) Low level of risk and no trade-off		
order weight	1	0	0
rank	1st	2nd	3rd
	(3) High level of risk and no trade-off		
order weight	0	0	1
rank	1st	2nd	3rd
	(4) Low level of risk and average trade-off		
order weight	0.8	0.2	0
rank	1st	2nd	3rd
	(5) High level of risk and average trade-off		
order weight	0	0.2	0.8
rank	1st	2nd	3rd
	(6) Average level of risk and no trade-off		
order weight	0	1	0
rank	1st	2nd	3rd

In fact using feature selection and select the importance data and then OWA method not only can prepare soil maps with multi-criteria decision, but also save time and money in soil science.

One of the main advantages of OWA is its ability in generating the wide variety of possibilities for different designs. In recent years some studies about soil fertility using OWA method is done by Delsouz Khaki et al. (2015), Bijanzadeh and Mokarram (2013) and Mokarram and Bardideh (2012). In some of them soil fertility is achieved by combining fuzzy algorithm and OWA method. In current research only a medium risk was used and the different risk levels is not evaluated. It is obvious that the OWA method with different risk levels can help a user such as farmer to make different decisions based on different financial situations and risk levels.

4. CONCLUSIONS

The aim of the present study was to produce the soil fertility maps based on feature selection algorithm and OWA operators of the GIS-based multi-criteria evaluation procedures in the west of Shiraz city of Fars province (Iran). Using the feature selection algorithm (Best-First, Greedy-Stepwise and Ranker) was selected the most importance parameters. Then using the OWA approach was provided a mechanism for guiding the decision maker/analyst through the multi-criteria combination procedures.

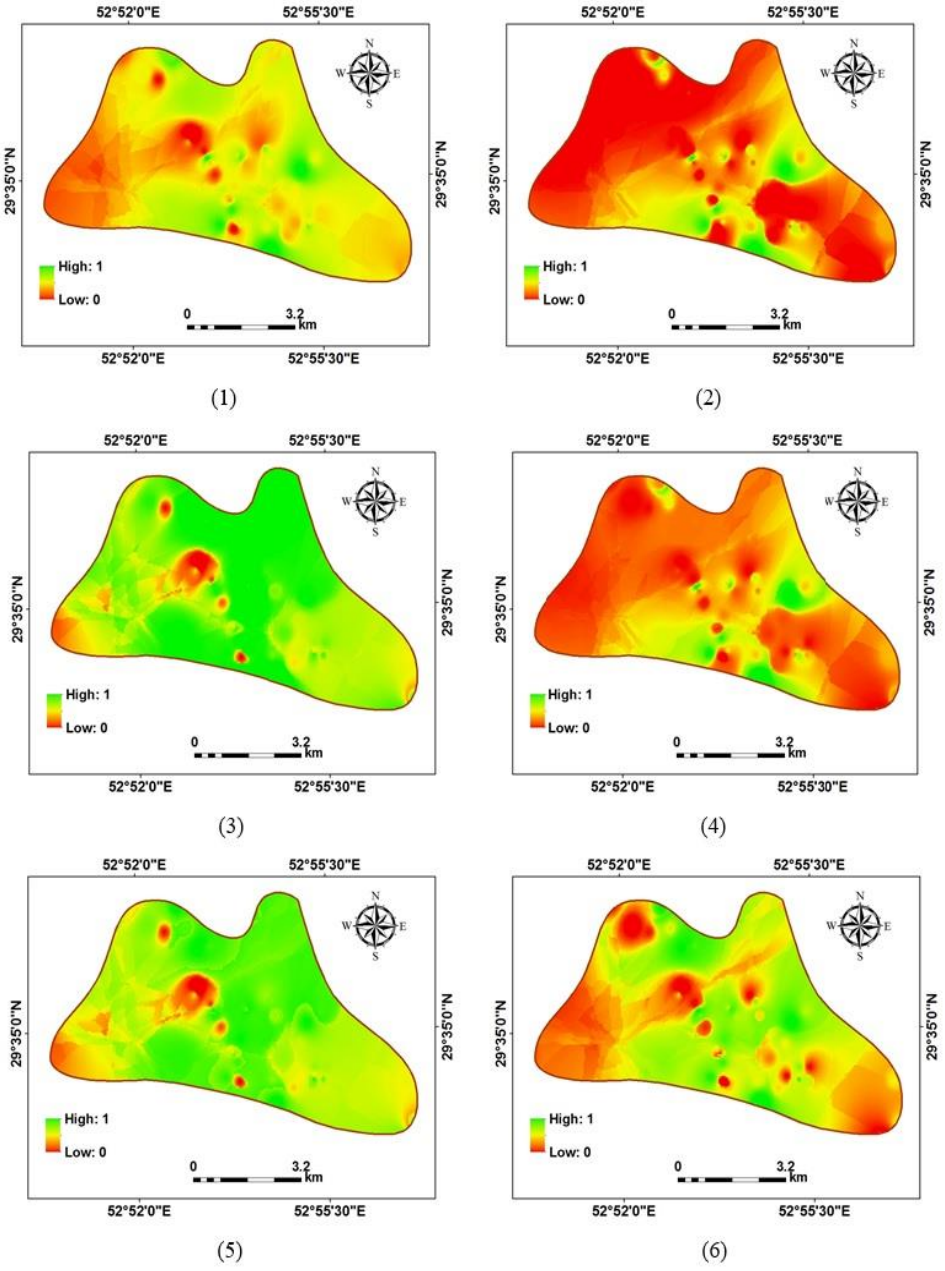

Fig. 6. The OWA map for study area based on different trade-offs. (1) an average level of the risk and a full trade-off, (2) a low level of the risk and no trade-off, (3) a high level of the risk and no trade- off, (4) a low level of the risk and an average trade-off, (5) a high level of the risk and an average trade-off, (6) an average level of the risk and no trade-off

Results showed that with decreasing the risk (no trade-off), the area with a high soil fertility was determined. Therefore, just parts of the east and southeast of the study area were considered suitable for the soil fertility. Furthermore, with increasing the risk (no trade-off), almost all of the study area had a good soil fertility. In fact using feature selection and select the importance data and then OWA method not only can prepare soil maps with multi-criteria decision, but also save time and money in soil science.

ACKNOWLEDGEMENTS

The authors would like to thanks to all personnel of Natural Resources Organization of Fars province and Organization of Agriculture Jahad Fars for their kind help.

R E F E R E N C E S

Asproth, V., Holm berg, S.C. & Håkansson, A. (1999) *Decision support for spatial planning and management of human settlements*, in Lasker, G.E. (Ed.): Advances in Support Systems Research, Vol. 5, International Institute for Advanced Studies in Systems Research and Cybernetics, Windsor, Ontario, Canada, 30–39.

Belkhiri, L., Boudoukha, A. & Mouni, L. (2011) A multivariate Statistical Analysis of Groundwater Chemistry Data, *International Journal of Environmental Research*, 5 (2), 537-544.

Bijanzadeh, E. & Mokarram, M. (2013) The use of fuzzy- AHP methods to assess fertility classes for wheat and its relationship with soil salinity: east of Shiraz, Iran : A case study. *Austoraliun journal of crop science*, 7(11), 1699-1706.

Burrough, P.A. & McDonnell, R.A. (1998) Principles of geographical information systems. *Spatial Information System and Geostatistics*. Oxford University Press, New York.

Dash, M. & Liu, H. (2003) Consistency-based Search in Feature Selection, *Artificial Intelligence*, 151, 155-176.

Delsouz Khaki, N., Honarjoo, N., Davatgar, A. & Torab, H. (2015) Soil Fertility Evaluation Using Fuzzy Membership Function (Case Study: Southern Half of Foumanat Plain in North of Iran). *Allgemeine forst undjagdzeitung*, 53-64.

Haidu, I. (2016). What Is Technical Geography. *Geographia Technica*, 11(1), 1-5. DOI: 10.21163/GT_2016.111.01

Makropoulos, C., Butler, D. & Maksimovic, C. (2003) A fuzzy logic spatial decision support system for urban water management. *Jornal of Water Resource. Planning. Manage*, 129 (1), 69–77.

Malczewski, J.A. (1996) GIS-based approach to multiplecriteria group decision making. *International Journal of Geographical Information Systems*, 10(8), 955-971.

Malczewski, J., Chapman, T., Flegel, C., Walters, D., Shrubsole, D. & Healy, M.A. (2003) GIS-multicriteria evaluation with ordered weighted averaging (OWA): case study of developing watershed management strategies. *Environment Planning*, A 35 (10), 1769–1784.

Malczewski, J. & Rinner, C. (2005) Exploring multicriteria decision strategies in GIS with linguistic quantifiers: a case study of residential quality evaluation. *Journal of Geography System*, 7(2), 249–268.

Mohammad, M., Sahebgharani, A. & Malekipour, E. (2013). Urban growth simulation through cellular automata (CA), analytic hierarchy process (AHP) and GIS; case study of 8th and 12th municipal districts of Isfahan. *Geographia Technica*, 8(2), 57-70.

Mohammad, M., Sahebgharani, A. & Malekipour, E. (2013). Urban growth simulation through cellular automata (CA), analytic hierarchy process (AHP) and GIS; case study of 8th and 12th municipal districts of Isfahan. *Geographia Technica*, 8(2), 57-70.

Mokarram, M. & Bardideh M. (2012) Soil fertility evaluation for wheat cultivation by fuzzy theory approache and compared with boolean method and soil test method in gis area. *Agronomy journal* (pajouhesh & sazandegi), 25(3), 111 -123.

Nagaraja, M. S., Bhardwaj, A. K., Reddy, G. V. P., Srinivasamurthy, C. A., and Kumar, S. (2016) Estimations of soil fertility in physically degraded agricultural soils through selective accounting of fine earth and gravel fractions. *Solid Earth*, 7, 897-903, https://doi.org/10.5194/se-7-897-2016.

Naseriparsa, M., Bidgoli, A.M. & Varaee, T. (2013) A Hybrid Feature Selection method to improve performance of a group of classification algorithms. *International Journal of Computer Applications*, Vol 69, No 17, 28-35.

Waikato University (2015) Weka software. Weka for Windows, v. 3.8.

Xie, L., W, Zhong, J., Chen, F.F., Cao, F.X., Li, J.J. & Wu, L.C.(2015) Evaluation of soil fertility in the succession of karst rocky desertification using principal component analysis, *Solid Earth*, 6, 515-524.

LAND COVER AND TEMPERATURE IMPLICATIONS FOR THE SEASONAL EVAPOTRANSPIRATION IN EUROPE

Mărgărit-Mircea NISTOR[1*], Titus Cristian MAN[2], Mostafa Ali BENZAGHTA[3], Nikhil NEDUMPALLILE VASU[4], Ştefan DEZSI[2], Richard KIZZA[1]

DOI: 10.21163/GT_2018.131.09

ABSTRACT:
Land cover and spatial variation of seasonal temperature may contribute to different evapotranspiration rates between the European regions. In order to assess the integral effect of land cover and climate on water resources, we implemented a procedure which allows defining favorability areas to high rate of evapotranspiration. Seasonal mean air temperature for the present (2011-2040) and future (2041-2070) combined with the seasonal crop coefficients of current future projections of land cover for the 2040s have been used to evaluate the various degrees of evapotranspiration at European scale. Extremely high and very high degree of evapotranspiration tendency were verified for Southern, Eastern, Western and Central of Europe during the mid-season period. The low and very low evapotranspiration favorability were found in the Scandinavian Peninsula and in the Alps, Dinarics, and Carpathian during the present period in all the seasons. In the cold season, the land cover favorability to evapotranspiration (LCFE) is low and very low in almost the whole Europe. These findings indicate that the southern and western regions of Europe are facing low water availability, decrease in surface water flow, and possible long periods of drought in the summers.

Key-words: Crop coefficients, Climate change, Evapotranspiration favorability, Europe.

1. INTRODUCTION

Europe is a dynamic continent from many points of view. Changes in land cover pattern after the 1980s and urban development were observed continuously in many locations, especially around the capitals and larger cities. Natural places, such as mountain areas and the wetlands indicate a low degree of urbanization, but at the same time, these regions are facing global natural changes. The climate is warming (Haeberli et al, 1999; IPCC, 2001) and most of the glaciers and ice lands have been retreating continuously in the last decades (Kargel et al, 2005; Oerlemans, 2005; Shahgedanova et al, 2005; Dong et al, 2013; Xie et al, 2013; Elfarrak et al, 2014; Nistor & Petcu, 2015). The main variations at

[1]*Nanyang Technological University, School of Civil and Environmental Engineering, 639798, Singapore;*
[*]*Corresponding author email: margarit@ntu.edu.sg; Last co-author email: kizz0001@e.ntu.edu.sg*
[2]*Faculty of Geography, University of Babeş-Bolyai, 400006, Cluj-Napoca, Romania, emails: man.titus@yahoo.com, stefan.dezsi@ubbcluj.ro*
[3]*Soil and Water Department, Faculty of Agriculture, Sirte University, 054, Sirte, Libya, email: benzaghta69@gmail.com*
[4]*British Geological Survey, Keyworth, Nottinghamshire, NG125GG, UK. email: nikil.nv@gmail.com*

global and continental scales come from changes in the mean air temperature which are expected to increase for the mid-century. Moreover, the natural systems are often influenced by climate change (Parmesan & Yohe, 2003; Aguilera & Murillo, 2009; Yustres et al, 2013; Jiménez Cisneros et al, 2014; Kløve et al, 2014). The most affected resources by climate change are the water resources, both freshwater and groundwater (Loàiciga et al, 2000; Bachu & Adams, 2003; Brouyère et al, 2004; Campos et al, 2013; Nistor et al, 2014; Prăvălie et al, 2014). The ecosystems are also facing climate change in many places from the globe, with significant changes in the biodiversity composition as well (Nistor, 2013; Nistor & Petcu, 2014).

In the last decades, climate change effects on water resources were claimed in details through numerous examples, regarding water quality and water quantity (Jiménez Cisneros et al, 2014). More than this, the climate change impact together with the land cover contributes to the hydrologic sensitivity of an area. Öztürk et al (2013) modelled the impact of land use on rural watershed from northern Turkey, mentioning that the hydrological processes influence watersheds with respect to meteorology, surfaces and underground characteristics. Thus, land cover represents a crucial factor in evapotranspiration, runoff, infiltration, and groundwater recharge (Öztürk et al, 2013). The runoff and evapotranspiration have been studied by Čenčur Curk et al (2014) in South-East Europe for groundwater vulnerability. Cheval et al (2017) used regional coupled models in the determination of aridity in South-Eastern Europe. In their survey, climate change and land cover have been carefully studied and several areas with high vulnerability were depicted, especially in locations with less water availability, aquifers characteristics, and pollution load index of each land cover type. Thus, an important role of surface and groundwater resources come from the evapotranspiration phenomena, which shows an essential concern for water balance and water surplus (Li et al, 2007; Rosenberry et al, 2007; Gowda et al, 2008). At the temperate zone, climate and land cover are directly responsible for evapotranspiration, a fact for which many investigations on this topic have been carried out in recent years by Ambas & Baltas (2012), Nistor & Porumb-Ghiurco (2015), Nistor et al (2016a), Nistor et al (2016b), Nistor et al (2017a), Nistor et al (2017b). They applied an original method, which assesses crop evapotranspiration at regional scale based on seasonal potential evapotranspiration, and standard seasonal crop coefficients (Kc) presented in the FAO Paper no. 56 (Allen et al, 1998; Allen, 2000). Considering this methodology, changes of climate and land cover could be problematic for many natural systems of the regions, e.g. groundwater and surface hydrology, agriculture and orchards, desertification in the dry grassland areas. Nistor (2016) determined the seasonal Kc for the Paris metropolitan area. In the Kingdom of Saudi Arabia, Güçlü et al (2017) calculated evapotranspiration using a regional fuzzy chain model. Based on the REMO and ALADIN regional climate models, Ladányi et al (2015) analyzed the drought hazard in south-central Hungary, in the Kiskunság National Park. Gao et al (2007) estimated the actual evapotranspiration over China during 1961-2002. The spatial-temporal characteristics of the actual evapotranspiration have been completed by Gao et al (2012) in the Haihe River basin from East China.

Regarding heterogeneity of the European continent and the current climate change, significant changes in the climate parameters such as temperature, rainfall, and evapotranspiration are expected for the mid-century. Considering the land cover projections for Europe, different visions over the economy, agriculture, industry, and natural ecosystems may be drawn. A method, which combines mean air temperature and land cover

to evaluate the synergy of climate and vegetation pattern on evapotranspiration parameter, could be a new issue for Europe, from many points of view.

The scope of the present paper is to propose a methodology to assess the effect of seasonal temperature and seasonal Kc on evapotranspiration following the spatial-temporal scale of Europe during 2011-2070. The second scope is to identify the favorability areas with different degrees for the evapotranspiration. Our results contribute both to the specialty literature of Europe and may be useful to policymakers for decision making

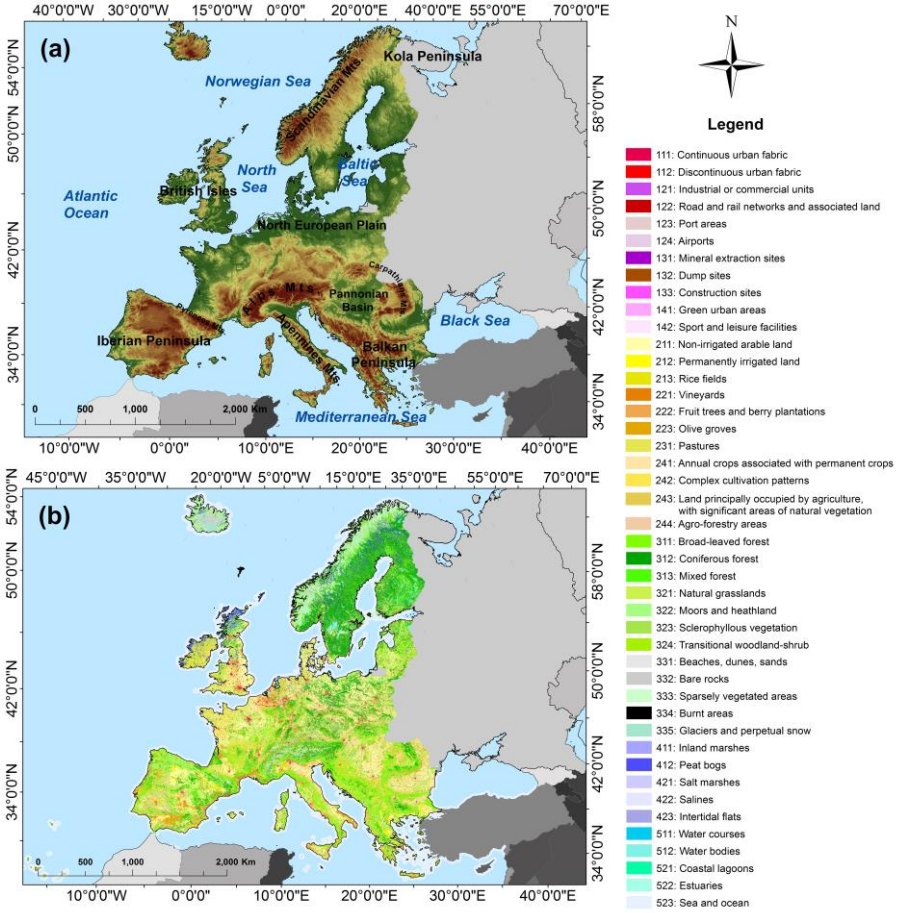

Fig. 1. (a). The physical map of European continent. **(b).** Land cover of the Europe.

regarding agricultural management and environmental planning.

2. STUDY AREA

The analyzed territory in this paper includes the Western, Northern, Southern, and Central regions of Europe. To these lands are added the British Islands and some islands from the Mediterranean Sea, e.g. Sardinia, Corsica, Aegean Islands, Baleares Islands. The

eastern sides of the continent, such as Russian, Ukraine, and Belarus have not been investigated here due to lack of land cover data. For future projections, Switzerland, Norway, and countries from the West of Balkan Peninsula do not have already completed land cover patterns. For Iceland, climate data are absent. The morphology of Europe indicates numerous landforms in correspondence with the main reliefs that are found in the territory (**Fig. 1a**). The highlands of the continent consist mainly of mountain chains: Alps Range, Carpathian Range, Dinarics Mountains, Pyrenees Mountains, Scandinavian Mountains and Apennines Mountains. The lowlands overlap to the North European Plain, Pannonian basin, South of British Islands, Romanian Plain, Po Plain. Between mountains and plains, hilly and plateau reliefs could be found. The coastline of Europe shows very articulated promontories, sea bays, fjords, and islands.

The geographical position, in the northern hemisphere between 34°35' to 80°42' latitude N and 8°59' longitude W to 66°42' longitude E and the presence of the Atlantic Ocean in the West are the main factors which influence the climate of Europe. Thus, in the North, there is more of a Baltic climate, while in the South, the Saharan and Mediterranean influences are felt. The western side of Europe together with the British Islands have more oceanic influences and in the eastern parts, the continentality is more presented. The relief arrangement and the regional wind movements induce local climate such as mountain climate, Pontic influence near the Black Sea and the transition climate between oceanic and continental could be identified in the East-central parts. The mean air temperature range from -12 °C to 21 °C and the maximum mean precipitation reaches 3500 mm $year^{-1}$. According to the Köppen-Geiger climate classification, the Cfa climate characterized by hot summers and a fully humid period was depicted in the Central, North-central, Southern, and Southeastern sides (Kottek et al, 2006). In the Scandinavian Peninsula and in the northeastern extremities, the Dfc class (cool climate) has been observed. The eastern and southeastern areas of Europe have Dfa and Dfb climates, which implies a cool climate but with hot and warm summers. The Csb climate was identified in the North of the Iberian Peninsula while in the South of the Iberian Peninsula, the Csa climate was depicted (Kottek et al, 2006). The high mountains and in the Scandinavian territory, the tundra climate is presented due to low temperatures (Kottek et al, 2006).

According to relief and climate, the vegetation of Europe is very diversified (**Fig. 1b**). The plains and hilly areas are favorable for agricultural lands, herbaceous vegetation, and grasslands. In the mountain areas up to 1800 m altitude, there extends the coniferous vegetation. Broad-leaved and mixed forests grow both in the mountains and hilly areas. The main species of trees that can be found in Europe include the oak (Quercus), elms (Ulmus), beech (Fagus), and hornbeam (Carpinus) (European Environment Agency, 2007). Transnational woodland, shrubs and pasture predominantly cover the elevated areas (over 1800 m). The coastal areas are often covered by green vegetation of various types of trees and sclerophyllous vegetation. Deltas, lagoons, and marshes are specifically for the low coastal areas such as Rhone Delta, Po Delta, and Danube Delta. European coastlines do not miss artificial port areas, man-made infrastructure and dams.

3. MATERIALS AND METHODS

3.1. Climate data

In order to determine the seasonal temperature of Europe at a spatial scale, we used the climate models of temperature for 30 years related to 2011 to 2040 (present) and 2041-2070 (future). Andreas Hamann, from Alberta University, Canada, constructed these climate

models at a very high resolution using the ANUSplin interpolation method. The mean monthly air temperature served to complete the raster datasets for four seasons according to the seasonal periods in the temperate zone but also in relationship with the growth plant calendar in Europe. The climate models were carried out based on the historical data from 1901 to 2013 followed the Mitchell & Jones (2005) method.

The ClimateEU v4.63 software package has been used to complete the climate models. The CMIP5 multi-model dataset, related to the IPCC Assessment Report 5 (2013) have been considered for the future projections. Representative Concentration Pathway (RCP) 4.5 by +1.4°C (±0.5) for the 2050s was used due to the global warming mean projections. The methodology of the models is exposed in a clear way by Hamann & Wang (2005), Daly et al. (2006), Mbogga et al (2009), and Hamann et al (2013). For the present study, the climate models spatial resolution was set at 1 km^2.

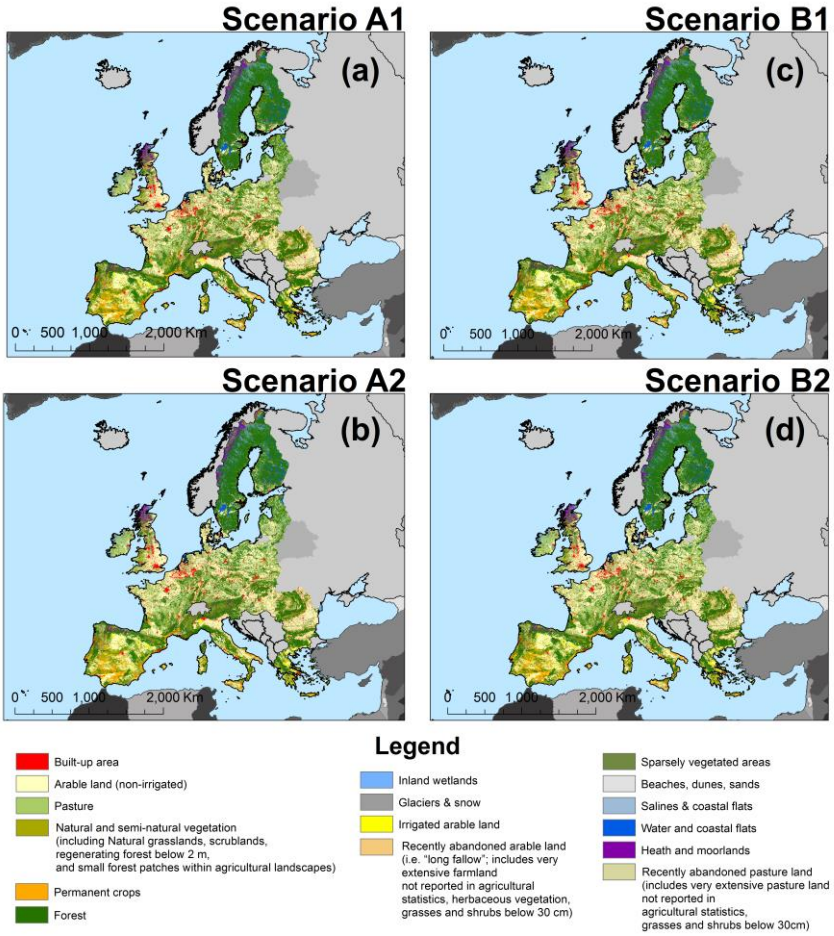

Fig. 2. Land cover projections of Europe. **(a)** Scenario A1. **(b)** Scenario A2. **(c)** Scenario B1. **(d)** Scenario B2. Source: Sustainable futures for Europe's HERitage in CULtural landscapES" project (http://www.hercules-landscapes.eu/).

3.2. Land cover data

CORINE Land Cover raster data from 2012 at 250 m^2 spatial resolution have been used to identify the main crops, shrubs and trees, and the land use in Europe. We agree with the CORINE Land Cover due to its georeferenced characteristics and the detailed classes up to 4^{th} level.

Table 1. Corine Land Cover classes and representative seasonal Kc coefficients in Europe during the present period.

Corine Land Cover		Kc ini season	Kc mid season	Kc end season	Kc cold season
CLC code 2012	CLC Description	Kclc	Kclc	Kclc	Kclc
111	Continous urban fabric	0.2	0.4	0.25	-
112	Discontinuous urban fabric	0.1	0.3	0.2	-
121	Industrial or commercial units	0.2	0.4	0.3	-
122	Road and rail networks and associated land	0.15	0.35	0.25	-
123	Port areas	0.3	0.5	0.4	-
124	Airports	0.2	0.4	0.3	-
131	Mineral extraction sites	0.16	0.36	0.26	-
132	Dump sites	0.16	0.36	0.26	-
133	Construction sites	0.16	0.36	0.26	-
141	Green urban areas	0.12	0.32	0.22	-
142	Sport and leisure facilities	0.1	0.3	0.2	-
211	Non-irrigated arable land	1.1	1.35	1.25	-
212	Permanently irrigated land	1.2	1.45	1.35	-
213	Rice fields	1.05	1.2	0.6	-
221	Vineyards	0.3	0.7	0.45	-
222	Fruit trees and berry plantations	0.3	1.05	0.5	-
223	Olive groves	0.65	0.7	0.65	0.5
231	Pastures	0.4	0.9	0.8	-
241	Annual crops associated with permanent crops	0.5	0.8	0.7	-
242	Complex cultivation patterns	1.1	1.35	1.25	-
243	Land principally occupied by agriculture, with significant areas of natural vegetation	0.7	1.15	1	-
244	Agro-forestry areas	0.9	1.1	1.05	0.3

Source: From Allen et al. (1998); Nistor and Porumb-Ghiurco (2015); Nistor (2017); Nistor et al. (2017)

Table 1. Corine Land Cover classes and representative seasonal Kc coefficients in Europe during the present period (continue).

Corine Land Cover		Kc ini season	Kc mid season	Kc end season	Kc cold season
CLC code 2012	CLC Description	Kclc	Kclc	Kclc	Kclc
311	Broad-leaved forest	1.3	1.6	1.5	0.6
312	Coniferous forest	1	1	1	1
313	Mixed forest	1.2	1.5	1.3	0.8
321	Natural grasslands	0.3	1.15	1.1	-
322	Moors and heathland	0.8	1	0.95	-
323	Sclerophyllous vegetation	0.25	0.9	0.8	-
324	Transitional woodland-shrub	0.8	1	0.95	-
331	Beaches, dunes, sands	0.2	0.3	0.25	-
332	Bare rocks	0.15	0.2	0.05	-
333	Sparsely vegetated areas	0.4	0.6	0.5	-
334	Burnt area	0.1	0.15	0.05	-
335	Glaciers and perpetual snow	0.48	0.52	0.52	0.48
411	Inland marshes	0.15	0.45	0.8	-
412	Peat bogs	0.1	0.4	0.75	-
421	Salt marshes	0.1	0.3	0.7	-
422	Salines	0.1	0.15	0.05	-
423	Intertidal flats	0.3	0.7	1.3	-
511	Water courses	0.25	0.65	1.25	-
512	Water bodies	0.25	0.65	1.25	-
521	Coastal lagoons	0.3	0.7	1.3	-
522	Estuaries	0.25	0.65	1.25	-
523	Sea and ocean	0.4	0.8	1.4	-

Source: From Allen et al. (1998); Nistor and Porumb-Ghiurco (2015); Nistor (2017); Nistor et al. (2017)

This database is available on Copernicus Land Monitoring Services (2012) website. The projections of future land cover for the main European countries were carried out in the "Sustainable futures for Europe's HERitage in CULtural landscapES" (Hercules) project, GA no. 603447 (Schulp et al, 2015). The Hercules models offer a spatial vision of the land cover dynamics based on the fourteen trajectories in the land cover trend. These trajectories incorporate the macro-economic and land use modes taking into account urbanization, agriculture, and forestry. The "Landscape Character Index", extracted from various landscapes such as land use intensity, structures, and patterns (Schulp et al, 2015) was considered during mapping of the future land cover. In the present paper, we used the projections of A1, A2, B1, and B2 land cover scenarios for the 2040s, which illustrate sixteen classes of land types (**Fig. 2**). Access to these scenarios could be done through the Hercules website (http://www.hercules-landscapes.eu/). Entire procedure to obtain the land cover models is exposed in Report no. 1 of the Hercules project (Schulp et al, 2015). All

maps were set at 1 X 1 km to be in line with the climate models resolution. The ArcGIS environment was used for this investigation due to its reliability in spatial analysis of territory (Chaieb et al, 2017; Nistor & Petcu, 2015).

3.3. Seasonal crop coefficients (Kc)

Each vegetation type has an evapotranspiration capacity called Kc. In order to calculate the crop evapotranspiration, Allen et al (1998) used the methodology based on standard Kc. These coefficients have been calculated both for single and dual crops, at different latitudes and in different climate types. According to Allen et al (1998), we set the seasonal Kc for the four seasons specific in the temperate zone. In the urban areas and bare soils, Grimmond & Oke (1999) completed the Kc in several cities and locations from the United States. In the European regions, such as Pannonian basin and South East Europe, Nistor et al (2017a) and Nistor et al (2017b) analyzed crop evapotranspiration at spatial scale incorporating climate models and land cover data. They provided the Kc values for CORINE land cover classes and they explained the time shifts for the four seasons in their study area.

Here, we adopted the above methodology to assess the Kc values both for the present land cover and for the future. We agree with four seasons like initial season ($K_{c\ ini}$) during March, April and May, the mid-season ($K_{c\ mid}$) during June, July and August, the end season ($K_{c\ end}$) during September and October, and the cold season ($K_{c\ cold}$) during January, February, November, and December. These periods were set first by Nistor & Porumb-Ghiurco (2015) who proposed the regional methodology at regional scale for Emilia-Romagna region. Further, Nistor et al (2016b) applied the same procedure for the Carpathian region. The stages, periods and the standard Kc values may slightly vary from place to place, with respect to latitude and local climate.

Table 1 reports the seasonal values of Kc used in this paper for the present period while **Table 2** illustrates the kc values for the projected land cover scenarios.

			Crop coefficient					
			0 - 2	0.21 - 0.6	0.61 - 0.8	0.81 - 1	1.01 - 1.3	> 1.3
		Susceptibility degree	Very low	Low	Medium	High	Very high	Extremely high
Temperature [° C]								
Very cool	< 0	Very low	Very low	Very low	Very low	Very low	Very low	Very low
Cool	0 - 4	Low	Very low	Low	Low	Medium	Medium	Medium
Temperate	5 - 10	Medium	Low	Low	Medium	Medium	High	High
Warm	11 - 15	High	Low	Medium	Medium	High	Very high	Very high
Hot	16 - 20	Very high	Medium	Medium	High	Very high	Very high	Extremely high
Very hot	> 20	Extremely high	High	High	Very high	Very high	Extremely high	Extremely high

Susceptibility degree for evapotranspiration					
Very low	Low	Medium	High	Very high	Extremely high

Fig. 3. The inference matrix used to assess the LCFE in Europe.

Table 2. Corine Land Cover classes and representative seasonal Kc coefficients used for the future scenarios in Europe.

Corine Land Cover		Kc ini season	Kc mid season	Kc end season	Kc cold season
CLC projection code	CLC Description	Kclc	Kclc	Kclc	Kclc
0	Built-up area	0.16	0.36	0.26	-
1	Arable land (non-irrigated)	1.1	1.35	1.25	-
2	Pasture	0.4	0.9	0.8	-
3	Natural and semi-natural vegetation (including Natural grasslands, scrublands, regenerating forest below 2 m, and small forest patches within agricultural landscapes)	0.45	1.1	1	-
4	Inland wetlands	0.15	0.45	0.8	-
5	Glaciers and snow	0.48	0.52	0.52	0.48
6	Irrigated arable land	1.2	1.45	1.35	-
7	Recently abandoned arable land (i.e. "long fallow"; includes very extensive farmland not reported in agricultural statistics, herbaceous vegetation, grasses and shrubs below 30 cm)	0.3	1.15	1.1	-
8	Permanent crops	0.5	0.8	0.7	-
10	Forest	1.2	1.5	1.3	0.8
11	Sparsely vegetated areas	0.4	0.6	0.5	-
12	Beaches, dunes and sands	0.2	0.3	0.25	-
13	Salines	0.1	0.15	0.05	-
14	Water and coastal flats	0.3	0.7	1.3	-
15	Heathland and moorlands	0.8	1	0.95	-
16	Recently abandoned pasture land (includes very extensive pasture land not reported in agricultural statistics, grasses and shrubs below 30cm)	0.6	1	0.9	-

Source: From Allen et al. (1998); Nistor and Porumb-Ghiurco (2015); Nistor (2017); Nistor et al. (2017)

3.4. NISTOR–LCFE method for assessing the land cover favorability for evapotranspiration

The goal of the survey is to assess the seasonal temperature and seasonal Kc for Europe and to determine a method, which defines the areas with different degrees of evapotranspiration favorability. New Implemented Spatial-Temporal On Regions–Land Cover Favorability to Evapotranspiration (NISTOR-LCFE) method has been set to map favorability areas to evapotranspiration, and accounting for both the seasonal mean air temperature and seasonal Kc values. NISTOR–LCFE approach is a new tool based on 6 × 6

matrix that provides six degrees of favorability and it is easy to implement at spatial-temporal scale. Nistor et al (2016a), Nistor & Mîndrescu (2017) have used an appropriate survey by matrix application in the hydrology study. Firstly, we classify the evapotranspiration favorability based on temperature and Kc values in six-degree classes: very low, low, medium, high, very high, and extremely high. The classification was done according to previous studies and observed thresholds of seasonal temperature and Kc values that may influence the evapotranspiration phenomena. We agree with the matrix classification due to climate and hydrological processes that may occur at different temperatures, in various types of vegetation cover. **Figure 3** shows the proposed matrix used in the present methodology.

4. RESULTS

The seasonal mean air temperature and seasonal Kc have been completed for Europe in two time shifts (present and future) on the basis of the presented methodology. **Figure 4** depicts the seasonal temperature in Europe for the 2011-2040 and 2041-2070 according to the four seasons of crop development. During the initial season, the mean air temperature reaches high values (over 12 °C) both in the present and in the future period, showing that the Iberian Peninsula, Pannonian basin, coastal areas of the Italian Peninsula, and in North of Balkan Peninsula are the regions more warm in this stage.

The low values (below 0° C) of temperature during the initial season could be found in the Scandinavian Mountains, Alps Range, Carpathian Range, Dinaric Mountains, and in the North of Europe (**Figs. 4a and 4b**). In the mid-season period, the high values of mean air temperature exceed 26 °C in the areas of Po Plain, South of Iberian Peninsula, Aegean Islands, and in the southeastern sides of the Balkan Peninsula. For the 2041-2070 period, the areas with high temperature extend at spatial scale of West and East parts of Italy and in the North of Balkan Peninsula. The low values of temperature in the mid-season were registered in the Alps Range, Scandinavian Peninsula, and in the North of British Islands (**Figs. 4c and 4d**). The air temperature in the end season reaches values over 20 °C especially in the central and West Iberian Peninsula, West of Sardinia, South of Sicily, and in the Aegean Islands. In the future period, areas with high values of temperature extend in the coastline of the Italian Peninsula, Po Plain, South of France, and in the East of Balkan Peninsula. The low values of mean air temperature could be depicted in the mountain areas, North of Europe and North of British Islands (**Figs. 4e and 4f**). In the cold season, both models illustrate low values of air temperature (below 4 °C) in most part of central, eastern, and northern Europe, and the mountain belts. Low values are also presented in the North of British Islands and some areas from the Balkan Peninsula, where the elevated heights are. During the cold season, the West and South of Europe, mainly the Atlantic coast of the Iberian Peninsula and the Mediterranean Islands register values around 10-13 °C of air temperature. Interestingly, the air temperature models indicate higher values for the future in all seasons (**Figs. 4g and 4h**). As we expected, the temperature changes are located in the South East, in the West and in the South of Europe and extend in the territory.

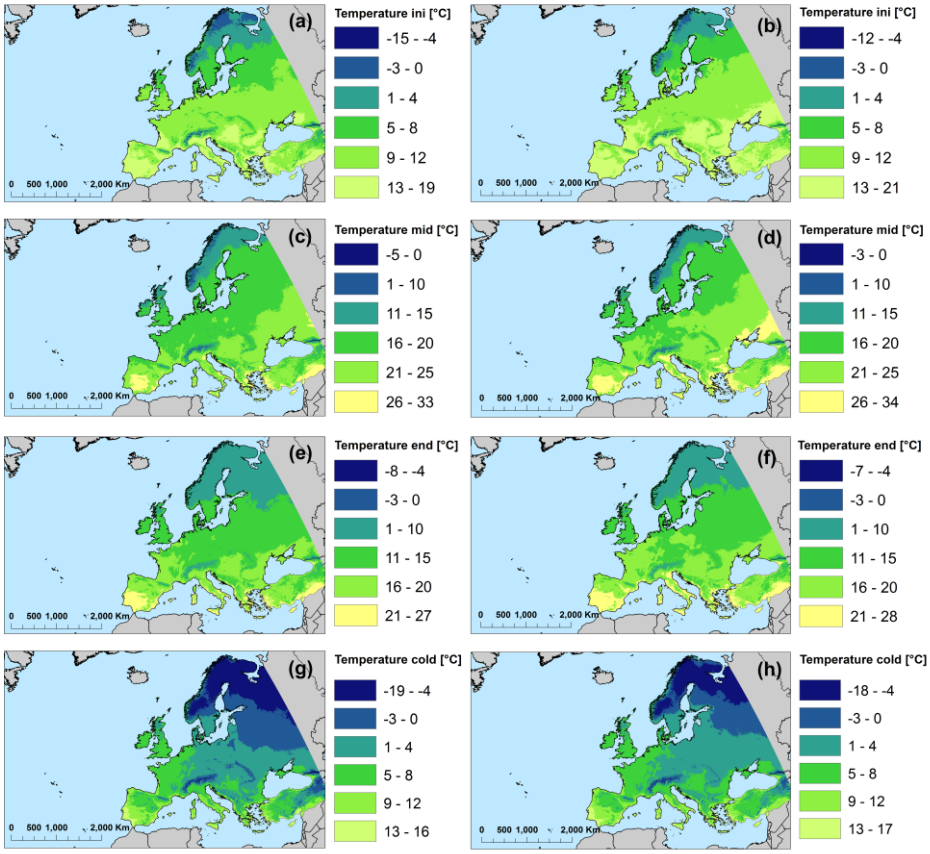

Fig. 4. Spatial distribution of seasonal air temperature in Europe. **(a)** Temperature for the initial (ini) season (2011 – 2040). **(b)** Temperature for the initial (ini) season (2041 – 2070). **(c)** Temperature for the mid-season (mid) (2011 – 2040). **(d)** Temperature for the mid-season (mid) (2041 – 2070). **(e)** Temperature for the end season (2011 – 2040). (f) Temperature for the end season (2041 – 2070). **(f)** Temperature for the cold season (2011 – 2040). **(h)** Temperature for the cold season (2041 – 2070).

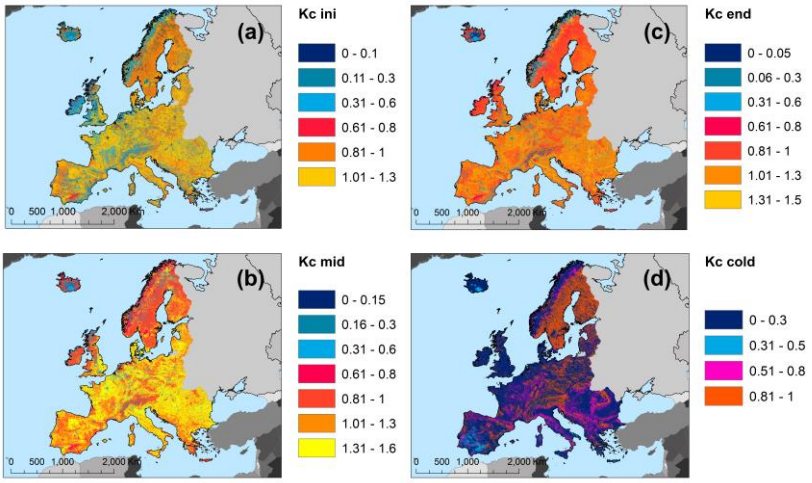

Fig. 5. Spatial distribution of Kc in Europe related to the present land cover. **(a)** Kc ini for the initial season. **(b)** Kc mid for the mid-season season. **(c)** Kc end for the end season. **(d)** Kc cold for the cold season.

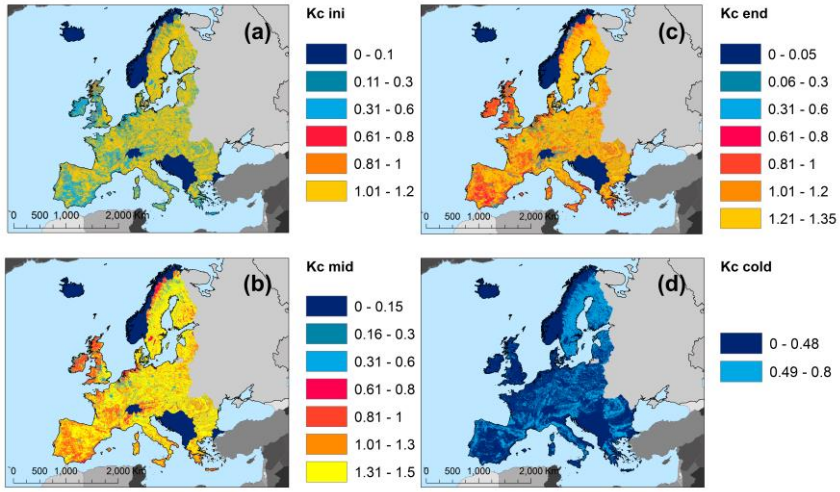

Fig. 6. Spatial distribution of K_c in Europe related to the projection of scenario A1. **(a)** Kc ini for the initial season. **(b)** Kc mid for the mid-season season. **(c)** Kc end for the end season. **(d)** Kc cold for the cold season.

During the present period, the Kc values range from 0 to 1.6 and register the maximum values in the mid-season stage (**Fig. 5**). The high values (1.31-1.6) could be depicted in the central, West, South-East, and South parts of Europe. The lower values of the Kc are related to the cold season when major parts of the continent have Kc values that range from 0 to 0.3. During the initial and end seasons, the Kc values reach 1.3 and 1.5 respectively and mean Kc indicates values around 0.81-1. The future land Kc illustrates values between 0 and 1.5, the maximum values being assigned for the mid-season stage. The cold season shows values up to 0.8 and the larger sides of the Europe have values of Kc between 0 and 0.48. Differences in the Kc pattern for the future are illustrated in **Figures 6-9**.

The LCFE map shows high and very high degree of favorability for the initial season in the East, South, and West sides of Europe, especially in the lowlands and on the coastal areas. The medium degree spread mainly in the Scandinavian Peninsula, Carpathian Mountains, Eastern Alps, central sides of the Europe, and in South of Iberian Peninsula. The low and very low LCFE were depicted in the North of Europe, North and West of the British Islands and in the mountain areas, especially in the Alps Range, Pyrenees, Central Apennines, and Dinaric Mountains. In the future period, increase in high degree has been observed in the Scandinavian Peninsula and in eastern Europe. The medium class of LCFE increases also for all scenarios in the Iberian Peninsula and in South of Europe, e.g. Sicily Island, Aegean Islands, South of Balkan Peninsula. **Figure 10** illustrates the favorability degree in Europe related to the initial season.

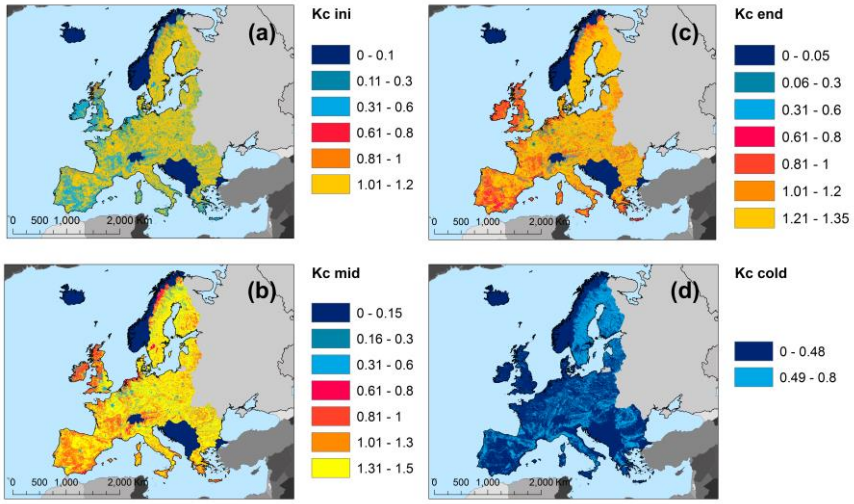

Fig. 7. Spatial distribution of Kc in Europe related to the projection of scenario A2. **(a)** Kc ini for the initial season. **(b)** Kc mid for the mid-season season. **(c)** Kc end for the end season. **(d)** Kc cold for the cold season.

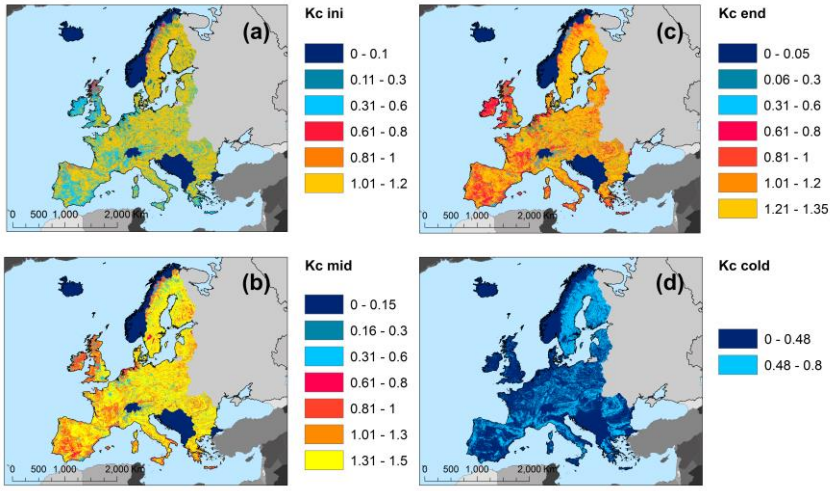

Fig. 8. Spatial distribution of Kc in Europe related to the projection of scenario B1. **(a)** Kc ini for the initial season. **(b)** Kc mid for the mid-season season. **(c)** Kc end for the end season. **(d)** Kc cold for the cold season.

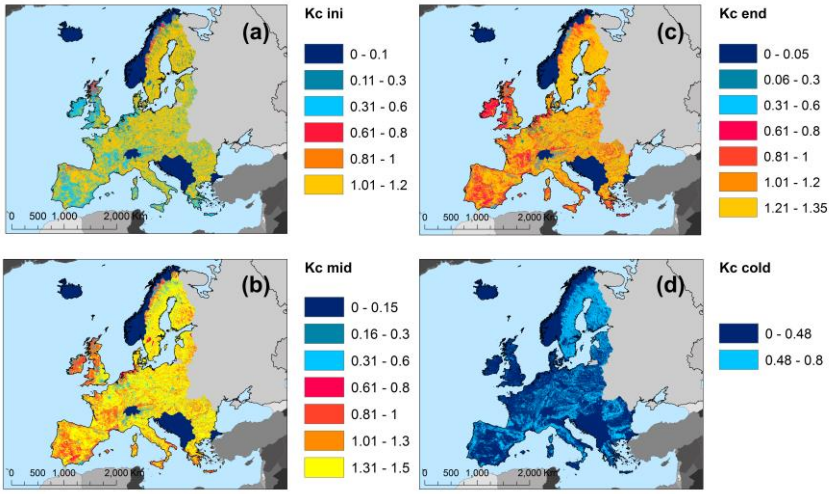

Fig. 9. Spatial distribution of Kc in Europe related to the projection of scenario B2. **(a)** Kc ini for the initial season. **(b)** Kc mid for the mid-season season. **(c)** Kc end for the end season. **(d)** Kc cold for the cold season.

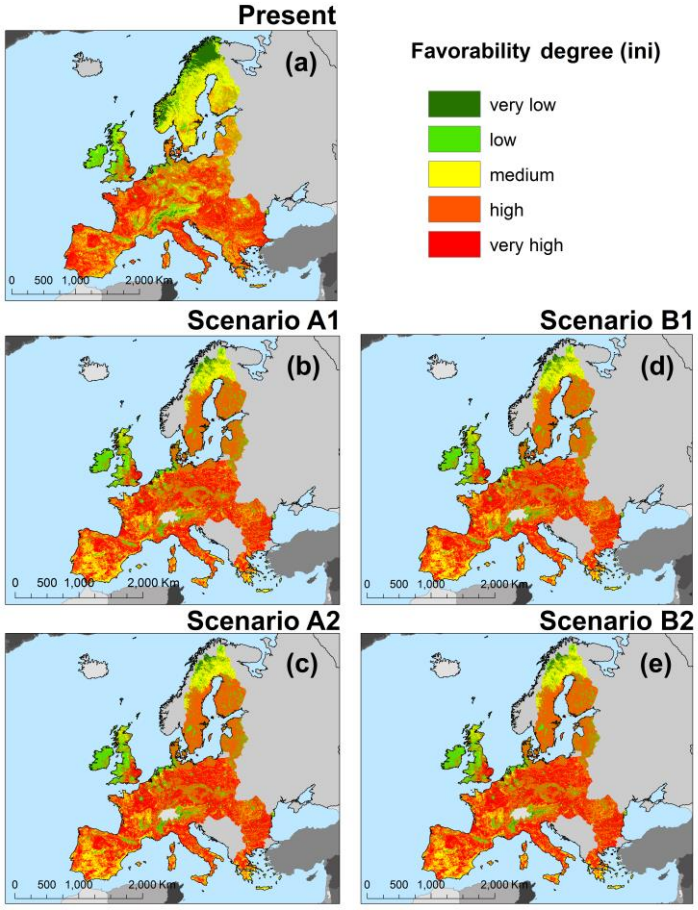

Fig. 10. Spatial distribution of LCFE in Europe during the initial season. **(a)** Present. **(b)** Scenario A1. **(c)** Scenario A2. **(d)** Scenario B1. **(e)** Scenario B2.

In the mid-season, the extremely high degree of LCFE was depicted in the lowlands of southern Europe, but also in the West, North, and East of Europe. In the Alps Range, Pyrenees and Scandinavian Mountains, the degree is low and very low, whereas, in the Carpathians, Dinarics, Scottish, and Apennines Mountains the LCFE is medium.

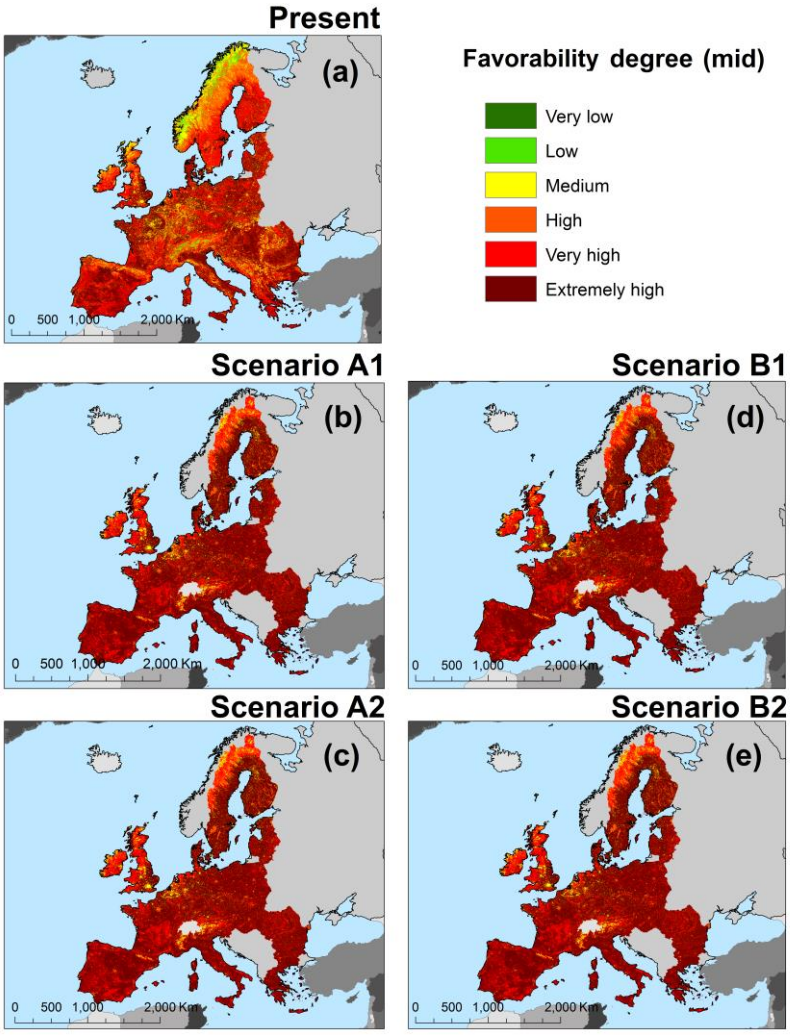

Fig. 11. Spatial distribution of LCFE in Europe during the mid-season. **(a)** Present. **(b)** Scenario A1. **(c)** Scenario A2. **(d)** Scenario B1. **(e)** Scenario B2.

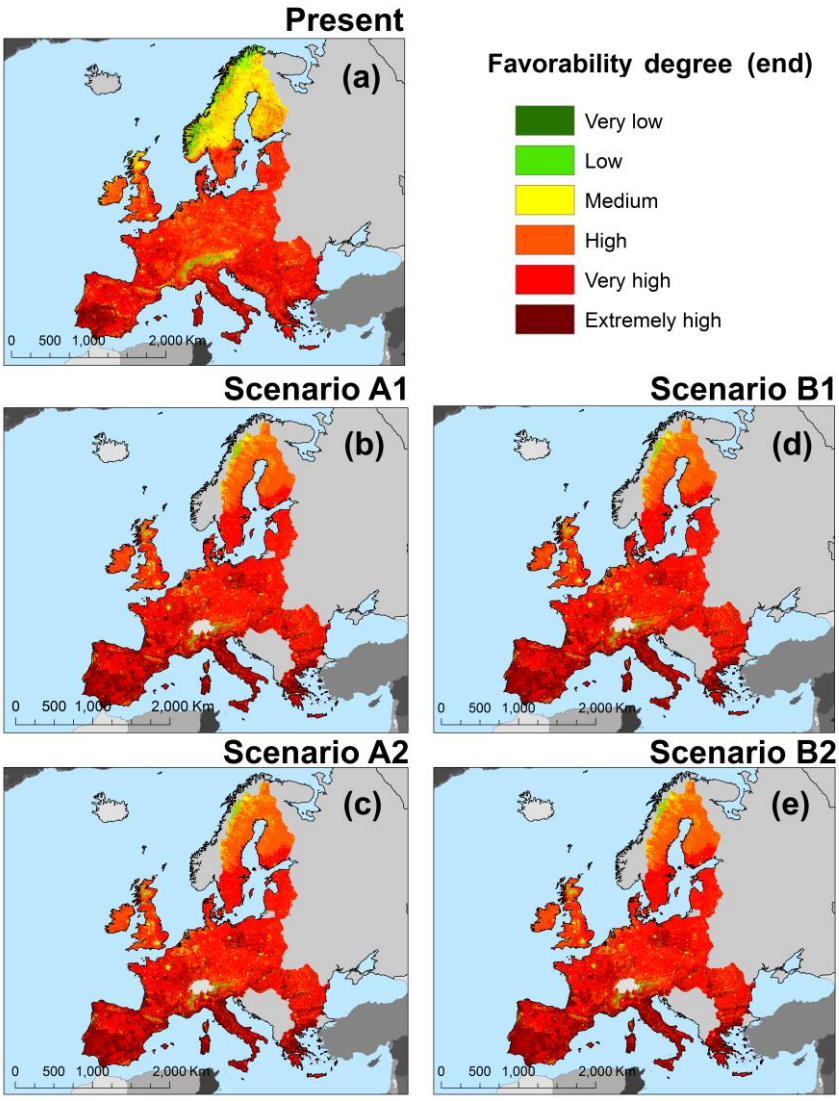

Fig. 12. Spatial distribution of LCFE in Europe during the end season. **(a)** Present. **(b)** Scenario A1. **(c)** Scenario A2. **(d)** Scenario B1. **(e)** Scenario B2.

The medium LCFE was found also in the large capitals and cities, e.g. London, Paris, Birmingham, and in the central and western sides of the Scandinavian Peninsula. The future scenarios indicate largest areas with an extremely high degree of the LCFE in the central, South, West, and some eastern sides of the Europe. **Figure 11** depicts the favorability degree in Europe related to the mid-season.

During the end season, the present LCFE map illustrates large areas with high and very high degree for evapotranspiration favorability, while the extremely high LCFE was depicted mainly in the West of Iberian Peninsula, South of Balkan Peninsula, Italian Peninsula, in some places from central Europe, and in the Mediterranean Islands. Medium, low, and very low degree were identified in the Alps Range, Scandinavian Peninsula, North of British Islands, Pyrenees Mountains, East of Sicily and in the Etna Mount. The medium LCFE extends also in the large urban areas, and in the central Iberian Peninsula, South of France, sparsely in the central and East of Europe. The future scenarios show increase of areas with extremely high degree of evapotranspiration favorability, especially in the southern, western, and eastern sides of Europe. The favorability degree in the end season of Europe is presented in **Figure 12**.

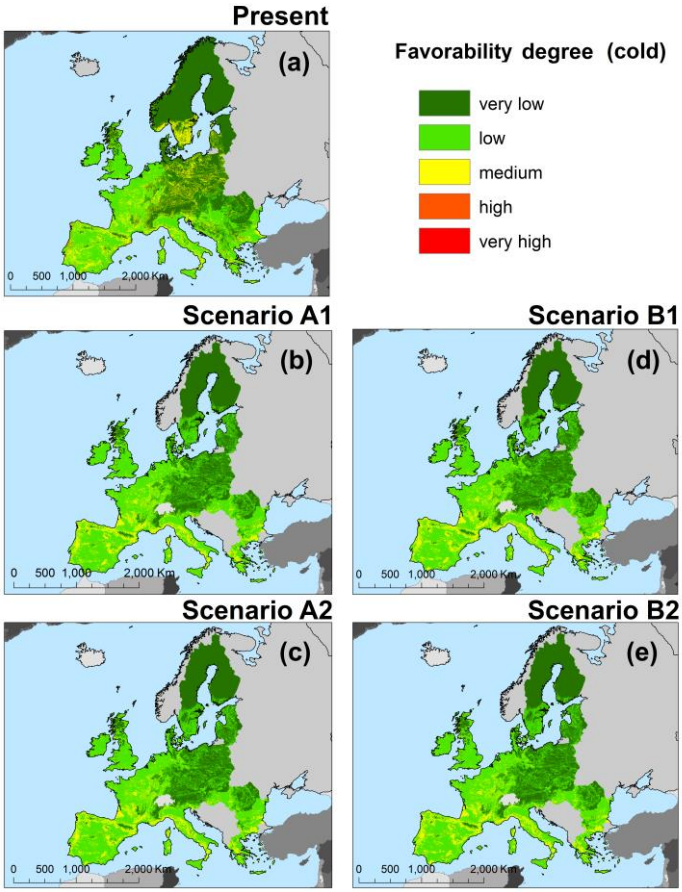

Fig. 13. Spatial distribution of LCFE in Europe during the cold season. **(a)** Present. **(b)** Scenario A1. **(c)** Scenario A2. **(d)** Scenario B1. **(e)** Scenario B2.

Very low degree of LCFE is depicted in the cold season mainly in the northern, central, and eastern sides of Europe. The low degree of LCFE is predominantly in the West and South of the continent, while medium LCFE appears in the West of the Iberian Peninsula

and sparsely in central and northern Europe, in Italian and Balkan Peninsula. This degree class extends also in the South of the Scandinavian Peninsula, but only for the present period. The future scenarios show an increase of low and very low degree in the East and North of Europe, whereas in the West and South of Europe, the medium class increases in the spatial distribution. A remarkable situation about high and very high degree of LCFE could be found only for the present in few locations from South of Italy, South of Balkan Peninsula, around the coastal areas of the Iberian Peninsula, and in the Aegean Islands. **Figure 13** depicts the favorability degree in Europe related to the cold season.

5. DISCUSSION

The main goal of this paper is to evaluate the seasonal mean air temperature and the seasonal Kc in Europe during 2011-2040 and 2041-2070 and to implement a methodology to identify areas with different degrees of favorability to evapotranspiration. The seasonality in Europe and, in general, in the temperate zone indicates four stages with various characteristics in the climate regime and growth of plants. As a parameter which indicates the exchange between vegetation and atmosphere (Chen et al, 2006), the evapotranspiration parameter is a useful indicator in hydrological and climate studies. First and the most important input for the evapotranspiration calculation is temperature because, without positive values of temperature, lack of energy as a result cannot produce evapotranspiration. Spatial distribution of seasonal mean air temperature is very diversified in Europe, with significant influences of Atlantic Ocean in the West and Mediterranean influences in the South sides, where temperatures are higher than in central, eastern and northern Europe. On the Eastern sides, North of the Black Sea, the high values of seasonal temperature are present also. These higher values of temperature were found in all seasons. A slight increase for the future period (2041-2070) could be observed. Continentality and large parts of land in eastern Europe contribute to the low and negative temperature in the cold season. The North of Europe is influenced by the Arctic cool zone, a fact for which the values of temperature are lower than in other parts of Europe, especially in the cold and initial season. As a consequence of the distribution of temperature in the European territory, evapotranspiration rate highly correlates to the quantity of heat and sunshine energy. For this reason, the southern and western regions of Europe are more susceptible to high evapotranspiration.

Land cover composition is the second factor which affects evapotranspiration, due to different absorption and hydrological exchanges of various vegetation types, and because of the crop calendar. In this sense, the non-vegetative land cover features such as glaciers, urban areas, or bare soil, contribute to evapotranspiration rate much in the mid-season period. In the northern lands of Europe and in the North of British Islands, low values of Kc are observed due to peat bogs areas, heath and moorlands fields. In the mountain areas, glaciers and coniferous forests influence the Kc. The ice covers have values of 0.48 (initial and cold season) and 0.52 (mid-season and end season), especially in the Alps, and the evergreen areas and the coniferous forest have a value 1 in all seasons. This is important because the evapotranspiration expectation could be higher also during the winter.

The future seasonal K_c does not reach the maximum value such as in the present due to simplified classes of the land cover. Thus, the forest class is not differentiated in the future by the broad-leaved and mixed forests, so one unique class for this type was used for the projections of land cover. The artificial areas are also represented only by one class, which

included all built-up areas. Due to these simplifications, the future spatial distribution of Kc that resulted from the scenarios indicate values lower than in the present up to 0.15 in the end season, but the Kc values are still within the range of previous literature studies. Analyzing the seasonal Kc patterns, it was observed that in the A1 scenario, lands with higher Kc are larger than in scenario B1 during all seasons. Comparing scenario A2 with scenario B2, areas with high Kc occupies more territory in scenario B2 than in scenario A2. From the analysis of scenario A1 and scenario B2, it was concluded that scenario A1 has more territory with high values of Kc in comparison with B2 scenario. The last, between scenarios A2 and B1, the analysis of patterns indicates larger areas with high Kc in scenario A2 than in scenario B1.

Incorporating the seasonal temperature and seasonal Kc of Europe in the 6 × 6 matrix as the NISTOR-LCFE method proposes, the favorability degree to evapotranspiration is highly dependent on the spatial distribution of both variables. The extremely high and very high LSCE is predominantly in the mid-season because mean air temperature is high in this season and also vegetation functions are more active than in other seasons. LCFE with very high and extremely high favorability was identified in the initial and end season, while in the cold season, the low and very low LCFE are predominant in Europe. In response to climate change, the future LCFE maps illustrate major changes in the high and very high degree class of favorability.

Even if we do not calculate crop evapotranspiration, the findings carried out through the NISTOR-LCFE method may be compared to the results obtained by Nistor & Porumb-Ghiurco (2015), Nistor et al (2016b), Nistor et al (2017a), Nistor et al (2017b) which assess the crop evapotranspiration in different regions of Europe. The above mentioned studies indicate high values of evapotranspiration during the mid-season, with an increase of areas with high and very high crop evapotranspiration. However, the key work of Nistor (2016) related to seasonal Kc in the Paris metropolitan area represented the base for Kc values decision for this paper.

Our work is not without limitations, considering that the complicated hydrological processes related to evapotranspiration are very complex. Here, we presented a reliable methodology to assess the LCFE at European scale. Based on climate models to extract seasonal temperature and using land cover database to determine the spatial distribution of Kc, the results could be slightly different at the local scale due to missing field measurements of Kc. The large territory of Europe and the multitude of land cover types do not permit us to complete an exhaustive survey using tensiometers and lysimeters. For this reason, we admit to using standard Kc knowing that evapotranspiration rate may fluctuate under the coefficients of evapotranspiration.

6. CONCLUSIONS

Spatial distribution of seasonal mean air temperature and seasonal K_c have been mapped for Europe in two time shifts with an aim to depict different degrees of evapotranspiration favorability using a new spatial-temporal approach. The application of the NISTOR-LCFE method combines climate models and land cover data in an efficient way that can be easily completed in ArcGIS environment. The power of our original method offers an overall view at spatial scale of favorability areas to evapotranspiration without the necessity to execute potential evapotranspiration which requires time and calculations. In addition, the NISTOR-LCFE approach has not been used in previous researches and this outcome may contribute to the specific literature.

The areas from West, South, and East Europe are susceptible to very high and extremely high degree of evapotranspiration during the mid-season and in the future, these areas would seem to extend. For the same season, the low and very low LCFE overlap to the mountain belts and on the northern territory. The medium LCFE is mainly presented in the initial season and spread over the northern sides of Europe, in the Iberian Peninsula, South of Europe, West-central parts of Europe (e.g. in France), and in the Carpathians Mountains. For an optimization of numerous environmental factors and for good practices in the society for decision making, our maps could be helpful to indicate drought areas during the summer periods, runoff and water surplus calculations, and to set up agricultural management planning.

Our findings fit also with climatology and hydrological sciences, for which further calculations of potential and actual evapotranspiration concerning groundwater vulnerability could be drawn. In this sense, the utilization of climate models and land cover scenarios are an exciting issue for many expertise fields. Future works will focus on water resources quantitative statement under climate change linking also land cover implications. To support the planning for environmental management, we provide out gridded data layers of seasonal temperature and seasonal Kc through an open access database (https://zenodo.org: 10.5281/zenodo.1193226).

Acknowledgements

The authors would like to thank Andreas Hamann from Alberta University for the climate model data, European Environmental Agency and Hercules team members for the land cover raster data. Previous affiliation of the corresponding author: Earthresearch Company, Department of Hydrogeology, Cluj-Napoca, Romania.

REFERENCES

Aguilera, H. & Murillo, J.M. (2009) The effect of possible climate change on natural groundwater recharge based on a simple model: a study of four karstic aquifers in SE Spain. *Environmental Geology*, 57(5), 963–974.

Allen, R.G., Pereira, L.S., Raes, D. & Smith, M. (1998) *Crop Evapotranspiration: Guidelines for Computing Crop Water Requirements.* FAO Irrigation and Drainage Paper 56. FAO: Rome, pp. 300.

Allen, R.G. (2000) Using the FAO-56 dual crop coefficient method over an irrigated region as part of an evapotranspiration intercomparison study. *Journal of Hydrology*, 229, 27–41.

Ambas, V.T. & Baltas, E. (2012) Sensitivity analysis of different evapotranspiration methods using a new sensitivity coefficient. *Global NEST Journal*, 14(3), 335–343.

Bachu, S. & Adams, J.J. (2003) Sequestration of CO2 in geological media in response to climate change: capacity of deep saline aquifers to sequester CO2 in solution. *Energy Conversion and Management*, 44, 3151–3175.

Brouyère, S., Carabin, G. & Dassargues, A. (2004) Climate change impacts on groundwater resources: modelled deficits in a chalky aquifer, Geer basin, Belgium. *Hydrogeology Journal*, 12, 123–134.

Campos, G.E.P., Moran, M.S., Huete, A., Zhang, Y., Bresloff, C., Huxman, T.E. et al. (2013) Ecosystem resilience despite large-scale altered hydroclimatic conditions. *Nature*, 494, 349–353.

Čenčur Curk, B., Cheval, S., Vrhovnik, P., Verbovšek, T., Herrnegger, M., Nachtnebel, H.P., Marjanović, P., Siegel, H., Gerhardt, E., Hochbichler, E., Koeck, R., Kuschnig, G., Senoner, T., Wesemann, J., Hochleitner, M., Žvab Rožič, P., Brenčič, M., Zupančič, N., Bračič Železnik, B., Perger, L., Tahy, A., Tornay, E.B., Simonffy, Z., Bogardi, I., Crăciunescu, A., Bilea, I.C., Vică, P., Onuțu, I., Panaitescu, C., Constandache, C., Bilanici, A., Dumitrescu, A., Baciu, M., Breza, T., Marin, L., Draghici, C., Stoica, C., Bobeva, A., Trichkov, L., Pandeva, D., Spiridonov, V.,

Ilcheva, I., Nikolova, K., Balabanova, S., Soupilas, A., Thomas, S., Zambetoglou, K., Papatolios, K., Michailidis, S., Michalopoloy, C., Vafeiadis, M., Marcaccio, M., Errigo, D., Ferri, D., Zinoni, F., Corsini, A., Ronchetti, F., Nistor, M.M., Borgatti, L., Cervi, F., Petronici, F., Dimkić, D., Matić, B., Pejović, D., Lukić, V., Stefanović, M., Durić, D., Marjanović, M., Milovanović, M., Boreli-Zdravković, D., Mitrović, G., Milenković, N., Stevanović, Z. & Milanović, S. (2014) *CC-WARE Mitigating Vulnerability of Water Resources under Climate Change*. WP3 - Vulnerability of Water Resources in SEE, Report Version 5. URL: http://www.ccware.eu/output-documentation/output-wp3.html.

Chaieb, A., Rebai, N., Ghamni, M.A., Moussi, A. & Bouaziz S. (2017) Spatial analysis of river longitudinal profils to cartography tectonic activity in Kasserine Plain Tunisia. *Geographia Technica* 12(2): 30–40.

Chen, S.B., Liu, Y.F. & Thomas, A. (2006) Climatic change on the Tibetan plateau: potential evapotranspiration trends from 1961 to 2000. *Climatic Change*, 76, 291–319.

Cheval, S., Dumitrescu, A. & Barsan, M.V. (2017) Variability of the aridity in the South-Eastern Europe over 1961–2050. *Catena*, 151, 74–86.

Copernicus Land Monitoring Services. (2012) CORINE Land Cover of Europe. URL: http://land.copernicus.eu/ (accessed 21 July 2016).

Dong, P., Wang, C. & Ding, J. (2013) Estimating glacier volume loss used remotely sensed images, digital elevation data, and GIS modelling. *International Journal of Remote Sensing*, 34(24), 8881–8892.

Elfarrak, H., Hakdaoui, M. & Fikri, A. (2014) Development of Vulnerability through the DRASTIC Method and Geographic Information System (GIS) (Case Groundwater of Berrchid), Morocco. *Journal of Geographic Information System*, 6, 45–58.

European Environmental Agency. (2007) *Land-use scenarios for Europe: qualitative and quantitative analysis on a European scale*. ISSN 1725-2237. EEA Technical report No 9/2007.

Gao, G., Chen, D., Xu, C.Y. & Simelton, E. (2007) Trend of estimated actual evapotranspiration over China during 1960–2002. *J. Geophys. Res.*, 112(D11120), 1–8, DOI: 10.1029/2006JD008010.

Gao, G., Xu, C.Y., Chen, D. & Singh, V.P. (2012) Spatial and temporal characteristics of actual evapotranspiration over Haihe River basin in China. Stoch. Environ. *Res. Risk Assess.*, 26, 655–669.

Güçlü, Y.S., Subyani, A.M. & Şen, Z. (2017) Regional fuzzy chain model for evapotranspiration estimation. *Journal of Hydrology*, 544, 233–241.

Gowda, P.H., Chavez, J.L., Colaizzi, P.D., Evett, S.R., Howell, T.A. & Tolk, J.A. (2008) ET mapping for agricultural water management: present status and challenges. *Irrigation Science*, 26(3), 223–237.

Grimmond, C.S.B. & Oke, T.R. (1999) *Evapotranspiration rates in urban areas, Impacts of Urban Growth on SurfaceWater and Groundwater Quality*. Proceedings of IUGG 99 Symposium HSS. Birmingham, July 1999.

Hamann, A. & Wang, T.L. (2005) Models of climatic normals for genecology and climate change studies in British Columbia. *Agricultural and Forest Meteorology*, 128, 211–221.

Hamann, A., Wang, T., Spittlehouse, D.L. & Murdock, T.Q. (2013) A comprehensive, high-resolution database of historical and projected climate surfaces for western North America. *Bulletin of the American Meteorological Society*, 94, 1307–1309.

Haeberli, W.R., Frauenfelder, R., Hoelzle, M. & Maisch, M. (1999) On rates and acceleration trends of global glacier mass changes. *Geografiska Annaler, Series A, Physical Geography*, 81A, 585–595.

IPCC. (2001) *Climate change 2001: the scientific basis.* In: Houghton, J.T., Ding, Y., Griggs, D.J., Noguer, M., van der Linden, P.J., Dai, X. (Eds), *Contribution of Working Group I to the Third Assessment Report of the Intergovernmental Panel on Climate Change*. Cambridge University Press: Cambridge and New York, New York, pp. 881.

Jiménez Cisneros, B.E., Oki, T., Arnell, N.W., Benito, G., Cogley, J.G., Döll, P., Jiang, T. & Mwakalila, S.S. (2014) *Freshwater resources.* In: Field, C.B., Barros, V.R., Dokken, D.J., Mach,

K.J., Mastrandrea, M.D., Bilir, T.E., Chatterjee, M., Ebi, K.L., Estrada, Y.O., Genova, R.C., Girma, B., Kissel, E.S., Levy, A.N., MacCracken, S., Mastrandrea, P.R., White, L.L. (Eds.), *Climate Change 2014: Impacts, Adaptation, and Vulnerability. Part A: Global and Sectoral Aspects. Contribution of Working Group II to the Fifth Assessment Report of the Intergovernmental Panel on Climate Change.* Cambridge University Press, Cambridge, United Kingdom and New York, USA, pp. 229–269.

Kargel, J.S., Abrams, M.J., Bishop, M.P., Bush, A., Hamilton, G., Jiskoot, H., Kääb, A., Kieffer, H.H., Lee, E.M., Paul, F., Rau, F., Raup, B., Shroder, J.F., Soltesz, D., Stainforth, S., Stearns, L. & Wessels, R. (2005) Multispectral imaging contributions to global land ice measurements from space. *Remote Sensing of Environment*, 99(1), 187–219.

Kløve, B., Ala-Aho, P., Bertrand, G., Gurdak, J.J., Kupfersberger, H., Kværner, J., Muotka, T., Mykrä, H., Preda, E., Rossi, P., Bertacchi Uvo, C., Velasco, C. & Pulido-Velazquez, M. (2014) Climate change impacts on groundwater and dependent ecosystems. *Journal of Hydrology*, 518, 250–266.

Kottek, M., Grieser, J., Beck, C., Rudolf, B. & Rubel, F. (2006) World Map of the Köppen-Geiger climate classification updated. *Meteorologische Zeitschrift*, 15(3), 259–263.

Ladányi, Zs., Blanka, V., Meyer, B., Mezősi, G. & Rakonczai, J. (2015) Multi-indicator sensitivity analysis of climate change effects on landscapes in the Kiskunság National Park, Hungary. *Ecological Indicators*, 58, 8–20.

Li, K.Y., Coe, M.T., Ramankutty, N. & De Jong, R. (2007) Modeling the hydrological impact of land-use change in West Africa. *Journal of Hydrology*, 337, 258–268.

Loàiciga, H.A., Maidment, D.R. & Valdes, J.B. (2000) Climate-change impacts in a regional karst aquifer, Texas, USA. *Journal of Hydrology*, 227, 173–194.

Mbogga, M.S., Hamann, A. & Wang, T. (2009) Historical and projected climate data for natural resource management in western Canada. *Agricultural and Forest Meteorology*, 149, 881–890.

Mitchell, T.D. & Jones, P.D. (2005) An improved method of constructing a database of monthly climate observations and associated high-resolution grids. *International Journal of Climatology*, 25, 693–712.

Nistor, M.M. (2013) Geological and geomorphological features of Kenai and Chugach Mountains in Whittier Area, Alaska. *STUDIA UBB GEOGRAPHIA*, LVIII(1), 27–34.

Nistor, M.M. & Petcu, I.M. (2014) The role of glaciers in the evolution of Prince William Sound landscape ecosystems, Alaska. *STUDIA UBB AMBIENTUM*, LIX(1-2), 97–109.

Nistor, M.M., Ronchetti, F., Corsini, A., Cervi, F., Borgatti, L., Errigo, D. & Marcaccio, M. (2014) *Vulnerability of groundwater in fractured aquifers, under climate and land use change in Northern Apennines*. National Meeting on Hydrogeology, Abstract volume Flowpath 2014, Viterbo June 18-20, 152–153.

Nistor, M.M. & Petcu, M.I. (2015) Quantitative analysis of glaciers changes from Passage Canal based on GIS and satellite images, South Alaska. *Applied Ecology and Environmental Research*, 13(2), 535–549.

Nistor, M.M. & Porumb-Ghiurco, G.C. (2015) How to compute the land cover evapotranspiration at regional scale? A spatial approach of Emilia-Romagna region. *GEOREVIEW Scientific Annals of Ştefan cel Mare University of Suceava, Geography Series*, 25(1), 38–54.

Nistor, M.M. (2016) Mapping evapotranspiration coefficients in the Paris metropolitan area. *GEOREVIEW Scientific Annals of Ştefan cel Mare University of Suceava, Geography Series*, 26(1), 138–153.

Nistor, M.M., Dezsi, St., Cheval, S. & Baciu M. (2016a) Climate change effects on groundwater resources: a new assessment method through climate indices and effective precipitation in Beliş district, Western Carpathians. *Meteorological Applications*, 23, 554–561.

Nistor, M.M., Gualtieri, A.F., Cheval, S., Dezsi, St. & Boţan, V.E. (2016b) Climate change effects on crop evapotranspiration in the Carpathian Region from 1961 to 2010. *Meteorological Applications*, 23, 462–469.

Nistor, M.M., Cheval, S., Gualtieri, A., Dumitrescu, A., Boţan, V.E., Berni, A., Hognogi, G., Irimuş, I.A. & Porumb-Ghiurco, C.G. (2017a) Crop evapotranspiration assessment under climate change in the Pannonian basin during 1991-2050. *Meteorological Applications*, 24, 84–91.

Nistor, M.M. & Mîndrescu, M. (2017) Climate change effect on groundwater resources in Emilia-Romagna region: An improved assessment through NISTOR-CEGW method. Quaternary International, https://doi.org/10.1016/j.quaint.2017.11.018.

Nistor, M.M., Ronchetti, F., Corsini, A., Cheval, S., Dumitrescu, A., Rai, P.K., Petrea, D., & Dezsi, Şt. (2017b) Crop evapotranspiration variation under climate change in South East Europe during 1991-2050. *Carpathian Journal of Earth and Environmental Sciences*, 12(2), 571–582.

Öztürk, M., Copty N., K. & Saysel A., K. (2013) Modeling the impact of land use change on the hydrology of a rural watershed. *Journal of Hydrology*, 497, 97–109.

Oerlemans, J. (2005) Extracting a Climate Signal from 169 Glacier Records. Science, 308, 675–677.

Parmesan, C. & Yohe, G. (2003) A globally coherent fingerprint of climate change impacts across natural systems. *Nature*, 421(2), 37–42.

Prăvălie, R., Sîrodoev, I. & Peptenatu, D. (2014) Detecting climate change effects on forest ecosystems in Southwestern Romania using Landsat TM NDVI data. *Journal of Geographical Sciences*, 24, 815–832.

Rosenberry, D.O., Winter, T.C., Buso, D.C. & Likens, G.E. (2007) Comparison of 15 evaporation methods applied to a small mountain lake in the northeastern USA. *Journal of Hydrology*, 340, 149–166.

Schulp, C.J.E., Tieskens, K.F., Sturck, J., Fuchs, R., van der Zanden, E.H., Schrammeijer, E. & Verburg, P.H. (2015) *EU scale analysis of future cultural landscape dynamics*. Report no. 1, WP 5 Fine- and broad-scale modelling of future landscapes.

Shahgedanova, M., Stokes, C.R., Gurney, S.D. & Popovnin, V. (2005) Interactions between mass balance, atmospheric circulation, and recent climate change on the Djankuat Glacier, Caucasus Mountains, Russia. *Journal of Geophysical Research*, 110(D16107), 1–12.

Yustres, Á., Navarro, V., Asensio, L., Candel, M. & García, B. (2013) Groundwater resources in the Upper Guadiana Basin (Spain): a regional modelling analysis. *Hydrogeology Journal*, 21, 1129–1146.

Xie, X., Li, Y.X., Li, R., Zhang, Y., Huo, Y., Bao, Y. & Shen, S. (2013) Hyperspectral characteristics and growth monitoring of rice (Oryza sativa) under asymmetric warming. *International Journal of Remote Sensing*, 34(23), 8449–8462.

VULNERABILITY ANALYSIS FOR TWO ACCIDENT SCENARIOS AT AN UPPER-TIER SEVESO ESTABLISHMENT IN ROMANIA

Lucrina ŞTEFĂNESCU[1], Camelia BOTEZAN[1]*, Iulia CRĂCIUN[1]

DOI: 10.21163/GT_2018.131.10

ABSTRACT:
Major accidents involving dangerous substances pose a serious threat to the health and safety of local communities and the environment, as well as to the integrity and development of infrastructure where Seveso establishments are located. In some cases, the disastrous effects may affect larger, even cross-border areas. At European level, there are continuous efforts to develop land-use planning policies and regulations to reduce consequences and to prevent future accidents from happening. Hence, research in this field comes to support the current actions and strategies of the European Commission to improve the capacity of the EU Member States to cope with and respond to the identified risks through effective prevention, preparedness and response measures. In Romania, the Seveso establishments are mostly located in or very close to urban areas. This paper analyses vulnerability in case of two different accident scenarios (explosion and toxic dispersion) in Targu-Mures, a city hosting one of the largest Seveso upper-tier establishments in Romania. The approach starts with exposure analysis - the first step in the process of vulnerability analysis - which identifies all the elements at risk, be they social (population, medical facilities, schools), environmental (protected areas, water bodies) or economic (transport infrastructure, buildings, utility and water supply networks, fuel or food storage facilities). Following the exposure analysis, vulnerability is assessed based on indicators selected in such way so that they cover the entire range of social, economic, environmental aspects, as well as the existing response capabilities in case of a major accident.

Key-words: *vulnerability, exposure, Seveso establishments, dangerous substances, chemical accident.*

1. INTRODUCTION

Risks induced by human activities increased proportionally to the development of industrial facilities. Disasters occurring in highly populated urban areas may be caused by various factors, from human error to equipment failure and natural events such as earthquakes, tornadoes, floods, tsunamis (the so-called NaTech events – Natural Hazard Triggering Technological Disasters) (Ruffi et al., 2017; Campedel, 2008).

Urban vulnerability has been defined as the liability of a city and its infrastructure to losses caused by disasters (Karashima et al., 2014). The urbanization and industrialization processes have led to increased exposure and risks, causing also significant changes in land cover and land-use. Smith (1992) lists among the reasons of increasing trends in disaster consequences: population growth, land pressure, economic growth, technological innovation, social expectations and growing interdependence of individuals, communities

[1] *Babeş-Bolyai University, Faculty of Environmental Science and Engineering, Research Institute for Sustainability and Disaster Management based on High Performance Computing – ISUMADECIP, 30 Fantanele, Cluj-Napoca, Romania, *Corresponding author: camelia.costan@ubbcluj.ro.*

and nations. Hence, these reasons are also at the foundation of increased vulnerability of urban communities.

Exposure is a component of disaster risk, together with vulnerability and hazard. The exposure, as a component of vulnerability, has a dynamic character, varying in both temporal and spatial scale (Botezan et al., 2015). It depends on a number of factors: economic, social, geographic, demographic, cultural or institutional. The lack of resilience and the ability to anticipate and adapt to extreme events are also important causal factors of exposure (Cardona, 2012). A high level of exposure is often the result of a distorted development process, such as the one associated with poor environmental management, demographic changes, rapid and unplanned urbanization, and limited life options for the poor people.

Several legislative instruments, especially the Seveso II Directive 96/82/EC with its amendment, Directive 2003/105/EC, and the SevesoIII (Directive 2012/18/EU) are already in force, with the specific aim of preventing and reducing the number of accidents and their consequences. The directives were named after the small town of Seveso, north of Milan, Italy, where an industrial accident occurred at the local chemical manufacturing plant on the 10th of July 1976. Accidents as those in Seveso (1976), Bhopal (1984), Enschede (2000) and Toulouse (2001) have clearly shown that the consequences of technological accidents can be amplified by the proximity of Seveso facilities to residential and highly populated areas (Christou, 2011; Li et al., 2010). As a consequence, the European legislation required major changes, which referred to the introduction of provisions related to land-use planning (Török et al., 2011). These legal instruments set safe distances for the building of new industrial facilities, separated from residential and commercial areas. These distances should be long enough to ensure the safety of the human population and the environment. Also, the established distance will depend on the vulnerability of the exposed community and on the risk level (facility type, dangerous substances involved, management systems etc.) (Cozzani et al., 2006). For example, it is expected that buildings where more vulnerable people spend their time, such as schools and hospitals, are located in safer areas, away from industrial areas. However, although land-use planning measures and transportation regulations are in place, including by the SevesoIII Directive, there are some old Seveso sites which are dangerously close to crowded places, like shopping malls, which is also the case of the current example.

2. CASE STUDY AND SCENARIOS

The case study chosen for this research is located in Targu Mures, Transylvania (**Fig. 1**). It is an important urban center and the county seat of Mures. The city experienced significant economic and social development, having in 2011 a population of 134,290 inhabitants. The analyzed Seveso site is the chemical plant in the western industrial area of Targu Mures, 4 km away from the city center and close to the European road E60 where a big shopping mall is located. From a geographical point of view, the chemical plant is located in the valley corridor of Mures, delimited in the North by the Transylvanian Plain and in the South by Madarasului Hills, included in the Tarnavelor Plateau.

The two types of hazards associated with the site are toxic ammonia dispersion and overpressure explosion of ammonium nitrate. In the first case, the potential amount involved is 15,000 tones, which might affect about 183,551 people in the hazard area.

Scenario 1: Massive discharge of ammonia in this industrial site may occur due to a severe damage caused by one of the following:

- earthquake or other natural disasters that may compromise the structural integrity of the tank storing the ammonia, followed by loss-of-containment (the Natech event);
- human error of operation due to failure to comply with the rules on technological workflow by exceeding the temperature and the pressure of the workflow;
- technological and mechanical damages;
- armed attack (military or terrorist);
- falling large objects in the atmosphere (airplane, meteorite);
- diversion/sabotage.

Fig. 1 Location of the study area.

The impact area with toxic dispersion depends on the weather conditions, and under unfavorable conditions it can extend over a radius of 10 km. Regarding the temporal position, the event can occur at any time of the day during the system operation and the duration of toxic effect depends in particular on the conditions of the toxic cloud formation (weather conditions, topography and roughness of the terrain).

Scenario 2: The second type of hazard - the overpressure explosion - can occur in the ammonium nitrate storage facility at the same chemical plant. This storage facility is located on the right bank of the Mures River and the number of inhabitants in the hazard area is 5,942. Considering that in the case of this hazard there is an explosion with overpressure, the transport (2.15 km of the E60 European road), public utilities (1 pumping station) and economical (Promenada Mall and 1 food store) infrastructure will be affected and their activity will be interrupted immediately.

The explosion of the ammonium nitrate packed in bags may be caused by one of the following:

- explosion in the neighborhood of the storage facility, leading to the explosion of the ammonium nitrate due to the resulting shock wave (Domino effect);
- fire in the neighborhood of the storage facility which might cause the Domino effect;
- human error due to failure to comply with the rules on handling the dangerous substances;
- armed attack (military or terrorist);
- large falling objects in the atmosphere (airplane, meteorite);
- diversion/sabotage.

The event can occur at any time of the day during the plant operation. In terms of duration, the explosion of the ammonium nitrate can occur suddenly if the cause of the explosion is another explosion produced in the neighborhood or it can last tens of minutes if the cause of the explosion is a fire burst inside the plant. The explosion of ammonium nitrate itself occurs suddenly and the effects are immediate, but the event may continue for a period of time that may take a few days, until the liquidation of the other events (fires/explosions, toxic dispersions) which a massive explosion at a fertilizer plant can generate through the Domino effect.

3. METHODOLOGY

3.1. Exposure analysis

In recent years, several attempts have been made to define and establish exposure assessment methodologies. Particular attention has been paid to the exposure of population and environment to chemical hazards and to the impact of these hazards on the mentioned components. Regarding the environmental risks, the exposure assessment is based on the characterization of the geophysical processes inducing the risks, including the magnitude, frequency, spatial dispersion, duration, rate of onset, time, and temporal spacing of physical conditions.

In order to assess the exposure of social factors, the number of inhabitants from the Territorial Administrative Units (TAUs) included in the scenarios was identified, respectively the estimated number of inhabitants in the hazard-prone area. The number of inhabitants in the hazard-prone area was estimated based on the density of population in the built-up area.

The surface of the residential areas in the hazard-prone area was also analyzed. This was weighted against the total surface of residential areas within the TAU contained in the buffer, using the GIS technique. A distinction has been made between residential areas where buildings were destroyed by explosion and the affected residential areas with no infrastructure destroyed by the toxic dispersion. The capacity of medical and educational units (the number of hospital beds, primary schools and high schools) was analyzed.

In order to assess the relevant environmental factors exposure, the rivers and the lakes (the areas obtained from the CORINE LAND COVER 2012 database) were analyzed, together with the protected natural areas designated according to the Habitats Directive (Sites of Community Importance - SCI and Avifaunistic Special Protection Areas - SPAs) in the hazard-prone area. The length of the rivers in the hazard area was determined and the areas of the lakes in the hazard-prone area were calculated. The protected areas located in the hazard-prone area have been weighted both against their surface within the TAU and against the total extent of the protected area. Their possible overlaps were also taken into account (SCI overlapping SPAs); in the end only one territorial footprint was considered.

In order to assess the exposure of economic components, the industrial sites, transport infrastructure, public utilities networks, drinking water supply networks and fuel, food and consumer goods warehouses were analyzed. In the case of industrial areas, their surface in the hazard area was analyzed against the total surface of the industrial areas within the TAUs contained in the buffer using the GIS technique. In the case of the transport infrastructure, the airports in the hazard area, as well as the transport routes were analyzed, their length being identified in the hazard-prone area. Concerning the public utility networks, their presence in the hazard-prone area and the possibility of their destruction due to explosions were analyzed. The power, thermal power, transformer power, gas pressure

measuring stations and wastewater treatment plants in the hazard-prone area were identified, as well as water catchments and pumping or water treatment stations. Also, the existence of fuel, food and consumer goods warehouses was monitored in the hazard-prone area.

3.2. Vulnerability analysis

Urban vulnerability to technological risks has been examined over the years in terms of four distinct factors: 1. the current pattern of hazardous technologies in relation to urban populations; 2. adequacy of land-use planning and control; 3. effectiveness of emergency planning and response; and 4. the socio-characteristics of the urban population (Liverman, 1986). Hence, these are also translated in a wide range of indicators used in numerous vulnerability assessment methodologies (Knox, 1980; Fedeski & Gwilliam, 2007; Zabeo et al., 2011; Das et al., 2012; Plummer et al., 2013; Constantin et al., 2015).

The vulnerability analysis is a systematic examination of buildings, utilities, population and economic components in order to identify the characteristics that are susceptible to be damaged by a disaster. In literature, it is considered that, for different categories of elements exposed, different vulnerability indices must be deployed and their average can be considered the vulnerability value of the system. In order to conduct an index-based vulnerability analysis, indicators for each index must be selected (Chuanglin & Yan, 2016; Lee, 2014; Armaș & Gavriș, 2016).

In this study, in order to set an index used in the vulnerability ranking of a system, arbitrary values of indicators quantification are determined, each indicator being qualitatively analyzed. The importance of the indicator is determined by its classification into one of the following three levels:

- Lesser importance – it has an indirect influence on the vulnerability – value 1;
- Moderate importance – it has a direct influence on the vulnerability – value 2;
- Great importance – it has a decisive influence on the vulnerability – value 3.

Furthermore, the vulnerability category of the indicator was classified into three levels:

- Low – value 1; Medium – value 2; High – value 3.

The vulnerability analysis was structured into social, economic, physical and environmental components. In this way, the main elements exposed to disaster risk are assessed: population, assets and environmental factors. Moreover, following the analysis of the selected scenarios, two categories of vulnerability indicators have been defined: general (common to all type of hazards) and specific (which characterize the analyzed hazards: accidents at Seveso upper-tier establishments).

The arithmetic mean of the indices values set for each indicator represents the total value of the system vulnerability. This value was furthermore divided into five levels: very low (0 – 1.8), low (1.8 – 3.6), medium (3.6 – 5.4), high (5.4 – 7.2), and very high (7.2 – 9) (Chuanglin & Yan, 2016).

The general indicators (i1-i10) cover the socio-demographic aspects (population density, demographic dependency ratio), the human capital aspects (unemployment rate, Gross Enrollment Ratio – GER, incomes, capacity of medical units, number of physicians per 1,000 inhabitants) and aspects related to physical and ecological vulnerability (hazardous industry, protected areas, water bodies). The data related to socio-demographic indicators were collected from the 2011 population and housing census, except the population density which was calculated by the authors for each particular scenario. For some indicators (population density, total demographic dependency ratio, number of physicians per 1,000 inhabitants) data were available at locality level and, therefore, the

vulnerability index was calculated also at locality level, i.e. more accurately. For the rest of the vulnerability indicators, statistic data at TAU level were used because data were missing at locality level.

Several studies on social vulnerability (Adger et al., 2004; Cutter et al., 2014; Lee, 2014) use disaster response capacities in their analyses. Of the disaster response capacity indicators, this paper considers the following specific indicators (i11-i16) as crucial: information/awareness campaigns for the population, training activities (exercises, simulations), population alarm systems coverage, existence of emergency shelters correlated to the number of population, existence of special CBRN (Chemical, Biological, Radiological and Nuclear) intervention teams, population endowment with individual protection equipment. These cover all measures of prevention, mitigation, preparedness and response that support the community to cope with and to recover after extreme events. These specific indicators were selected according to hazard type (Seveso accidents) and they were evaluated based on data from the official reports and studies of the county inspectorate for emergency situations.

4. RESULTS AND DISCUSSION

4.1. Exposure analysis

The exposure to Seveso upper-tier establishment hazards was assessed considering the elements at risk within the hazard-prone area: population, residential areas, sanitary units, educational units, protected natural areas, water bodies, industrial areas, transport infrastructure, public utilities, fuel deposits and large population agglomerations, drinking water supply networks.

The degree of exposure is larger for the first scenario and the exposed elements are affected differently. These differences are generated by the fact that the hazard-prone areas differ from one scenario to another and the two types of hazards are affecting the exposed elements in different ways. Even though the area affected by the toxic dispersion is larger and more elements are exposed and affected, the effects are not as severe as the effects of the explosion which are more direct and have a physical impact. For example, the toxic dispersion can affect 55.33% of the residential areas, without damaging the infrastructure, while the explosion can affect just 5.06% of the residential area, but in this case the building infrastructure can be damaged. The results show the same situation when considering the medical and educational units: the toxic dispersion can disturb the activities without affecting the infrastructure (the total number of hospitals in TAU – 16, total number of education units in TAU – 45), while the explosion can damage the infrastructure of these units (however, there are no medical and educational units in the hazard-prone area). The same situation is found in the case of protected natural areas (the surface of the natural area located in the hazard-prone area is 32.89 km^2). These could be affected only in the case of toxic dispersion as the area affected by explosion does not include protected natural areas.

The industrial areas have a similar exposure percentage for both scenarios (35% and 22.16%, expressed as ratio between the surfaces of the industrial area located in the hazard-prone area/total surface of industrial area in TAU). However, in the case of explosion the infrastructure can be affected. In the case of transport infrastructure, the toxic dispersion can affect the airport activities, while the explosion can damage 2.15 km of the road.

Based on the assessment of the factors described above, exposure maps have been made for each analyzed scenario (**Fig. 2**). The maximum radius of hazard-prone area for the

first scenario was 10,765 m, while for the second scenario it was 941 m (the radius was calculated based on the most unfavorable weather conditions).

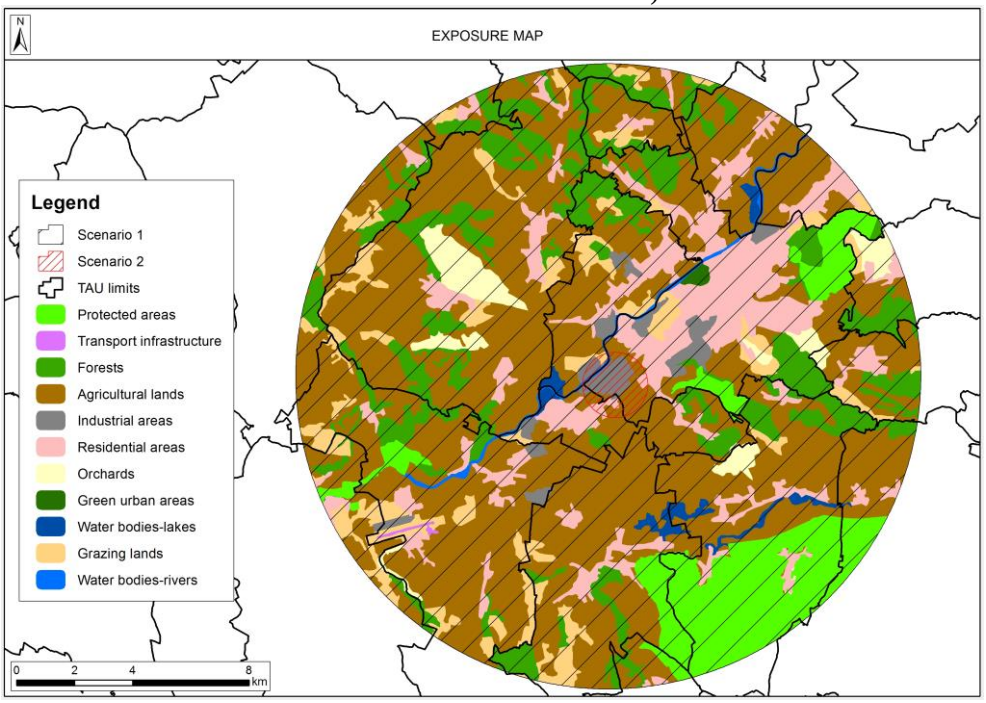

Fig. 2 Exposure map for the two analyzed scenarios

4.2. Vulnerability analysis

Following the analysis of selected indicators, the values for the two scenarios were summarized in **Table 1**.

The total vulnerability index for Scenario 1 – toxic dispersion (ammonia) is 4.8, and for Scenario 2 – explosion (ammonium nitrate) is 4.3, both falling under the moderate vulnerability category.

In terms of general indicators analyzed, the two scenarios were assigned similar values in some cases (unemployment rate of 2.68%, capacity of medical units – 19 beds per 1,000 inhabitants, as compared to the average national value of 6.6 beds/1,000 inhabitants). High values were recorded for population density, demographic dependency ratio and average income (lower than the national value). The general indicators that really differentiate the two scenarios are the hazardous industries, natural protected areas and water bodies. In Scenario 1 there are two more other Seveso establishments in the hazard-prone area, leading to a high vulnerability from this point of view. Moreover, 35% of the protected areas are located in the area of the scenario (moderate vulnerability); while 42.60 % of the water bodies are within the scenario limits (also moderate vulnerability). In the second scenario, the lower vulnerability is given by the lack of other Seveso establishments and lack of natural protected areas and water bodies in hazard-prone area. Campaigns for raising awareness are developed annually in Târgu-Mureș and in the neighboring villages, indicating a low vulnerability level.

Table 1.

Vulnerability results for the two scenarios.

Indicator	Vulnerability indicator	Importance	Scenario 1		Scenario 2	
			Category	**Total**	Category	**Total**
i1.	Population density (inhab./km^2)	3	2 (250– 2000)	**6**	3 (>= 2000)	**9**
i2.	Demographic dependency ratio	3	3 (>40%)	**9**	3 (>40%)	**9**
i3.	Unemployment rate	1	1 (<3%)	**1**	1 (<3%)	**1**
i4.	Gross Enrolment Ratio (GER)	2	3 (< 60%)	**6**	2 (60-75%)	**4**
i5.	Average income	1	3 (< 1800)	**3**	3 (< 1800)	**3**
i6.	Capacity of medical units (no. of beds/1,000 inhabitants)	3	1 (>10)	**3**	1 (>10)	**3**
i7.	Number of physicians per 1,000 inhabitants	3	3 (<1.3)	**9**	2 (2.6 – 1.3)	**6**
i8.	Hazardous industries	2	3 (>1)	**6**	1 (0)	**2**
i9.	Protected areas	1	2 (10-50%)	**2**	1 (10-50%)	**1**
i10.	Water bodies	1	2 (10-50%)	**2**	1 (<10%)	**1**
i11.	Information/awareness campaigns for the population	3	1 (in 2016)	**3**	1 (in 2016)	**3**
i12.	Training activities (exercises, simulations)	3	1 (in 2016)	**3**	1 (in 2016)	**3**
i13.	Population alarm systems coverage	3	1 (>50 %)	**3**	1 (>50 %)	**3**
i14.	Existence of emergency shelters correlated to the number of population	3	3 (<20 %)	**9**	3 (<20 %)	**9**
i15.	Existence of special CBRN intervention teams	3	1 (public and private)	**3**	1 (public and private)	**3**
i16.	Population endowment with individual protection equipment	3	3 (<20 %)	**9**	3 (<20 %)	**9**
Total vulnerability			**4.8**		**4.3**	

Furthermore, these general campaigns are doubled by training activities, developed on a regularly basis, for both the employees of the studied Seveso establishment, as well as for the population outside the manifestation area. The result is an informed and trained population, able to respond in an adequate manner to emergency situations, which can be of significant importance in case of toxic dispersion, as the entire town population may be affected by its consequences. In case of ammonium nitrate explosion, it is more important for the employees on the site to know the adequate measures to be taken in order to protect themselves and their colleagues.

The coverage with alarm systems is very high (246%), thus reducing the vulnerability degree, especially in case of toxic dispersion, when the early warning of the population may reduce the number of victims. These alarms are installed on the main buildings in the residential areas, as well as on the main industrial facilities in the affected area. In case of toxic dispersion, it is recommended to evacuate the surrounding area situated in wind direction; therefore, the existence of alarms systems is very important for saving human lives. If the population must remain inside the buildings, they should close the windows, to

ensure the sealing of the buildings and to unplug the electrical devices, in order to prevent a fire. The alarm system covers also the studied Seveso establishment, allowing the rapid warning of the employees and of the surrounding population (especially the visitors of the city mall located across the site).

On the other hand, there are two indicators that contribute to the increase of the vulnerability level: the poor capacity of emergency shelters related to the number of population (5%) and the lack of population endowment with individual protection equipment (0%). For example, for the toxic dispersion of ammonia, hands, skin and eyes should be protected by using personal protective equipment, such as gloves, air-proof safety goggles, dust-proof suit, and safety footwear. The lack of protective equipment increases the risk of injuries for the city population: headaches, cough and breathing difficulties, eye injuries. The employees can use the protective equipment available on site. In Târgu-Mureş, there are special CBRN intervention teams at the County Inspectorate for Emergency Situations and within private industrial facilities (Seveso establishments). The existence of these intervention teams reduces vulnerability, the intervention in case of chemical accident being much more rapid and efficient. The CBRN intervention team on site includes the adequate means and equipment necessary for a rapid intervention, as well as trained personnel.

5. CONCLUSIONS

Considering that the analyzed case study is one of the major Seveso establishments in Romania, vulnerability reduction measures are necessary. For both scenarios it is proposed to improve traffic lines (for more efficient evacuation) and allocation of medical services, and include vulnerability assessment in land-use planning to reduce future risks.

Moreover, in the case of the first scenario (toxic dispersion), better sealing of windows and doors would be recommended, together with clear instructions for population evacuation and special care requirements for vulnerable groups (children and elderly people). To slow down the toxic cloud, vegetation barriers would be necessary around the water bodies.

In the second scenario (explosion), considering the proximity of the shopping mall (a few hundred meters), very strict safety measures, continuous monitoring and rigorous training of the personnel are required throughout the entire area of the industrial site.

In order to protect the population of the city and reduce the number of victims, it is necessary to build new shelters or improve the existing ones, to ensure a perfect sealing from the outside atmosphere. Furthermore, it is recommended to endow the exposed population with individual protective equipment, increasing the individual protection level and, thus, reducing the overall vulnerability.

ACKNOWLEDGMENT

This paper was supported by the European Social Fund, Administrative Capacity Operational Programme (POCA) SIPOCA grant 30, Disaster Risk Assessment at national level – RoRISK.

REFERENCES

Adger, W.N., Brooks, N., Bentham, G., Agnew, M. & Eriksen, S., (2004) *New Indicators of Vulnerability and Adaptive Capacity*. Technical Report 7, Tyndall Centre for Climate Change Research, University of East Anglia, Norwich.

Armaș, I. & Gavriș, A., (2016) Census-based social vulnerability assessment for Bucharest. *Procedia Environmental Sciences*, 32, 138 - 146.

Botezan, C., Ozunu, Al. & Ștefănie, H., (2015) Vulnerability Assessment: the Case of the Aries River Middle Basin, *Journal of Environmental Protection and Ecology*, vol. 16, no. 4, 1316 – 1326.

Campedel, M., (2008), *Analysis of major industrial accidents triggered by natural events reported in the principal available chemical accident database*. JRC Scientific and Technical Report, 38 pp.

Cardona, O.D., van Aalst, M.K., Birkmann, J., Fordham, M., McGregor, G., Perez, R., Pulwarty, R.S., Schipper E.L.F. & Sinh, B.T. (2012) Determinants of risk: exposure and vulnerability. In: *Managing the Risks of Extreme Events and Disasters to Advance Climate Change Adaptation*. A Special Report of Working Groups I and II of the Intergovernmental Panel on Climate Change (IPCC). Cambridge University Press, Cambridge, UK, and New York, NY, USA, pp. 65-108.

Christou, M., Gyenes, Z. & Struckl, M., (2011) Risk assessment in support to land-use planning in Europe: Towards more consistent decisions?, *Journal of Loss Prevention in the Process Industries*, 24, 219-226.

Chuanglin, F. & Yan, W., (2016) A comprehensive assessment of urban vulnerability and its spatial differentiation in China. *Journal of Geographical Sciences*, 26(2): 153–170.

Constantin, V., Ștefănescu, L. & Kantor, C.M., (2015) Vulnerability assessment methodology: A tool for policy makers in drafting a sustainable development strategy of rural mining settlements in the Apuseni Mountains, Romania. *Environmental Science & Policy*, 52, 129-139.

Cozzani, V., Bandini, R., Basta, C & Christou, M.D., (2006) Application of land-use planning criteria for the control of major accident hazards: A case-study, *J. Hazard. Mater.*, A136, 170–180.

Cutter, S.L., Ash, K.D. & Emrich, C.T., (2014) The geographies of community disaster resilience, *Global Environmental Change*, 29, 65–77.

Das, A., Gupta, A.K., Mazumdera, T.N., (2012) Vulnerability assessment using hazard potency for regions generating industrial hazardous waste. *Journal of Hazardous Materials*, 209– 210, 308–317, doi:10.1016/j.jhazmat.2012.01.025.

Fedeski, M., Gwilliam, J., (2007) Urban sustainability in the presence of flood and geological hazards: The development of a GIS-based vulnerability and risk assessment methodology, *Landscape and Urban Planning*, 83, 50–61, doi:10.1016/j.landurbplan.2007.05.012.

Karashima, K., Ohgai, A. & Saito, Y., (2014) A GIS-based Support Tool for Exploring Land Use Policy Considering Future Depopulation and Urban Vulnerability to Natural Disasters - A Case Study of Toyohashi City, Japan, *Procedia Environmental Sciences.* 22 (2014) 148 – 155.

Knox, P.L., (1980) Measures of accessibility as social indicators: A note. *Social Indicators Research* 7(1-4), 367-377, DOI 10.1007/BF00305607.

Lee, Y.-J., (2014) Social vulnerability indicators as a sustainable planning tool, *Environmental Impact Assessment Review*, 44, 31–42.

Li, F.Y., Bi, J., Huang, L., Qu, C.S., Yang, J. & Bu, Q.M., (2010) Mapping human vulnerability to chemical accidents in the vicinity of chemical industry parks, *J. Hazard. Mater.*. 179, 500–506, doi:10.1016/j.jhazmat.2010.03.031.

Liverman, D. M., (1986) The vulnerability of urban areas to technological risks: An overview of US and European experience, *Cities*, Volume 3, Issue 2, Pages 142-147.

Plummer, R., de Grosbois, D., Armitage, D. & de Loe, R.C., (2013) An integrative assessment of water vulnerability in First Nation communities in Southern Ontario, Canada. *Global Environmental Change*, 23, 749-763, doi:10.1016/j.gloenvcha.2013.03.005.

Ruffi, M.G., Piegau F. & Monnani G., (2017) Natech risk analysis in "Seveso" plants, *AES Bioflux – Advances in Environmental Sciences – International Journal of the Bioflux Society* 9(1): 77-91.

Smith, K., (1992), *Environmental Hazards: Assessing and Reducing Disaster*. Routledge, London.

Török, Z., Ajtai, N., Turcu, A.-T. & Ozunu, A., (2011) Comparative consequence analysis of the BLEVE phenomena in the context on Land Use Planning; Case study: The Feyzin accident. *Process Safety and Environmental Protection*, 89, 1–7, doi:10.1016/j.psep.2010.08.003.

Zabeo, A., Pizzol, L., Agostini, P., Critto, A., Giove, S. & Marcomini, A., (2011) Regional risk assessment for contaminated sites Part 1: Vulnerability assessment by multicriteria decision analysis. *Environment International*. 37, 1295–1306, doi:10.1016/j.envint.2011.05.005.

LOCALIZATION THEORY OF REGIONAL DEVELOPMENT AND AGGLOMERATION EFFECTS: A CASE STUDY OF THE ICT SECTOR IN THE CZECH REPUBLIC

Kamila TUREČKOVÁ [1]

DOI: 10.21163/GT_2018.131.11

ABSTRACT:
The localization theory of the regional development constitutes even these days the permanent groundwork for the possible explanations of the local distribution of the firms in relation to their economic prosperity and potential for the future development. In this paper, factors and contributions of the firm concentration will be theoretically defined using the theory of the core-periphery, taking into consideration their location either in the core of the region or in its periphery. The theoretical assumptions of the chosen subtheories of the group core-periphery, i.e. the theory of cumulative causation and the general theory of polarized development, will be confronted in the paper with the actual findings based on the questionnaire survey among the ICT firms in two regions of the Czech Republic, namely in The South Moravian Region and The Moravian-Silesian Region (NUTS3). The regional capital defined on the regional level of LAU1 formed the core of the region, while the periphery was formed by the remaining districts in the given region. The research confirmed that the ICT firms concentrated in the cores of the regions possess and are aware of the agglomeration effects (advantages) connected with the dominance of the positive (net) externalities combined with relatively undemanding mutual information sharing, knowledge, experience and innovation. The central agglomeration of concentrated ICT firms supports and creates conditions for the existence of the specialized (technological) infrastructure, the availability and sharing of the qualified workforce based on the advanced division of labour, and the participation in the sectoral arrangement (clusters), or more precisely in research and development centres. The discovered data unambiguously support the polarization of the chosen economic structures, specifically the economic sector of ICT, which is then reflected in the dynamic development of the innovation and the growth of investments, a highly specialized structure of workforce, the growth of living standards and the increase in the competitiveness of the given firms, and through the sector and the region leads to the growth of the competitiveness of the whole national economy.

Key-words: *Core-periphery theory, Sectoral agglomeration, ICT sector, Regional Development, Czech Republic.*

1. INTRODUCTION

Information and communication technologies (ICT) play a key role in the context of current societal and economic change. In the 1990s free and public information began to spread through the use of the internet and soon it was possible to produce, to access and to share own, private data. All these steps have led to the promotion of cooperation between different groups of actors, to the digitization of processes and the network integration of enterprises. Through information and communication technologies the process of incorporating foreign processes into their own business activities has been continually

[1] *School of Business Administration in Karvina, Silesian University in Opava, Univerzitni Nam. 1934/3, 733 40 Karvina, Czech Republic, tureckova@opf.slu.cz*

stepped up in order to simplify, streamline and, in particular, to reduce and cost-effectively reduce the important, especially corporate, processes and activities (Friedman, 2006). The ICT sector continues to increase its share in the life of individuals, the functioning of businesses and public administration, and also plays an important role in product or service creation. Last but not least, it is an important factor affecting local, national and global economic performance (Basl, 2010). The ICT sector is characterized by multiplier effects in the economy, where activities in this sector directly or indirectly affect outputs in other sectors, contribute to significant savings and productivity gains, increased intellectual capital, the growth of social value generated by the synergy of knowledge, information and technology, which are being developed, developed and supported by this sector of the economy. All these positive effects associated with business activity in the ICT sector increase the competitiveness of the regions in which they operate and contribute to improving a quality of life and living standards (Turečková, 2017). The agglomerating process of territorial concentration of the ICT industry would be interested in ICT firms themselves and should be actively supported by their leadership and management as well as by the national economic authorities (see also Roche, 2016 or Hong & Fu, 2011).

The selected theoretical approaches to regional development should define the theoretical benefits of the regional specialization in the ICT sector, respectively sectoral agglomeration of the ICT firms and define the factors that support this concentration process, i.e. to characterize the relevant causes of interregional differences forms the specific sectoral agglomerations. Generally defined localization factors of sectoral specialization related to the ICT sector include agglomeration savings related to the prevalence of positive (network) externalities, mutual sharing of information, knowledge, experience and innovation, the existence of specialized (technological) infrastructure, accessibility and sharing skilled labor based on advanced division of labor or the existence of sectoral clusters, respectively research and development centers (Pařil et al., 2015; Turečková, 2014 and Turečková, 2015).

Regarding the methodological perspective, the current research is based on economic-geographical methods which are part of Economic geography. On the background of localization theories were selected theories from the group of the "core-periphery" because of its most important contribution of localization theories that can be referred to as the development of agglomeration effects, which are part of regional development theories today (Šimanová & Trešl, 2011 and Baldwin et al., 2005).

The objective of this paper is to determine differences in the perception of the sectoral concentration between the core (centre) of the region and its periphery. In particular, we will be interested in some agglomeration effects and their differences with respect the location of ICT firms in the region. This information was obtained through an email questionnaire survey done between ICT firms that have been conducted in the area of two regions on regional level NUTS3 in the Czech Republic. These regions are The South Moravian Region and The Moravian-Silesian Region at the turn of the years 2016 and 2017.

The article is organized as follows. Section "Theoretical framework of the study" describes the theoretical approach towards the sectoral concentration in the context of theory "core-periphery" with an emphasis on the main theoretical contributions to this problem. Most of the questions used in the questionnaire survey were based on finding out from the theoretical background. The section "Methodology and data" provide information about primary survey and research. The next section "Agglomeration effects of ICT firms in the core and in the periphery" presents concrete basic empirical results on differences

between centre and periphery. The last part, the conclusion, provides us with concluding comments, and it highlights some of the major conclusions from the analysis provided.

2. THEORETICAL FRAMEWORK OF THE STUDY

The presented paper is from the theoretical point of view based on economic-geographical assumptions of the "core-periphery" theory, especially on the theory of cumulative causes and the general theory of polarized development. The question asked is if there are some differences between the effects of the concentration of ICT firms located in the centres (core) and on the periphery of the region.

The core-periphery theory, respectively "the general theory of polarized development (regional imbalances)" was most intensely developed in the Keynesian period, especially in the 50´s and 70´s of the 20th century. The concepts of core-periphery have introduced by John Friedmann who used this term (word) at the first time. It was a set of partial theories explaining the long-standing divergent processes between regions in the context of the development in the sectoral structure of the economy, whose main theorists include G. Myrdal (1957), J. Friedmann (1966), F. Perroux (1950), A. Hirschman (1967) and D. North (1955). The assumption of these theories is unequal regional development and emphasis on the importance of factors on the demand side, especially investments. Other factors that cause regional divergence in the context of sectoral development include external savings, agglomeration benefits (savings), selective migration of labour, and mobility of capital (especially human). The theory assumes long-standing inequality in regional development, which requires the need for government intervention, which as the only institution in the country is capable of stopping the deepening process of regional divergence.

One of the most important ideas is the theory of cumulative causes of the Swedish economist Gunnar Myrdal (Myrdal, 1957) which argues that the change does not trigger a reaction in the opposite direction, but other changes that enhance it, i.e. a change in one factor will also change the orientation of other factors, the initial difference, i.e. the difference between the regions (the core) will be further deepened (periphery). Market forces, the movement of capital, resources and labour do not lead to a balance but cause widening of regional differences. In the context of its theory, the initial development of a region for whatever reason will cause the region to develop faster than other regions, and the differences between it and the group of other regions will continue to grow. In the less developed regions, resources (capital and prospective labour force) that accumulate in more developed regions are being drained.

Friedmann (1966) within the framework of his "general theory of polarized development", understands the centre as an autonomous region with the ability to capture the main impulse of the given development and to create the required innovations, while the periphery as an area that does not capture these changes. Strengthening dominance and deepening asymmetry of the centre over the periphery explains through six effects: (1) the effect of dominance, (2) the effect of links, (3) the information effect, (4) the psychological effect, (5) the modernization effect and (6) the production effect. The core has a better ability to generate innovation and achieves a greater degree of autonomy with respect to the periphery - independence from other regions. Friedmann's theory is significant in view of the fact that it does not only cover a narrow range of economic variables (for example in comparison to Perroux's economic theory) but emphasizes the importance of institutional structures and social, political and cultural developments in the geographic space (behavioural factors for regional development).

Perroux (1950) in his theory of growth poles, emphasizes the importance of cross-sectoral links, the regional multiplier, and the existence of agglomeration savings that cause the growth of some driving industries at the expense of others. The driving industry in the region is one that is rapidly developing against the backdrop of large and innovative firms. These differences in economic structure are behind the rise and growth of interregional differences. In this case, unequal development is considered to be self-evident as growth cannot occur everywhere and on the same scale. Another concept introduced by Perroux is the growth pole, a certain point (place), respectively points (places) in time and space that lead to growth (Wokoun et al., 2008).

Hirschmann (1967) perceives interregional differences as a basic, natural and indispensable condition for growth where regions (cores) with agglomerating advantages are more abundant at the expense of peripheral areas that lag behind the "cores". Thus cyclical causality processes occur in the territory which in the context of dissertation work can be characterized as the long-term development of the sectoral core (cores) and the decline of sectoral activities on the periphery. Cores are characterized by advanced infrastructure and a higher level of knowledge and skills that are characteristic of a skilled workforce.

The core-periphery theory began to be criticized at the end of the 1960s, particularly by J. R. Lasuén (1969) who accused them of neglecting institutional issues and abandoning the concept of innovation. On the other hand, Lasuén supported and emphasized the importance of innovation (especially their creation and implementation) as a key element for the development of the economy. At the same time, he emphasized the growth potential of the tertiary and quaternary sector firms (Higgins, Higgins & Savoie, 1995).

On the same background was elaborated the concept of sectoral industrial agglomeration at the beginning of the 21st century where firms are concentrated on a certain, limited territory, operating mainly in the same sector, interconnected by a network of mutually meaningful and non-binding relationships and links that complement other participating private and public institutions that are with the firms or industries concerned, direct or indirect and exist in the same territory. The reason for the evolutionary formation and the existence of industrial agglomerations are the benefits of participation in this agglomeration, especially in the form of deepening specialization, externalities and economies of scale (Turečková, 2015 or Campos, 2012). For example, Kim et al. (2009) based on the DEA method demonstrated a positive effect of externalities on the efficiency of the biotech industry in the USA. Driffield and Munday (2001) in their UK research have confirmed that the regionally concentrated industry improves its technical efficiency and shifts it to the production possibilities. The most concentrated manufacturing enterprises showed the highest production efficiency. Mitra and Sato (2007) and Otsuka and Goto (2015) came to similar conclusions. Improving efficiency and enhancing competitiveness resulting from the concentration of firms was confirmed at the microeconomic level in the textile industry in India (Mitra, 1999), salmon production in Norway (Tveteras & Battese, 2006) and in tourism industry in Czech Republic (Ruda, 2016).

3. METHODOLOGY AND DATA

As a first step of the presented research, detailed literature retrieval was performed to understand the problem, nature and specifics of the localization theory of regional development and agglomeration effects of the concentration of firms. From these theories and in context of the aim of the research was selected a group of theorems "core-

periphery", especially the theory of cumulative causes and the general theory of polarized development which were extended by the concept of the sectoral agglomerations. There were defined question and structure of the questionnaire based on these theoretical approaches.

The South Moravian Region (SMR) **The Moravian-Silesian Region (MSR)**

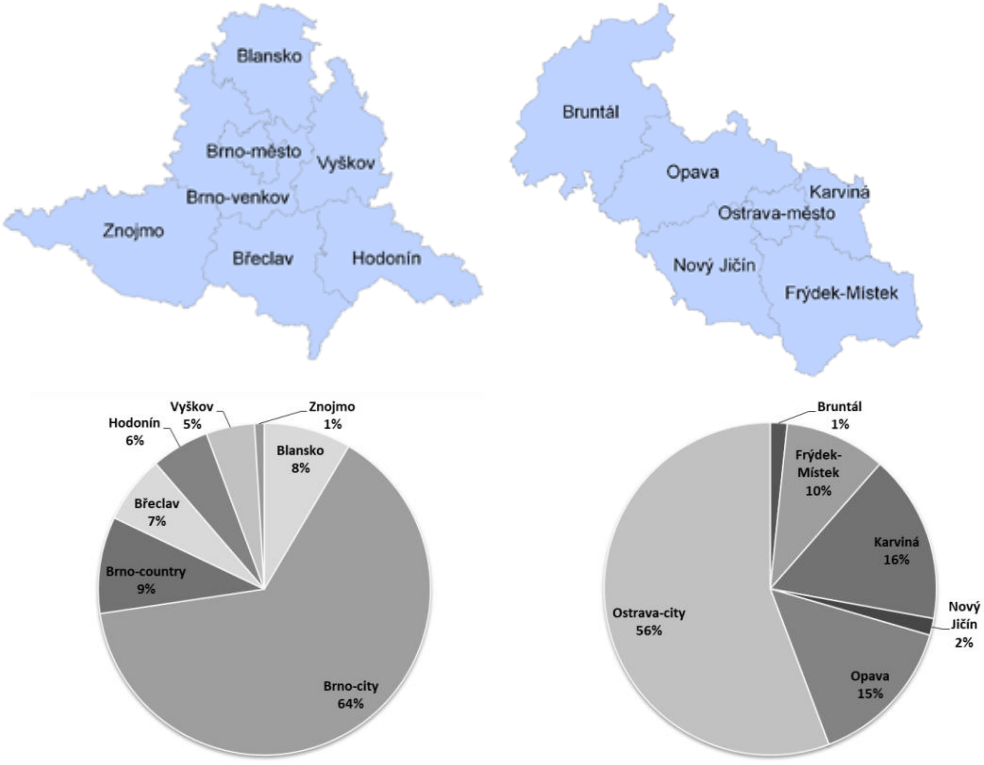

Fig.1 Localization of the ICT firms (n_{SMR}=106, n_{MSR}=61).
Sources: Regional Information Service and questionnaire survey, own processing, 2017.

Primary data to determine the effects of ICT firm´s agglomeration was obtained via email questionnaire survey (email correspondence). Individual phases of conducted research were performed simultaneously in two Czech regions on level NUTS3, in The South Moravian Region (SMR) and in The Moravian-Silesian Region (MSR) in 2016 and 2017 (**Fig. 1**). These two regions were selected against the background of previous studies on regional disparities (Turečková & Nevima, 2017 or Turečková, 2017). In order to ensure the electronic addresses of ICT companies, MERK company database by IMPER CZ, s.r.o. was used. The questionnaire survey was done among 1601 firms operating in the ICT sector (1021 firms in The South Moravian Region and 580 firms in The Moravian-Silesian Region. The ICT sector is defined by NACE Rev. 2, Section J. The return was 167 completed questionnaires, what mean 10.43 % of the total number of respondents. The questionnaire has been created on the basis of previous studies and contained 9 questions

concerning the aspects of the company´s position in the context of the agglomeration (sectoral concentration) effects and the six questions to identification issues characterizing the firm´s respondents. The evaluation of the data obtained took into account the division of firms into the centres (cores) of the regions (regional cities on regional level LAU1) and their periphery (the rest regions LAU1 of the region NUTS3).

If we distribute ICT firms to firms located in the centre (core) and the periphery we have 102 firms in the centre and 65 firms located in the periphery. This division is very important for the further analysis of the agglomeration effects and is necessary to get required results. This is the main content of the next chapter.

4. RESULTS - AGGLOMERATION EFFECTS OF ICT FIRMS IN THE CORE AND IN THE PERIPHERY

This part of the paper analyses the answers obtained from the questionnaire survey and puts it in context with the theoretical assumptions and conclusions resulting from selected regional development theories in the context of the division at the core and the periphery. As already mentioned earlier, the regional cities (centres) of two selected regions will be geographically defined by the territory of the LAU1 regions. It will be Brno-city and Ostrava-city. The remaining districts will form the periphery. In The South Moravian Region, the districts (periphery) defined by the regional level LAU1 as well are Blansko, Brno-country (Brno-venkov), Břeclav, Hodonín, Vyškov and Znojmo, in The Moravian-Silesian Region there are Bruntál, Frýdek-Místek, Karviná, Nový Jičín and Opava.

Table 1.

Distribution of ICT firms in the districts of The South Moravian Region and The Moravian-Silesian Region in 2008 and 2015

Districts (LAU1) of The South Moravian Region/year	Blansko	Brno - city	Brno - country	Břeclav	Hodonín	Vyškov	Znojmo
2008	6.4%	63.7%	11.0%	4.6%	6.2%	4.0%	4.1%
2015	4.7%	64.9%	13.9%	4.4%	5.1%	3.8%	3.2%
Districts (LAU1) of The Moravian-Silesian Region/year	Bruntál	Frýdek - Místek	Karviná	Nový Jičín	Opava	Ostrava - city	
2008	5.7%	16.1%	18.3%	9.3%	10.3%	40.3%	
2015	5.4%	16.2%	16.0%	10.5%	13.0%	38.9%	

Source: Database of the Business Register, Czech Statistical Office, 2017.

Table 1 shows the relative distribution of ICT firms in the districts of the respective regions in 2008 and 2015 according to the Czech Statistical Office (Register of Economic Subjects). It can be seen from the Table 1 that in The South Moravian Region ICT firms are more concentrated in the Brno-city (65%; 2015), while in The Moravian-Silesian Region the distribution of ICT firms in the districts is not so polarized. Most firms are located in the Ostrava-city (less than 40%, 2015). In The South Moravian Region, next 14% of ICT firms are concentrated in the Brno-country, while in the other districts 21% of them are

located. In The Moravian-Silesian Region, except the Bruntál district, the distribution in the remaining regions is rather even and ranges from 10.5% to 16.2%. On the basis of the above, we can conclude that from the point of view of ICT firms, the centre of ICT sector in The South Moravian Region is Brno-city district and in The Moravian-Silesian Region it is Ostrava-City, but the position of this centre is not as strong as in the first case. There is also necessary to emphasize that the percentage of ICT firms in the districts of the analyzed regions corresponds to the distribution of firms in the answers received in the questionnaire survey.

Table 2 shows come different manifestations in the answers between centre and periphery. There is a considerable demand for higher education at technical staff in the centre (more than 22%). Also, respondents from the core think that the wage in the centre is higher than usual which may be related to the difficulty of retaining employees what we can explain increased competition between firms spilling into the labour market. In the centre with the problem of retaining employees about 53% of ICT companies while on the periphery it is only 37%. ICT firms in the core also require higher education of their employees (in 47%) than companies in other districts (in 25%). What is surprising is the perceived independence of addressed firms from other ICT companies: in 65% ICT firms feel to be independent as well as in the centre as well as on the periphery. For ICT firms in the centre are also characteristic that they know more other ICT firms (they know more than 5 similar firms around in 56%) in their neighbourhood than the firms in peripheral parts of the region (only in 23%). This can be explained by the higher concentration of ICT firms in smaller territorial areas and hence by increased market concentration when companies actually need to know their competitors. In Table 2, there is finally to be seen that the firms in the core (in 65%) more aware of the positive effects of company concentration and be part of a sectoral agglomeration. Companies in the periphery in 54% think it is good to be part of such an agglomeration. In both cases, ICT firms perceive the positive effects of company concentration.

Table 2.

Selected differences in the results of the questionnaire survey among cores and periphery in The South Moravian region and The Moravian-Silesian region (Czech Republic).

Variables	Centre - Core (102 firms)	Periphery (65 firms)
Requirement to recruit next workers	45%	31%
Wage higher than usual	38%	26%
Requirement for university education	47%	25%
Independence from other ICT firms - yes	65%	65%
The difficulty of retaining your employees	53%	37%
Awareness about 5 or more similar firms around	56%	23%
Do business in an environment with more similar firms is positively perceived	65%	54%

Source: questionnaire survey, own processing, 2018.

The histogram in **Fig. 2** shows the cumulative responses for each concentration effect from both regions divided by the location of ICT firms in the centre and in the periphery. Respondents could choose more variants for answering this question. For this reason, the number of answers does not match the total number of addressed ICT firms.

The most positive assessment of the concentration for ICT firms is the natural pressure to continually innovate and improve existing processes in the company (with this answer agree 82 respondents what is 49% of all addressed firms, see also **Fig. 3**). There were 53 respondents from the centres (52%) and 29 companies (45%) on the periphery. Companies also appreciate better transfer of expertise, knowledge and information (25% of firms from centres and 14% from peripherals). A qualified workforce is valued by firms located only in the centres of the regions (at 17%). So, sectoral concentration has a positive impact on the number of skilled workers on the labour market and on easier sharing of information and knowledge. Increased competition among ICT firms in their agglomeration has a positive effect of the need to constantly innovate and improv processes.

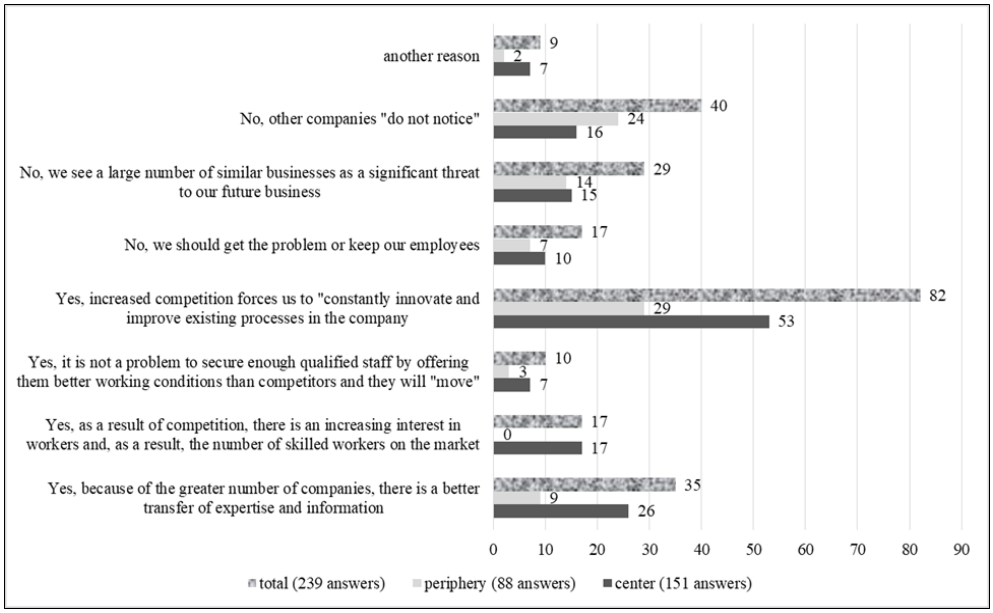

Fig. 2. Agglomeration effects of ICT firms in the core and periphery (number of responses).
Sources: questionnaire survey, own processing, 2018.

Negative to increased competition is the feeling of a threat to another potential business (29 replies in total, 22% of companies come from peripheral districts and only 16% from centres). However, many ICT firms have admitted that they do not notice the behaviour of other similar companies in their area (40 companies, i.e. 24%), more companies in peripheral areas (37%) voted for the answer. In the centres, it was only 16%. This division of responses is typical in context of their localization in the core and in the periphery.

The results of agglomeration (concentration) effects correspond to the answers summarized in Table 2. The above information is complemented by the fact, get from the of questionnaire research, that independently of the location of ICT firms, these

companies together work and cooperate from 90% but in 65% feel completely independent on other similar firms. The current favourable economic situation contributes, among other things, to the positive expectations of ICT companies regarding future developments while more than 88% of ICT companies anticipate further growth: increasing product production or provision of services, modernization of their production processes and technical infrastructure or expansion of current business partnership. Companies also consider increasing the number of their employees. For existing employees ICT firms generally, support further education and actively call for cooperation with other ICT companies.

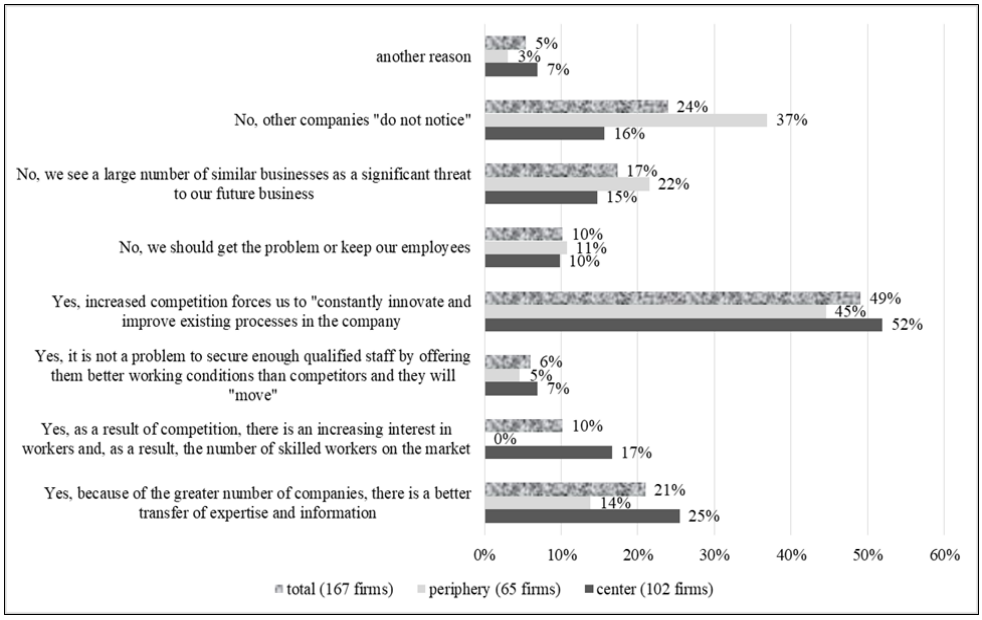

Fig. 3. Agglomeration effects of ICT firms in the core and periphery (in % of the number of companies).
Sources: questionnaire survey, own processing, 2018.

5. CONCLUSIONS

The aim of the paper was to examine the factors and contributions of the firm concentration and selected agglomeration effect, taking into consideration their location either in the core of the region or in its periphery. The case study was done on primary data gained from email questionnaire survey which was carried out in the Czech Republic in two regions on regional level NUTS3, The South Moravian Region and The Moravian-Silesian Region between firms doing their business in Information and Communication Technologies. Through the findings from the questionnaire survey and the background of the analysis of answers, we can find partial relevant links and elements between the examined issues and some specific theories of regional development, especially "core-periphery" theory.

From the concentration of the ICT sector, the following agglomeration effects are emerging for firms: the most positive element of the concentration of the ICT sector is that the addressed firms are pressured by competition, leading to the constant need to implement innovation (in a positive sense) in these companies and to improve their current processes and practices in their company. A total of 82 ICT firms (49%) opted for this answer. 35 companies (21%) perceive, as a further substantial benefit of sectoral concentration, easier exchange and transfer of expertise and knowledge and, in general, better access to information and data. The undesirable effect of sectoral concentration for the firms is the risk of failure in further (next) business (due to increased competition). This option was chosen by 29 companies, i.e. 17%. Overall, the effects of the concentration of ICT companies are perceived by 61% as clearly positive what corresponded with another answer that 65% firms in the core and 54% in the periphery are aware generally of the positive effects of sectoral agglomeration. For "core" is more characteristic and are more pronounced these agglomeration advantages: (1) skilled and specialized workforce, (2) mutually reinforcing technology and innovation in the industry (necessity and response to competition), and (3) the interdependence of local businesses in the form of subcontracting and joint use of specialized infrastructure (in about 90%). There is a need to add a significant cumulative effect that contributes to the region's specialization in certain economic activities, and thus positive expectations.

From the concept of sectoral industrial agglomerations, it is possible to emphasize the parallel between the actual findings and the thesis that the dissemination of information, knowledge, technological processes and practices and innovations enhances efficiency, success, growth dynamics and the competitiveness of the system itself.

ACKNOWLEDGMENT

This paper was supported by the project SGS/13/2015 "Influence of Selected Macroeconomic and Microeconomic Determinants on the Competitiveness of Regions and Firms in Countries of the Visegrad Group Plus".

REFERENCES

Baldwin, R., Forslid, R., Martin, P., Ottaviano, G. & Robert-Nicoud, F. (2005). Economic Geography and Public Policy. University Presses of California, CA: Columbia and Princeton.

Basl, J. (2010). Přístupy a trendy v inovacích informačních a komunikačních technologií ve společnosti a ekonomice. [online] Available from: https://is.muni.cz/do/econ/soubory/oddeleni/centrum/papers/19Basl.pdf [Accessed 20th September 2017]

Campos, C. (2012). The Geographical Concentration of Industries. [online] Available from: Dostupné z: http://www.ons.gov.uk /ons/ dcp171766_ 272232.pdf. [Accessed 25th September 2017]

Czech Statistical Office. (2017). Database of the Business Register. [online] Available from: https://www.czso.cz/csu/res/business_register [Accessed 20th December 2017]

Driffield, N. & Munday, M. (2001). Foreign manufacturing, regional agglomeration and technical efficiency in UK industries: A stochastic production frontier approach. Regional Studies 35(5), 391–399.

Friedman, T. L. (2006). The World is Flat – The globalized world in the Twenty-first century. 2nd edition. New York: Penguin Books.

Friedmann, J. (1966). Regional development policy: a case study of Venezuela. Cambridge: MIT Press.

Higgins, B. H., Higgins, B. & Savoie, D. J. (1995). Regional development theories and their application. London: Transaction Publishers.

Hirschman, A. O. (1967). Development Projects Observed. Washington, D. C.: The Brookings Institution.

Hong, J. & Fu, S. (2011). Information and Communication Technologies and the Geographical Concentration of Manufacturing Industries. Urban studies 48(11), 2339-2354.

Kim, M. K., Harris, T. R. & Vusovic, S. (2009). Efficiency analysis of the US biotechnology industry: Clustering enhances productivity. AgBioForum, 12(3-4), 422-436.

Lasuén, J. R. (1969). On growth poles, Urban Studies 6(2), 137-161.

Mitra, A. & Sato, H. (2007). Agglomeration economies in Japan: Technical efficiency, growth and unemployment. Review of Urban and Regional Development Studies 19(3), 197-209.

Mitra, A. (1999). Agglomeration economies as manifested in technical efficiency at the firm level. Journal of Urban Economics 45(3), 490-500.

Myrdal, G. (1957). Economic Theory and Under-developed Regions. London: Gerald Duckwords.

North, D. (1955). Location Theory and Regional Economic Growth. Journal of Political Economy 63(3), 243-258.

Otsuka, A. & Goto, M. (2015). Regional policy and the productive efficiency of Japanese industries. Regional Studies 49(4), 518-531.

Pařil, V., Kunc, J., Šasinka, P., Tonev, P. & Viturka, M. (2015). Agglomeration effects of the Brno city (Czech Republic) as exemplified by the population labour mobility, Geographia Technica, 10(1), 66-76.

Perroux, F. (1950). Economic Space: Theory and Applications. The Quarternaly Journal of Economics 64(2), 89-104.

Regional Information Service. (2017). Maps. [online] Available from: http://www.risy.cz/cs/mapy-ke-stazeni [Accessed 10th September 2017]

Roche, E. M. (2016). Information and Communication Technology Still a Force for Good? Journal of global information technology management 19(2), 75-79.

Ruda, A. (2016). Exploring tourism possibilities using gis-based spatial association method, Geographia Technica, 11(2), 87-101.

Šimanová, J. & Trešl, F. (2011). Vývoj průmyslové koncentrace a specializace v regionech NUTS3 České republiky v kontextu dynamizace regionální komparativní výhody. Ekonomie a management 1(1), 38-52.

Turečková, K. & Nevima J. (2017). Cluster analysis in context of ICT sector in NUTS3 regions of Czech Republic. In: Proceedings of the 13th International Conference Liberec Economic Forum 2017. Liberec: Technical University of Liberec, 153-161.

Turečková, K. (2014). Dekompozice faktorů konkurenceschopnosti regionů v oblasti ICT sektoru. In: Sborník recenzovaných příspěvků z 2. ročníku mezinárodní vědecké konference Ekonomika a řízení podniku ve 21. století. Ostrava: VŠB-TU Ostrava, 187-193.

Turečková, K. (2015). Sectoral industrial agglomeration and network externalities: concept of ICT sector. In: Proceedings of 5th International Conference on Applied Social Science. USA: IERI, 50-55.

Turečková, K. (2017). Selected Microeconomic Effects of ICT firms in context of level of Sectoral Concentration: case study in selected regions of the Czech Republic, Trends Economics and Management 11(30), 61-72.

Tveteras, R. & Battese, G. E. (2006). Agglomeration externalities, productivity and technical inefficiency. Journal of Regional Science 46(4), 605-625.

Wokoun, R. et al., (2008). Regionální rozvoj: východiska regionálního rozvoje, regionální politika, teorie, strategie a programování. Praha: Linde.

METHODS OF MAXIMUM DISCHARGE COMPUTATION IN UNGAUGED RIVER BASINS. REVIEW OF PROCEDURES IN ROMANIA.

Anna Izabella VODA[1], Adrian Constantin SARPE[2], Mihai VODA [3]

DOI: 10.21163/GT_2018.131.12

ABSTRACT:
Maximum discharge determination on small river basins with no hydrological measurement utilities is important for the rainfall-runoff correlation and the accurate assessment of the watershed surface flow effects. Discharge transfer time calculation from rainfall to runoff requires correct determined hydrological parameters. The focus of this article is the evaluation of Romanian methodologies used for maximum discharge computation in ungauged river basins. Our research for ungauged small river basins study methodology was carried on using remote sensing, GIS and regional datasets. Field work on significant small catchments was necessary for the basin morphological features assessment and land cover characteristics validation. We found that the Romanian rational methodology is widely used according to national landscapes features classification, applicable to a considerable number of ungauged river basins. Our study presents the benefits and limitations of the official Romanian methodologies used for small ungauged river basins scientific assessment and hydrological calculations.

Key-words: *river basin, ungauged basin, rational method, GIS, maximum discharge.*

1. INTRODUCTION

The maximum discharge correct computation for ungauged river basins has a significant importance for the safety and reliability of water works planning, flooding estimation and floods protection measures. There is a considerable difficult delimitation between ungauged river basins from the maximum discharge approach. The limit varies according to the geographical position, from upstream mountain river basins to hilly and downstream plain regions.

Romanian ungauged river basins maximum discharge computation is determined using various research approaches, such as Romanian national rational standard methodology (RNS), general or synthesis relations methodology, Q200 and rainfall computation methodology (Diaconu & Miță, 1997).

Small river basins surfaces under 5–10 km^2 are analyzed with the RNS method. The maximum discharge determination for ungauged watersheds surfaces below 1000 km^2 is developed with synthesis relations methodology, using measured data from hydrological stations network in representative neighboring river basins or experimental hydrological stations, having the maximum discharge obtained from regular statistical calculations, and from pluvial network system. The methodology based on rain computation is used for the maximum discharge of 1% probability determination in 5-100 km^2 river basins and the Q200 method for 10-1000 km^2 river basins (Sarpe & Voda, 2017; Diaconu & Miță, 1997; Mustață, 1991).

[1] Babes Bolyai University, 400006 Cluj Napoca, Romania, vodaizabella@yahoo.com;
[2] Lorraine University, Laboratory LOTERR EA-7304, 57045 Metz, France, adriansarpe@yahoo.com;
[3] Dimitrie Cantemir University, 540545, Targu Mures, Romania, mihaivoda@cantemir.ro;

The maximum discharge computation methodologies require soil, vegetation and land cover assessment. Remote sensing technology is important for river basins outlining process. Eilander et al. (2014) used MODIS and Landsat for maps elaboration and Radarsat for watershed monitoring.

Small river basins rainfall-runoff models constitute indicators of regional water system evolution, being also important for national water resources policies and management plans (Sarpe & Voda, 2017; Deitch et al., 2016; Haidu & Ivan, 2016). Reistetter and Russell (2011), analyzed the duration time between the maximum precipitation value and peak flow discharge, emphasizing the importance of rainfall. Fan et al. (2013), suggested that rainfall-runoff correlation is considerably dependent on soil typology. Zégre et al. (2013), assessed the influence of land coverage on overland flow. Choi et al. (2013) created the LSM (land surface model) for catchments stream flow assessment and management. Haidu et al. (2017), created `*The Cluj model*` for peak flow computation in any point of a hill slope. Bozzano et al. (2017) validated remote sensing methodology with field trips. Ungauged watershed stream flow computation could present errors without onsite validation surveys.

As the National Institute of Hydrology and Water Management (NIHWM) is increasingly recommending the use of RNS for the ungauged small river basins maximum discharge computation, it is worth examining its impact in Romania, where SCS-CN is a pioneer in the process (Sarpe & Voda, 2017). According to OMMD (2016), Grimaldi et al. (2012, 2013, 2015) the Rational Formula has to be updated to the new technological trends, which determined significantly improved methodology for river basins maximum discharge evaluation.

2. RESEARCH METHODOLOGY

Geographical information system (GIS) represents the main geospatial technology that facilitates the use of DEM (digital elevation model), CLC (Corine Land Cover) and HWSD (Harmonized World Soil Database) for the virtual hidro-maps ellaboration and catchments morphological features comprehension. INIS GeoPortal, developed on Esri Geoportal Server Extension Technology and Google Earth are utilized for geographical data validation, environmental factors assessment (Diaconu & Serban, 1994; Yu et al., 2000; Reistetter & Russell, 2011; Jung & Jasinski, 2015; Győri et al., 2016).

An assessment will first be made of the geographical features of the river basins themselves, on an individual basis. Secondly, the existing hydrological registered measurements are analyzed and then, according to the available hydrometrical database, the proper maximum discharge computation methodology is selected.

Preliminary evaluation phase impose the measurement of the analyzed river basin surface, the forest canopy coefficient calculation, soil types determination and climatic characterization.

The hydrometrical data from the river basin are analyzed based on annual database collected from the hydrological stations, with focus on the exceptional maximum discharges registered, maximum flow volumes and the major floods hydrograph (Diaconu & Miță, 1997).

A considerable number of ungauged river basin parameters can be determined from regional synthesis studies and should be validated in the field, such as land cover, soil typology and watershed morphometric features (Diaconu & Serban, 1994; Sarpe & Voda, 2017).

3. THE Q_{200} METHOD

The *Q_{200} method* is applied when 200 Km^2 river basins are selected as reference, with already computed 1% maximum discharges. For the given surface F_b of the river basin that needs to be analyzed, the maximum discharge calculus formula will be (Mustaţă, 1991):

$$Q_{max1\%B} = q_{200}(200/F_B)^n F_B \quad (1)$$

Where q_{200} represents the specific maximum discharge with 1% probability, determined on the 200 km^2 river basins surface and expressed in m^3/s per km^2 (**Fig. 1**). The *n* parameter is extracted from the *n* reduction coefficient maps (Diaconu & Miţă, 1997).

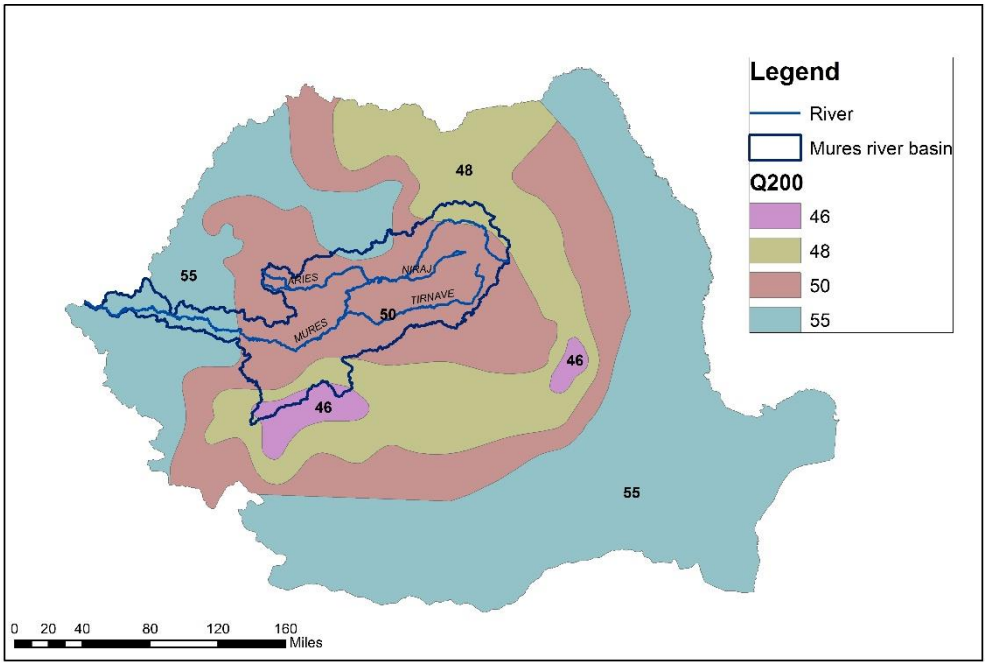

Fig. 1 The *q_{200}* specific maximum discharge map.

4. THE *H RAINFALL* METHOD

The H rainfall method presents a computation formula for the maximum discharges with 1% probability determination in the river basins with surfaces between 5 and 100 km^2 (Mustaţă, 1991):

$$Qmax1\% = (0{,}28*C_s*F*H60)/(F+1)^n \quad (2)$$

where the hourly maximum precipitations layer (H_{60}) and the *n* subunitary coefficient are provided by the Romanian standard regionalization (**Fig. 2**) annexes (Diaconu & Miţă, 1997). The C_s parameter represents the runoff coefficient, obtained from the Romanian experimental hydrological stations and representative river basins (Miţă & Muscanu, 1986).

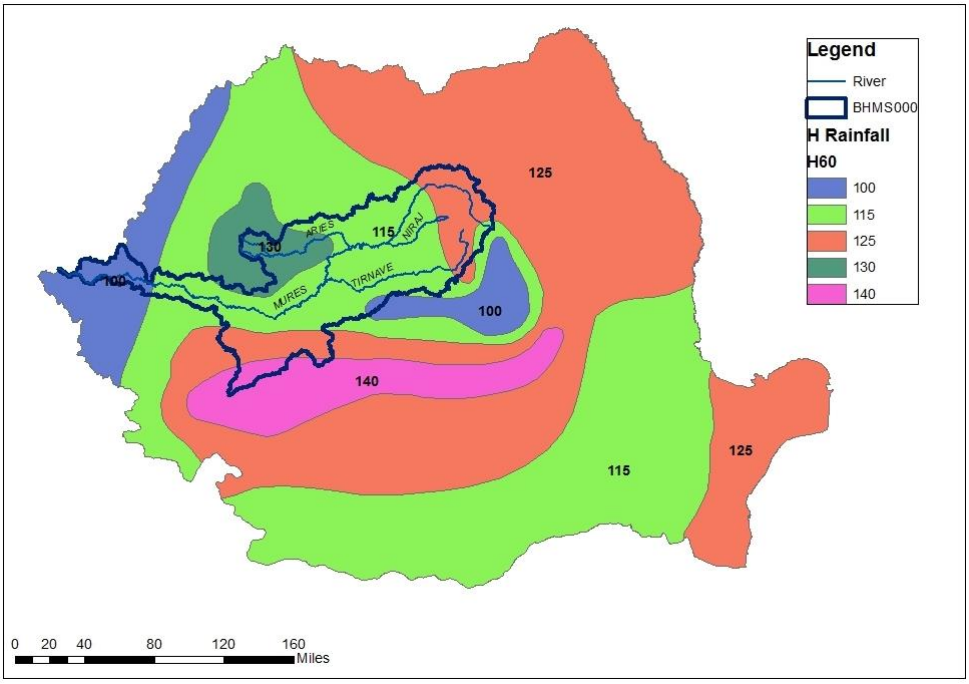

Fig. 2 The *H rainfall* map.

The C_s (runoff coefficient) is determined taking into account the river basin soil textures, average slope gradients and forest canopy coefficient. The Arc GIS facilitates the extraction of the slope layer for the analysed river basin providing the catchment slopes and soil textures. LANDCOVER layer computes the forest canopy coefficient (Diaconu & Mișă, 1997).

5. GENERALIZATION METHOD

The generalization or synthesis method is considered an indirect approach, applied when hydrological data are missing. The maximum discharge computation is based on neighbouring similar river basins hydrological determinations. The necessary data have to be registered at 4-5 hydrometrical stations located in the analysed watershed proximity. The maximum discharges origins in Romanian river basins are represented mainly by the rainfalls (Mustață, 1991).

This methodology cannot be applied in certain situations, such as considerable morphological catchment features differences between the analysed river basin and the referenced ones. Furthermore, the existence of significant surfaces exposed to flooding, the presence of specific soils, for example sandy soils or the water works constructions that are influencing the runoff regime are restricting the methodology application (Diaconu & Mișă, 1997).

The average altitude of the referenced river basins and their surface have to be relatively similar in order to qualify for generalization methodology establishment (Diaconu & Serban, 1994).

6. THE RATIONAL METHOD (RNS)

The Romanian national rational standard (RNS) method represents the main maximum discharge computation methodology applied for small ungauged river basins in Romania (Sarpe & Voda, 2017). The registered rainfalls are considerably influencing the small watersheds water balance. The rational calculus formula is taking into account the average precipitation intensity that is generating the maximum discharge and has a duration that equals the runoff watershed lag time, the runoff coefficient and the analysed river basin surface in square kilometres. $Q_{max1\%}$ is expressed in $m^3/s*km^2$:

$$Q_{max1\%} = B_{1\%} * F^{(1-n)} \qquad (3)$$

Where F is the river basin surface in km^2, (1-n) is a subunitary parameter and $B_{1\%}$ represents the 1% probability maximum discharge for 1 km^2 surface. The $B_{1\%}$ parameter is adjusted through an iterative procedure so the maximum discharge calculated from the formula:

$$Q`_{max1\%} = 16.7 * I_{r1\%} * C_r * F, \qquad (4)$$

has to coincide with the discharge determined with formula (3) under the 5% acceptable error. C_r is the river basin runoff coefficient and $I_{r1\%}$ represents the generating rainfall intensity, directly dependent on the $B_{1\%}$ parameter through the overland flow concentration time.

The precipitations that are generating the maximum discharge are considered uniformly distributed on the river basin surface. This is the reason why the application of RNS is limited to the small ungauged river basins with surfaces up to 1000 ha, situated in the hilly and mountainous regions (Diaconu & Mița, 1997).

The RNS method takes into account the watershed surface typology, the vegetation coverage gradient and the vegetation type (grass, shrubs, forest) before maximum discharge computation. In practice, the following hydrographical parameters are determined (Diaconu & Serban, 1994):

- **F** *river basin surface* – determined with GIS tools
- **La** *river bed length* – measured between the river origins and the closing watershed section with GIS tools
- **ΣL** *the total river bed length including tributaries*–**ΣL= La+ ΣLafl**
- **Lv** *the average slopes length*- **Lv=0,55*F/ ΣL**
- **Ia** *the average river bed slope* - **Ia(m/km)= ΔH(m)/ La(km)**

Environmental factors are conditioning the maximum discharge genesis, the river bed runoff and the overland water flow. The watershed morphological parameters such as soil textures, vegetation typology, watercourse body class, forest canopy gradient and human settlements characteristics have to be evaluated owing to their influence on river flow and maximum discharge formation. On field assessment is recommended for ungauged catchments (Sarpe & Voda, 2017).

The roughness coefficient determination is preceded by the riverbed barriers or flow obstacles appraisal, water vegetation placements and meandering grade estimation. According to Diaconu & Mița (1997), the reduction coefficient values for different Romanian geographical areas, the riverbed and slope roughness coefficients are extracted

from designated tables, elaborated by the National Institute of Hydrology and Meteorology (Diaconu & Serban, 1994).

7. DISCUSSION

The RNS methodology is founded on tailored-made maps, regional stereotypes and generalization documents. According to Musy (1998), Jeon *et al.* (2014), land cover and soil type assessment have a significant importance for curve number estimation in ungauged river basins. Assigning values for soil permeability, vegetation density and hill slope, the curve number is estimated and used for the maximum potential water retention computation but in ungauged catchments the curve number appraisal is using only land cover and soil type characteristics. Huang et al. (2006) performed the slope inclusion into the curve number estimation method and showed the runoff depth connection to slope values. Jeon *et al.* (2014) presented the ungauged catchments surface runoff assessment errors generated by the unadjusted curve number variables.

Sarpe & Voda (2017), observed that the RNS methodology field validation is considerably increasing the maximum discharge computation accuracy if it is correlated with the calibrated river basin surface parameters in GIS data base. Satellite imagery can indicate land cover typology changes, which are considered important predictors for small river basins hydrological processes development. Legal and illegal deforestation activities are significantly disturbing the rainfall-runoff processes, with disastrous effects on a considerable number of Romanian rural communities. Choi (2013) and Posner *et al.* (2014), showed the importance of mapping products and simulation models for the small watershed protection and flood prevention for refined prognosis of water system evolution.

8. CONCLUSIONS

This paper findings are illustrating the rational methodology significant adjustability to Romanian ungauged watershed geographical characteristics. The maximum discharge determination is more accurate and the lag time duration remarkably follows the runoff influencing parameters variation. The time interval between the maximum rainfall moment and the peak stream flow is dependent on the river basin hydrographical features, proving the RNS method flexibility. Furthermore, on field validation required for small catchments hidro-morphology and forest canopy assessment, considerably contributes to RNS methodology proficiency.

The maximum discharge computation methodology for small ungauged watersheds is presenting special particularities, with different elements, in comparison with the maximum discharge determination procedures for bigger river basins.

In small catchments, the rainfall repartition on the basin is more concentrated as compared with the same precipitation quantity registered in larger river basins.

The peak runoff and the floods *formed on small watersheds are composing floods on small watersheds* in a shorter time interval compared with the wider basins surfaces. This faster runoff concentration process leads to a different methodology approach for the maximum discharge computation according to the size of the ungauged river basins.

The watershed surface roughness characteristics are influencing the *conceiving*?? and the conditional factors of the peak runoff dynamics. River basin slopes degradation, fast erosional processes and deforestation activities can produce important changes in years or decades.

The ungauged river basins surface evolution, the runoff coefficient, the roughness effects on the rainfall-runoff system are all quantified in the RNS methodology used for maximum discharge computation.

REFERENCES

ArcGIS Server, (2017). *Website of ArcGIS Server* [Online]. Environmental Systems Research Institute, Available from: www.esri.com/software/arcgis/arcgisserver/, [Accessed December 2017].

Bozzano, F., Mazzanti, P., Perissin, D., Rocca, A., De Pari, P., & Discenza, M.E. (2017). Basin Scale Assessment of Landslides Geomorphological Setting by Advanced InSAR Analysis. *Remote Sens*ing, 9, 267.

Choi, H.I. (2013). Application of a Land Surface Model Using Remote Sensing Data for High Resolution Simulations of Terrestrial Processes. *Remote Sens*ing, 5, 6838-6856.

Deitch, M.J., Docto, M., & Feirer, S.T. (2016). A spatially explicit framework for assessing the effects of weather and water rights on streamflow. *Applied Geography*, 67, 14-26.

Diaconu, C., & Serban, P. (1994). *Sinteze si regionalizari hidrologice*, Editura HGA: Bucuresti, Romania, pp. 151–185, 973-98530-8-0.

Diaconu, C., & Miță, P. (1997). *Instrucțiuni pentru calculul scurgerii maxime în bazine mici*. I.N.M.H., București, Romania.

Eilander, D., Annor, F.O., Iannini, L., & van de Giesen, N. (2014). Remotely Sensed Monitoring of Small Reservoir Dynamics: A Bayesian Approach. *Remote Sensing*, 6, 1191-1210.

FAO/IIASA/ISRIC/ISS-CAS/JRC. (2009). *Harmonized World Soil Database (version 1.1)*., FAO, Rome, Italy and IIASA, Laxembourg, Austria.

Fan, F., Deng, Y., Hu, X., & Weng, Q. (2013). Estimating Composite Curve Number Using an Improved SCS-CN Method with Remotely Sensed Variables in Guangzhou, China. Remote Sensing, 5, 1425-1438.

Grimaldi, S., Petroselli, A., & Romano, N. (2013). Green-Ampt Curve Number mixed procedure as an empirical tool for rainfall-runoff modelling in small and ungauged basins. *Hydrological Proces*sing, 27, 1253–1264.

Grimaldi, S., & Petroselli, A. (2015). Do we still need the Rational Formula? An alternative empirical procedure for peak discharge estimation in small and ungauged basins. *Hydrological Science J*ournal, 60(1), 1-11, DOI:10.1080/02626667.2014.880546.

Grimaldi, S., Petroselli, A., Tauro, F., & Porfiri, M. (2012). Time of concentration: a paradox in modern hydrology. *Hydrological Science J*ournal, 57(2), 217-228, DOI:10.1080/02626667.2011.644244.

Győri M-M., Haidu I., & Humbert J., (2016). Deriving the floodplain in rural areas for high exceedance probability having limited data source. *Environmental Engineering and Management Journal*, 15(8), 1879-1887.

Haidu, I., Batelaan, O., Crăciun, A.I., & Domniţa, M. (2017). GIS module for the estimation of the hillslope torrential peak flow. *Environmental Engineering and Management Journal*, 16(5), 1137-1144.

Haidu, I., & Ivan, K. (2016). Évolution du ruissellement et du volume d'eau ruisselé en surface urbaine. Étude de cas: Bordeaux 1984-2014, France. *La Houille Blanche*, 5, 51-56.

Haidu, I., & Ivan, K. (2016). The assessment of the impact induced by the increase of impervious areas on surface runoff. Case study the city of Cluj-Napoca, Romania. *Carpathian Journal of Earth and Environmental Sciences*, 11(2) 331 – 337.

Huang, M., Gallichand, J., Wang, Z., & Goulet, M.A. (2006). Modification to the Soil Conservation Service curve number method for steep slopes in the Loess Plateau of China. *Hydrological Processes*, 20, 579–589.

Jeon, J.-H., Lim, K.J., & Engel, B.A. (2014). Regional Calibration of SCS-CN L-THIA Model: Application for Ungauged Basins. *Water*, *6*, 1339-1359.

Jung, H.C., & Jasinski, M.F. (2015). Sensitivity of a Floodplain Hydrodynamic Model to Satellite-Based DEM Scale and Accuracy: Case Study—The Atchafalaya Basin. *Remote Sens*ing, 7, 7938-7958.

Kim, U., & Kaluarachchi, J.J. (2008). Application of parameter estimation and regionalization methodologies to ungauged basins of the Upper Blue Nile River Basin, Ethiopia. *Journal Hydrology*, 362, 39–56.

Miță, P., & Muscanu, M. (1986). *Small river basins runoff coefficients*, Studii şi cercetări de hidrologie : Bucuresti, Romania, pp. 45-58. 53.

Mustață, I. (1991). *Instrucțiuni pentru calculul scurgerii maxime în bazine mici*. I.N.M.H., București, Romania.

Musy, A. (1998). *Hydrologie appliquée*. H*G*A*, Bucuresti, Romania, 368 p.

Ordinul MMDD nr. 976/2008. [Online]. Available from: https://lege5.ro [Accessed December 2017].

Posner, A., Georgakakos, K., & Shamir, E. (2014). MODIS Inundation Estimate Assimilation into Soil Moisture Accounting Hydrologic Model: A Case Study in Southeast Asia. *Remote Sensing*, 6, 10835-10859.

Reistetter, J.A., & Russell, M. (2011). High-resolution land cover datasets, composite curve numbers, and storm water retention in the Tampa Bay, FL region. *Applied Geography*, *31*, 740–747.

Sarpe, C. A., & Haidu, I. (2017). Temporal sampling conditions in numerical integration of hydrological systems time series. *Geographia Tech*nica, 12, Issue 1, 2017, 82- 94.

Sarpe, C. A., & Voda, I. (2017). Small Watershed Hydrological Models - Lag Time Comparation. 3rd PannEx workshop on the climate system of the Pannonian basin. Cluj-Napoca, Romania, 20-21 March 2017; Horvath, C., Croitoru, A. E., Guettler, I., Man, T. C, Bartok, B. Eds.; Romania.

United States Department of Agriculture, Soil Conservation Service (USDA-SCS). (2004). Estimation of Direct Runoff from Storm Rainfall. In National Engineering Handbook; USDA-SCS: Washington, DC, USA.

USGS (2017) *The United States Geological Survey* [Online]. Land Cover Trends Geotagged Photography. Available from: https://lta.cr.usgs.gov/lct_photos [Accessed December 2017].

Yu, B., Rose, W.C., Ciesiolka, C.A., & Cakurs, U. (2000). The relationship between runoff rate and lag time and the effects of surface treatments at the plot scale. *Hydrological Scienc*e, 45(5), 709-726.

Zégre, N.P., Maxwell, A., & Lamont, S. (2013). Characterizing streamflow response of a mountaintop-mined watershed to changing land use. *Applied Geography*, 39, 5-15.

.

Aims and Scope

Geographia Technica is a journal devoted to the publication of all papers on all aspects of the use of technical and quantitative methods in geographical research. It aims at presenting its readers with the latest developments in G.I.S technology, mathematical methods applicable to any field of geography, territorial micro-scalar and laboratory experiments, and the latest developments induced by the measurement techniques to the geographical research.

Geographia Technica is dedicated to all those who understand that nowadays every field of geography can only be described by specific numerical values, variables both oftime and space which require the sort of numerical analysis only possible with the aid of technical and quantitative methods offered by powerful computers and dedicated software.

Our understanding of ***Geographia Technica*** expands the concept of technical methods applied to geography to its broadest sense and for that, papers of different interests such as: G.I.S, Spatial Analysis, Remote Sensing, Cartography or Geostatistics as well as papers which, by promoting the above mentioned directions bring a technical approach in the fields of hydrology, climatology, geomorphology, human geography territorial planning are more than welcomed provided they are of sufficient wide interest and relevance.

Targeted readers:

The publication intends to serve workers in academia, industry and government.
Students, teachers, researchers and practitioners should benefit from the ideas in the journal.

Guide for Authors

Submission

Articles and proposals for articles are accepted for consideration on the understanding that they are not being submitted elsewhere.

The publication proposals that satisfy the conditions for originality, relevance for the new technical geography domain and editorial requirements, will be sent by email to the address editorial-secretary@technicalgeography.org.

This page can be accessed to see the requirements for editing an article, and also the articles from the journal archive found on www.technicalgeography.org can be used as a guide.

Content

In addition to full-length research contributions, the journal also publishes Short Notes, Book reviews, Software Reviews, Letters of the Editor. However the editors wish to point out that the views expressed in the book reviews are the personal opinion of the reviewer and do not necessarily reflect the views of the publishers.

Each year two volumes are scheduled for publication. Papers in English or French are accepted. The articles are printed in full color. A part of the articles are available as full text on the www.technicalgeography.org website. The link between the author and reviewers is mediated by the Editor.

Peer Review Process

The papers submitted for publication to the Editor undergo an anonymous peer review process, necessary for assessing the quality of scientific information, the relevance to the technical geography field and the publishing requirements of our journal.

The contents are reviewed by two members of the Editorial Board or other reviewers on a simple blind review system. The reviewer's comments for the improvement of the paper will be sent to the corresponding author by the editor. After the author changes the paper according to the comments, the article is published in the next number of the journal.

Eventual paper rejections will have solid arguments, but sending the paper only to receive the comments of the reviewers is discouraged. Authors are notified by e-mail about the status of the submitted articles and the whole process takes about 3-4 months from the date of the article submission.

Indexed by: **CLARIVATE ANALYTICS**
SCOPUS
GEOBASE
EBSCO
SJR
CABELL

ISSN: 1842 - 5135 (Print)
ISSN: 2065 - 4421 (Online)